DZIEDZINA: Nauki Inżynieryjno-techniczne
DYSCYPLINA: Inżynieria Środowiska, Górnictwo i Energetyka

ROZPRAWA DOKTORSKA

METODY ANALIZY DANYCH Z SYSTEMÓW O ARCHITEKTURZE INTERNETU RZECZY I PRZETWARZANIA W CHMURZE NA POTRZEBY MONITOROWANIA PROCESÓW TECHNOLOGICZNYCH POZYSKIWANIA RUDY MIEDZI

Mgr inż. Bartłomiej Ziętek

Promotor:
prof. dr hab. inż. Radosław Zimroz
Wydział Geoinżynierii, Górnictwa i Geologii

Promotor pomocniczy:
dr inż. Jacek Wodecki
Wydział Geoinżynierii, Górnictwa i Geologii

Słowa kluczowe: Górnicze procesy technologiczne, Prototypowanie układów pomiarowych, Analiza danych, Przetwarzanie sygnałów, Monitorowanie stanu, Internet Rzeczy, Chmura obliczeniowa

Wrocław 2025

FIELD OF SCIENCE: Engineering and Technology
DISCIPLINE OF SCIENCE: Environmental Engineering, Mining and Energy

DOCTORAL DISSERTATION

IOT AND CLOUD COMPUTING DATA ANALYSIS METHODS FOR MONITORING TECHNOLOGICAL PROCESSES OF COPPER ORE EXTRACTION

Bartłomiej Ziętek, MSc

Supervisor:
Radosław Zimroz, PhD, DSc, Full Professor
Faculty of Geoengineering, Mining and Geology

Assistant supervisor:
Jacek Wodecki, PhD
Faculty of Geoengineering, Mining and Geology

Keywords: Mining technological processes, Measurement systems prototyping, Data analysis, Signal processing, Condition monitoring, Internet of Things, Cloud Computing

Wrocław 2025

Per Aspera Ad Astra

Autor pracy pragnie podziękować:

Prof. Radosławowi Zimrozowi i dr. inż Jackowi Wodeckiemu za ich ogromną wiedzę i motywację, za wsparcie na każdym etapie pracy badawczej oraz za wskazówki udzielone podczas pisania pracy doktorskiej.

Dr inż. Pawłowi Śliwińskiemu i współpracownikom z KGHM za możliwość wspólnej realizacji projektów badawczych.

Współautorom artykułów za swój wkład, poświęcony czas we wspólnie prowadzonych badaniach.

Koleżankom i kolegom z zespołu badawczego Digital Mining Center (DMC) za możliwość współpracy i wszelkie udzielone wsparcie.

Rodzinie za nieustającą wiarę we mnie.

Streszczenie

Rozwój technologii informatycznych i ich wpływ na wiele obszarów przemysłu staje się obecnie podstawową metodą ich dalszego rozwoju. Część z nich, takie jak Internet Rzeczy (IoT) i korzyści z wykorzystywania zasobów chmury obliczeniowej (Cloud Computing) może w ogromnym stopniu wzbogacić również nowoczesną działalność przemysłu wydobywczego. Technologie te pomagają dziś firmom i organizacjom podejmować decyzje na podstawie danych. Ta zmiana jest również widoczna w przemyśle górniczym, gdzie główny nacisk jest kładziony na zwiększenie możliwości monitoringu procesów technologicznych i odpowiednie wnioskowanie na podstawie otrzymanych danych pomiarowych.

Aby sprostać wymaganiom stawianym przez branżę górniczą, w niniejszej pracy przedstawiono opracowane metody analizy danych z systemów o architekturze internetu rzeczy i przetwarzania chmurowego na potrzeby monitorowania procesów technologicznych pozyskiwania rud miedzi. W pracy zawarto zagadnienia związane z m.in. prototypowaniem układów pomiarowych na potrzeby wykorzystania w środowisku górniczym oraz przetwarzaniu i analizie zebranych sygnałów w celu monitorowania stanu środowiska, maszyn i parametrów pracy wybranych fragmentów procesów technologicznych.

Zaproponowanie nowych metod pomiarowych, dostosowanie technologii robotycznych dla wymagań górnictwa podziemnego oraz analiza danych długoterminowych procesów związanych z wydobyciem rud miedzi m.in. z zastosowaniem przetwarzania chmurowego umożliwi nie tylko głębsze poznanie procesów, ale i również przyczyni się do zwiększenia bezpieczeństwa pracowników dołowych. Efekty przygotowywanej pracy doktorskiej pozwalają na opracowanie nowoczesnych metod akwizycji i przetwarzania danych z maszyn górniczych i środowiska w kopalni podziemnej wraz z uwzględnieniem ryzyk związanych z wdrażaniem nowych technologii informatycznych. Odpowiednia ich analiza umożliwia dalszy rozwój wiedzy w zakresie procesów technologicznych (np wiercenie, kotwienie, monitorowanie zagrożeń naturalnych) w kopalniach rud miedzi.

Słowa kluczowe: *Górnicze procesy technologiczne, Prototypowanie układów pomiarowych, Analiza danych, Przetwarzanie sygnałów, Monitorowanie stanu, Internet Rzeczy, Chmura obliczeniowa*

Abstract

The development of information technologies and its impact on a broad ranges of industry becomes a basis method for further growth nowadays. Some of them, such as Internet of Things and benefits coming from using Cloud Computing can enormously enrich also modern mining activities. These technologies help companies and organizations to make a data-driven decisions. This change is also evident in the mining industry, where the focus is on increasing process monitoring capabilities and making appropriate inferences based on the obtained measurement data.

In order to comply with the requirements of the mining industry, this work presents methods for analysing data from systems with an Internet of Things architecture and Cloud Computing for the purpose of monitoring technological processes of copper ore extraction. The thesis includes issues related to, among other things, the prototyping of measurement systems for use in the mining environment, as well as the processing and analysis of the collected signals to monitor the state of the environment, machinery and operating parameters of selected fragments of technological processes.

The proposal of new measurement methods, the adaptation of robotic technologies for the requirements of underground mining and the analysis of long-term data of processes related to the mining and copper ores extraction, among others, using Cloud Computing will not only enable a deeper understanding of the processes, but will also contribute to increasing the safety of underground workers. The results of the doctoral thesis allow for the development of modern methods for the acquisition and data processing from mining machinery and the underground mine environment including the risk analysis related to the implementation of new technologies. Appropriate analysis of these make it able to allow the development of specialized knowledge of some technological processes (e.g. drilling, bolting, monitoring of environmental hazards) in copper ore mines.

Keywords: *Mining technological processes, Measurement systems prototyping, Data analysis, Signal processing, Condition monitoring, Internet of Things, Cloud Computing*

List of Publications

1. **Bartłomiej Ziętek**, Paweł Śliwiński, Jarosław Szrek, and Radosław Zimroz. Laser-based measurement system for drilling and bolting operations monitoring in deep underground copper ore mine. *Measurement, 253:117425, 2025*

2. Paweł Trybała, Jarosław Szrek, Błażej Dębogórski, **Bartłomiej Ziętek**, Jan Blachowski, Jacek Wodecki, and Radosław Zimroz. Analysis of lidar actuator system influence on the quality of dense 3D point cloud obtained with SLAM. *Sensors, 23(2):721, 2023*

3. Hamid Shiri, Jacek Wodecki, **Bartłomiej Ziętek**, and Radosław Zimroz. Inspection robotic UGV platform and the procedure for an acoustic signal-based fault detection in belt conveyor idler. *Energies, 14(22), 2021*

4. Jarosław Szrek, Paweł Trybała, Mateusz Góralczyk, Anna Michalak, **Bartłomiej Ziętek**, and Radosław Zimroz. Accuracy evaluation of selected mobile inspection robot localization techniques in a GNSS-denied environment. *Sensors, 21(1):141, 2020*

5. Agnieszka A Tubis, Sylwia Werbińska-Wojciechowska, Mateusz Góralczyk, Adam Wróblewski, and **Bartłomiej Ziętek**. Cyber-attacks risk analysis method for different levels of automation of mining processes in mines based on fuzzy theory use. *Sensors, 20(24):7210, 2020*

6. Jacek Wodecki, Mateusz Góralczyk, Pavlo Krot, **Bartłomiej Ziętek**, Jaroslaw Szrek, Magdalena Worsa-Kozak, Radoslaw Zimroz, Paweł Śliwiński, and Andrzej Czajkowski. Process monitoring in heavy duty drilling rigs—data acquisition system and cycle identification algorithms. *Energies, 13(24):6748, 2020*

7. **Bartłomiej Ziętek**, Aleksandra Banasiewicz, Radosław Zimroz, Jarosław Szrek, and Sebastian Gola. A portable environmental data-monitoring system for air hazard evaluation in deep underground mines. *Energies, 13(23), 2020*

List of Conference Papers

8. Adam Wróblewski, Paulina Kujawa, Jacek Wodecki, and **Bartłomiej Ziętek**. Design of structured meshes of mining excavations based on variability trends of real point clouds from laser scanning for numerical airflow modeling. *IOP Conference Series: Earth and Environmental Science, volume 1295, 2024*

9. **B. Ziętek**, P. Krot, and P. Borkowski. An overview of torque meters and new devices development for condition monitoring of mining machines. *IOP Conference Series: Earth and Environmental Science, volume 684, 2021*

10. **Bartłomiej Ziętek**, Jacek Wodecki, Anna Michalak, and Pawel Śliwiński. Drill bit state-oriented drilling process classification with time-series data for wheeled drilling rigs. *IOP Conference Series: Earth and Environmental Science, volume 942, 2021*

11. O. Sukhanova, O. Larin, and **B. Ziętek**. Dynamics of glass windows in mining vehicles under the impacts of rock pieces: Numerical and analytical comparison for computational models validation. *IOP Conference Series: Earth and Environmental Science, volume 942, 2021*

Contents

1 Introduction

Monitoring of technological processes is the key part of ensuring continuity of mining operations. Current significant developments in measurement technologies, signal acquisition capabilities and process exploration provide the basis for many new initiatives involving an in-depth understanding of copper ore mining processes. The key challenges of today's raw materials industry involve identyfying, optimising process efficiency and improving the safety of underground workers. Nevertheless, the technological processes of ore extraction are complex, as the work of many different machines, systems and miners in many separate tasks, must be combined in order to extract the ore as profitably as possible.

In Fig. 1 it is presented how many technological operations are incorporated into the copper ore extraction process. The room-and-pillar mining system is used at copper mines in Poland, thus the preparation of the work front starts through the drilling of the blast holes. By inserting explosive charges into the holes and detonating explosives, the ore is ready for transportation by loaders and trucks. Subsequently, as the process continues, the mining front progresses, the bolting rigs arrive to secure the roof by installing rock bolts. The steps mentioned above are repeated at multiple locations in the mine to produce a continuous stream of new ore. Further transport of the excavated material takes place using conveyor belt systems from a screen, where the largest rock fragments are crushed into smaller pieces. With the usage of hoisting skips, vertical transport is performed to transfer the ore to the surface. The final part is to use the belt conveyors once again and transport the excavated material to the ore enrichment plant, where further processes take place to transform copper ore into the copper ore concentrates.

From the operational perspective, the monitoring of drilling cycles is a key procedure for obtaining valuable information on the efficiency of mining processes and the correctness of work execution in underground mines using blasting technologies. Therefore, there is a need for a data acquisition system that can be used on a variety of machines. In addition, the system is going to allow the automation of data analysis procedures. This will enable useful information to be collected and used by other decision support systems to optimise machine operation and determine the quality parameters of the drilling process.

All leading manufacturers of mobile drilling machines have made significant advances in monitoring systems over the past three decades to improve process control and quality [2]. Nevertheless, on-board monitoring systems used for this purpose are only installed on a limited number of machines. In Fig. 2 the population of machines with implemented monitoring system

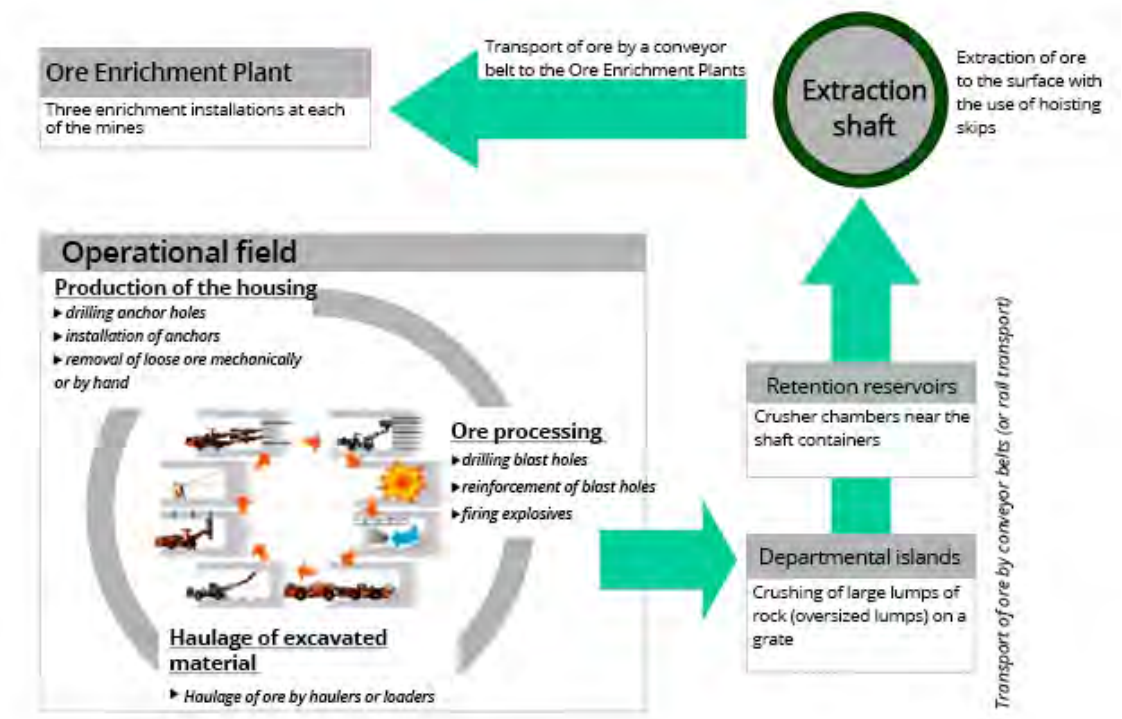

Figure 1: Technological operations in the copper ore extraction process [1]

is presented. The yellow bars correspond to the overall balance of machines with system applied whereas green and blue bars represent new and withdrawn machines per year. Such systems are mainly based on measurements of oil flow in hydraulic systems with complex design to estimate the pressure. Moreover, the construction can vary significantly from machine to machine. The analysis of data from such systems is characterized by a high level of complexity and subject to frequent failures. As with any indirect measurement method, additional measurement uncertainties arise, related to, among other things, variable temperature in the excavation area.

The next area of interest is to use data from the process of drilling holes for rock bolts. In the mining sector, measuring devices that are mechanically or hydraulically coupled to the mining machine are mainly used for the precise measurement of the feed of the drilling tool [4]. This implies limitations, mainly in terms of the value of the sampling frequency by the aforementioned equipment. The use of other measuring devices, including those based on laser techniques, allows for more efficient recording and accurate analysis of the variability of kinematic parameters.

In this work, methods for analysing data from systems with Internet of Things (IoT) and Cloud Computing (CC) architecture for monitoring technological processes of copper ore extraction are described. The issues related to the presented topic are based on, among others, prototyping of

Figure 2: Population of machines with SYNAPSA monitoring in the mining divisions of KGHM [3]

measurement systems for the use in the mining environment and the analysis and processing of the collected signals to monitor the state of the environment, machinery and operating parameters of selected fragments of technological processes. The dissertation focuses on the development of data acquisition systems on selected machines and their analysis in the context of identifying duty cycles.

The next stage is to develop a concept for integrating the measurement systems placed on the platform of the wheeled inspection robot to study environmental conditions. An important part of this stage is the implementation of a Light Detection and Ranging (LiDAR) control system to build a precise map of the excavations and unification with the robot's operating system. Further applications are conveyor belt damage detection or roof state assessments of underground excavations.

The final stage of work within the framework of the dissertation consists in enabling routine procedures, carried out in the mine, related to the monitoring of environmental parameters (hazardous gas measurements) as well as the implementation of mechatronic systems for 3D modeling of underground mine workings. By proposing the use of IoT technology and further data processing in a distributed architecture (acquisition and preprocessing on edge devices) a set of prerequisites has been gathered to enable further analysis in a cloud environment [5, 6].

Proposing new measurement methods, adapting robotic technologies for the requirements of underground mining and analysing long-term data of copper ore mining processes, among others, using Cloud Computing will not only enable a deeper understanding of the processes, but will also contribute to increasing the safety of underground workers.

The results of this work will allow the development of modern methods for the acquisition and processing of data from mining machinery and the environment in the underground mine. Appropriate analysis of this data will provide the development of specialized knowledge of, among other things, technological processes (e.g. drilling, bolting, monitoring of natural hazards) in copper ore mines. Moreover, monitoring of the extensive underground infrastructure can be more achievable thanks to laser scanning data in order to create digital twin of mine. Owing that, the miner localication (rescue operations) and gas hazard monitoring can be possible thanks to creation of spatial map of the mine.

2 Problem formulation

As a result of enormous development of information technology, measurement systems, large-scale data processing capabilities, and widespread access to large computing capacities, it becomes clear to find parts of mining activity that can be digitally transformed to take advantage of new available possibilities in this area. Nevertheless, the mining activities, as many of engineering procedures, have significant level of difficulty. This creates problems for the adoption of such solutions, which are very important for the further development of the mining industry and the increase of labour productivity.

In order to rise this challenge, based on previous research, literature studies and close cooperation with industry, several technological processes have been identified. Selected mining processes include drilling for blasting and securing corridor excavations using bolting bolt rods. Moreover, some of routine procedures such as monitoring of environmental parameters in mine workings or transportation system inspection with robot platform are selected. The representation of technical processes above is initially defined as the potential of an approach using IoT technology.

Following the diagram from the Fig. 3, there is a need for the objective knowledge creation about the technological processes in mines. To achieve this, the new measurements methods applied to selected mining machines and devices, backed by the original data-processing techniques are proposed.

Due to the size of the mine, the variety of mining technologies and machines used, the number of underground workers, the quality of the big data generated and the nature of its variability, there is a necessity to create one common scheme to deploy many new measurement sources into existing processes.

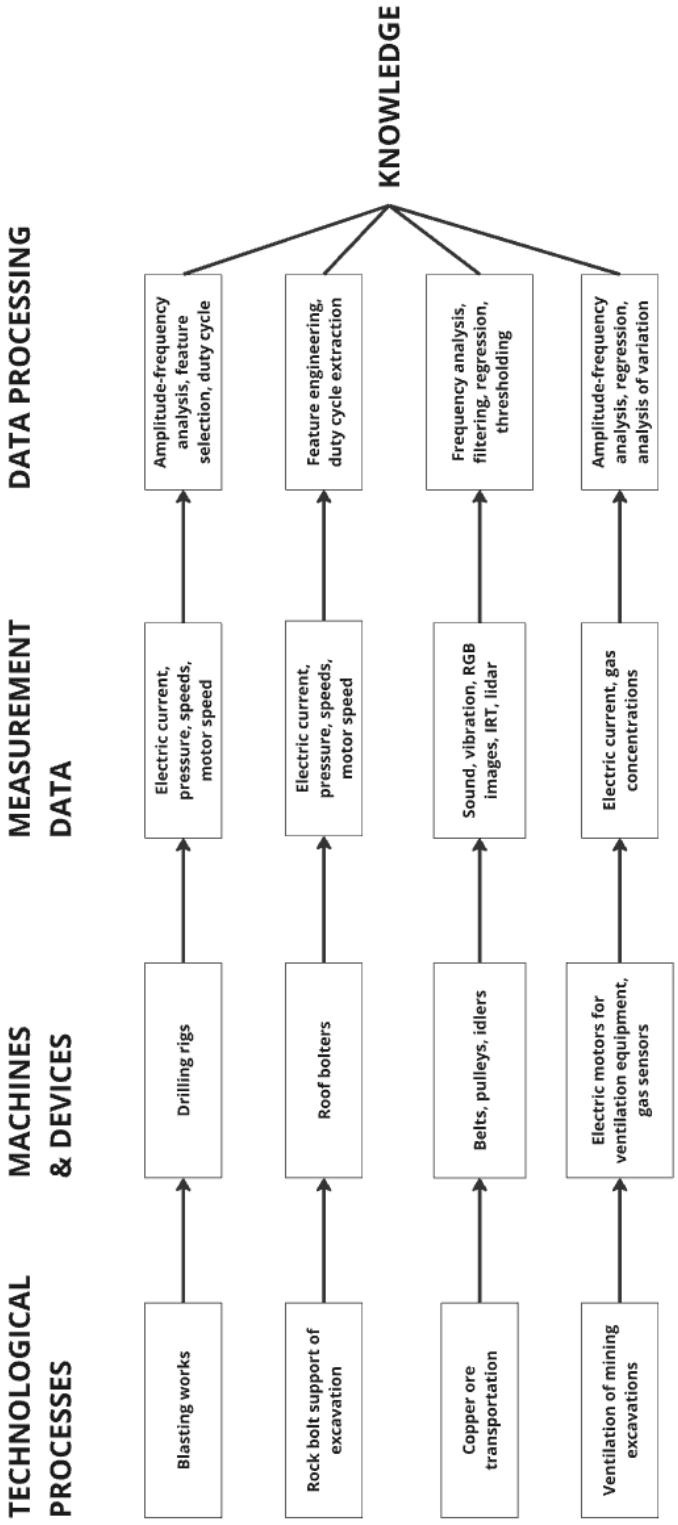

Figure 3: Data flow for mining technological procesess

2.1 The aim of the dissertation

Taking into account the state of the art knowledge, domain expertise within mining industry and author experience, the following research hypothesis are presented:

- Through the usage of advanced measurement systems and data transmission (based on the Internet of Things) and advanced data processing and analysis (based on Cloud Computing technology) it is possible to develop a system of decision support to optimise the operation of the mining machines work and improve the safety of miners.
- In order to predefine the potential of an approach using IoT technology in mining industry, several technological processes and routine procedures carried out in the underground mine have been identified.
- Taking into the consideration the fact of the underground mine size, mining technology used, number of utilized machines, number of underground miners, the quality of the data and the nature of its variability it is viable to use the novel, scale-effective analytical procedures.
- The hybrid cloud data architecture can help to overcome the limitations of mining environment, considering the need of reliable data workflows, and efficient utilization of aggregated big data scopes.

To confirm the above, the adoption of cloud system architecture is proposed. With usage of the latest analytical technologies within one common architecture it is possible to manage key parts of the software delivery for a distributed data processing system both at the edge and in a centralised manner using Cloud Resources (CR). That approach highlights the requirements from the specific analytical procedures proposed in this work based on the deep understanding of the process, analysis of data properties and appropriate selection of analytical techniques.

Usage of IoT technology for measurement systems development are a key part for obtaining all of data sources above. Based on the original methods for data processing it is possible to convert these new data sources into knowledge. It creates the fundamental layers for modern Big Data processing architecture in a repetitive, prone-to-error and cost efficient manner thanks to Cloud Computing technologies advantages.

3 State of the art

In this section, the state of the art is presented in areas related to the data acquisition from mining machines and mining processes interpretation. Many research articles on the process of digital transformation in the mining industry have been enumerated. The main emphasis is on the use of IoT devices for mining use cases. Moreover, the integration of measurement devices with cloud services has been shown. Their impact on data-driven management systems in mining to perform end-to-end analytics based on machine learning algorithms reasoning is also discussed. Finally, important research topics and cybersecurity trends in industrial systems show how they impacted mining activities enhanced by digital transformation.

3.1 Monitoring of mining machines and processes

The start of the copper ore mining processes is initialised by the work of the drilling machines. Hence, the development of research work in the context of drilling equipment operation is desirable from both a mining industry and research perspective. Measurement While Drilling (MWD) method provides many information about the actual parameters of the drilled rock mass and the process. Owing that, numerous studies has been examined to determine drilling performance and monitor the state of the machine based on many sensor units. The general overview of MWD in many mining use cases is presented in [7]. Based on pressure data from drill machine subsystems it is possible to determine rock samples strenghts [8]. The void detection method based on feed and rotation pressure of bolting rig is examined in laboratory conditions [9], but describes the possible application of pattern recognitions algorithms, which can be used for real mining condition applications [10]. Another approaches of unifying the drilling parameters with terrestrial digital photogrammetry images to describe the rock mass are also known in the literature [11]. In [4], another approach with usage of cord encoder is presented in order to detect discontinuities during drilling with bolting rig machine.

Drilling cycles identification for mining machines is one of the most important tasks from the point of view of the organization of work and management of these machines. The software architecture for condition monitoring for mining machinery [12] is an important step in developing solutions that enable the correct data acquisition to fulfill that expectations. Effectiveness of the drilling process for drilling rigs based on drill parameters such as: drill preccusion, rotation, and tool feed system pressures from monitoring system helps to assess, identify and segment machine work [13]. Based on long-term data analysis of the drilling process it is possible to

detect the work cycles for wheeled drilling machines [14]. Nevertheless, real data analysis is problematic, and it is needed to develop increasingly innovative methods to enhance noisy data into more informative [15]. There is a number of parameters that affect the variability of drilling processes. The previously mentioned influence of local variations in rock lithology is not the only factor. It is also worth paying attention to machine wear, particularly on drilling tools. Especially for drilling rigs, the impact of tool wear on the efficiency of the drilling process is considerable. The assessments covering the drill bit deterioration based on machine learning algorithms are presented in [16, 17]. A new analytical approaches to determine the blasting process parameters to obtain a favourable blast outcomes are revealed in [18]. In meanwhile, it is important to properly manage the mining machines work in order to mitigate the impact of downtimes [19]. Working at the mining face is difficult and demanding for the machines and their operators, hence adequate supervision of the work is required. For drilling rig machine case, some important from management perspective effectiveness metrics (such as availability, utilization rate) can be determined based on the long-term data analysis [20]. Data integration from different sources of drilling and blasting processes and usage of geospatial queries can be found in [21]. Operational data consolidated in a mine's data warehouse enables tracking the performance of drilling operations even at the single blast hole granularity level.

Another significant research problem is the mining process automation. Nowadays, the increasing integration of different types of sensors together with dedicated algorithms enables the automation of more and more mining processes. In [22], the autonomous system for Load Haul Dump Machines (LHD) loading work is presented. With usage of several laser scanners, encoders, and pressure sensors it is automated the loading routine handled by Robot Operating System (ROS). However, to enable the automated work it is necessary to resolve the problem of localization determination in underground mines. Due to existence of GNSS-denied conditions, another methods of localization techniques are needed [23]. Based on inertial measurements [24], stereo camera [25] or laser scanners data analysis [26] taken from underground conditions, it is possible to overcome that problem. Nevertheless, mining activities are complex and before any enhancements in machine autonomous work will be considered, the proper risk management due to safety and operational issues should be concerned [27, 28].

The use of machine-mounted sensors and data transfer is undoubtedly an effective method of acquiring data during the operation of machinery and equipment in mining. Nevertheless, some machines are powered by underground electrical networks, making it possible to use electrical current measurements to identify the operation of equipment. In [29], it is presented the electrical

load identification method using non-invasive measurements based on Sweep Frequency Analysis Response (SFRA). An alternative method for power consumption usage for household appliances based on current signal measurements and waveforms classification is discussed in [30]. Fault detection and localization of electromechanical devices such as three-phase inverters based on current measurement is also possible [31]. The detailed analysis of computional demand for application of low-cost IoT modules to identify various devices connected to the network grid is revealed in [32]. Based on alternate current measurements and further transformation to characterize parameters such as resistive, inductive, and capactive loads, the device classification is possible using machine learning approaches. Finally, the IoT systems with cloud analytics integration services performing the time and frequency analysis over current consumption are able to identify the devices work [33].

A separate aspect of measurement in underground mining is related to air hazard evaluation. Gas concentration measurements are the key part of ensuring the safety of underground miners. The main emphasis is put on assessing the concentration of hydrogen sulfide (H_2S) and carbon monoxide (CO) as well NOx gases. The origin of these gases is determined both by natural sources (H_2S) and by mining activities caused by wheeled machines work or blasting procedures (CO, NOx), to name a few [34–36]. Hence, it is important to analyse the long-term trends and gas concentration variability to understand the underground mine air environment better. In [37], it is determined the amount of time after the blasting procedure when CO concentration level is below the maximum values. Another significant analysis is put on correlation research aiming to bond together the ventilation schedule with H_2S concentration patterns in mine excavation [38]. The examples presented above indicate how important gas measurement data acquisition in the mining industry is nowadays to perform mining activities based on a detailed analysis of the environment.

The next important type of infrastructure in the process of ensuring the continuity of mining activities are the belt conveyors systems. Their continuous inspection is the key part from the maintenance point of view. The efficiency of the haulage process can be maximized thanks to the scheduled maintenance in order to repair or replace worn out machine elements. Components deterioration is usually determined via visual inspections. Nevertheless, the demand for automation of this process is growing. In the literature there are widely known approaches using vibration [39–43], and acoustic [44–46] signals. There are many additional measurements systems enabling the analysis of the belt condition with usage of magnetic sensors [47, 48]. In parallel, the possibilities of image acquisition from cameras and data processing algorithms are also under constant development. With usage of machine learning-based image processing, there

are attempts to perform fault diagnosis of rotating elements [49]. An automated data acquisition becomes increasingly popular in the mining industry as well. Examples of use cases for inspection robot utilization in the mining diagnostics mission are described in [50]. In [51, 52] data is acquired by inspection robots to detect the thermal defects of idlers. To enhance the proper scheduling of the maintenance operations, the historical data can be utilised to enable predictive modelling of conveyor belt deterioration. Based on the different operating conditions and specific variables describing the belt parameters it is feasible to predict the characteristics associated with the wear of a conveyor belt with usage of neural networks [53].

3.2 Digital transformation

Using a digital technologies in order to improve the overall organization business model is the key part of digital transformation [54]. In the mining industry, replacement of analog devices with digital ones, utilization of adapted methods and systems to generate and use digitised data, are the most impactful actions to transform mining practices. In [55] the text-mining technique is revealed to identify the key digital technologies and their adoption levels for the mining industry. The outcomes of the analysis above reveal methods related to general process automation and the usage of robotics and IoT in order to obtain real-time data (and big data) from mining activities. The results demonstrate machine learning and artificial intelligence usage along with 3D printing as the leading technologies. Nevertheless, every technology adaptation relies on many factors. For smaller mining organizations, it can be faster and uncomplicated to fulfill the tailored needs. However, digital transformation in case of larger companies can be more complex and, the economy of scale will determine the adaptation of new solutions.

Enabling smart monitoring with usage of the above technologies focuses primarily on the development of current technical solutions used in the industry. Widely used systems like Supervisory Control and Data Acquisition (SCADA) or Distributed Control System (DCS) are often upgraded with new features corresponding to the techniques above. Nevertheless, benefits as well as disadvantages need to be analysed for every use case [56].

In words above, the impact of digital transformation is depicted mainly on technical solutions. However, as a part of the next phase of industrial revolution, impacts on the society, organization, and competences development as well as change for work environment might affect the mining organizations altogether [57]. Especially for mining industry, thanks to the enhancements coming from the advantages of digital transformation adaptation, numerous problems related to

occupational health and safety problems can be solved and make the mine environment work more sustainable. Due to that, it will take significant effort to reform mining production into data-driven decision management approach in the future to enable the long-term competitiveness [58]. This will require an integration of many areas of the organization. To achieve this, it will be necessary, among other things, to use services that enable data management in a cloud environment. Accelerating the adoption of new technologies would require prototyping the small scope of the system, with usage of digital twins to create a digital object fully covering the features and characteristics of the real objects [59]. Due to the nature of the mining environment, extensive underground areas, processing and inference with machine learning algorithms will have to be done to some extent on edge. To achieve this, a well-prepared automation framework is necessary to automate many orchestration tasks for the distributed computing system [60].

3.3 Internet of Things in mining

Internet of Things (IoT) is a term, describing the ability of the physical devices enhanced by digital sensors, communication interfaces, computational elements and actuators, which have an ability to communicate with each other to achieve specific goals [61]. There are many existing technologies considering the communication protocols, middleware, and service components to address specific goals of application areas in i.e. environment research, transportation and logistics, healthcare, personal and social [62].

Many use cases with IoT successful implementations in underground mines can be found in the literature. Starting from the comprehensive review of IoT systems in mining industry, there are presented the most popular applications emerging at the usage for mining operations prediction, increase of mining safety, and surveillance systems [63]. With usage of IoT devices and dedicated data processing algorithms tied with expert knowledge about the mining operations, it is viable to optimize the work of self-propelled machines. In [64], based on inertial sensors measurements a method is revealed in order to detect dynamic overloads, which significantly impact machine deterioration. In [65], an approach with usage of MQTT protocol to predict the machine state incorporated to the IoT device with vibration sensors is presented. Not only machine state can be entrenched by IoT set of devices. It is also possible to determine the structural stability of mine. Condition monitoring of the mine's corridors roof utilizing a Fiber Bragg Grating sensors is presented in [66]. That IoT management platform for structural monitoring is hosted on web server for data integration, visualization, and damage detection analysis.

Another important area of IoT systems usage in mining are safety systems. Sensors types, and communication technologies used in safety monitoring systems for underground mines are revealed in [67]. In [68], the usage of Bluetooth Low Energy (BLE) technology for real-time localization of the mine workers is published. A case study of early-warning system for underground coal mine is described in [69]. The platform consists of devices installed in many locations with several sensors for environment parameter measurement with microcontroller connected via BLE protocol, and smartphone nodes. For visualization, alerting, and event identification based on K-means clustering algorithm, a webserver hosts the processing software. As a development of the system above, the authors expand system features in [70]. Air quality monitoring system is enhanced by machine learning pipelines based on cloud services in order to forecast the air quality in the mining environment. Another example of IoT devices usage for ensuring the occupational safety and health of miners in underground conditions can be found in [71]. Based on data retrieved from wearable terminals (electronical bracelet and a miner lamp), a real-time monitoring system is created. It enables the miner's health state based on vital signs collection. Afterwards, the use of the neural network helps estimate the fatigue level and generate early warnings by the system administrator.

Digital transformation cannot be successfully adopted by industry without the development in some key areas. In [72], it is presented a redundant data transmission from source devices within Condition Monitoring Systems (CMS). The next phase is measurement data validation with usage of many statistical metrics describing the desired dataset to limit i.e. data inconcistency [73]. Implementation of error-prone real signal parameters calculation is not a trival problem and should be handled likewise [74].

3.4 Introduction to Big Data and Cloud Computing

Big Data term refers to the definition of a dataset of significant size which is characterized by 5V's: volume, velocity, variety, veracity and value [75]. The volume deals with the physical quantity of the disk storage needed to save the given dataset. The velocity concerns how data flows should be quickly stored or processed. The variety relates to multitude of data formats, veracity covers dataset completeness aspects, and value is about the possible financial impact determined by the decisions taken using the dataset. The mentioned aspects reveals the situation where the computational capacity of a single computer is not enough to perform data processing and analysis efficiently.

Instead of providing the organization's data centers to process the Big Data, it is often necessary to use appropriate resources via the Cloud Computing model [76]. The first occurence of Cloud Computing term came in the 1960s as supplying the computing capabilities to the general public as an utility [77]. From the business model perspective, cloud services models refers to three types: private (on-premises), hybrid, and public cloud [78]. The shift from full responsibility for all aspects of the data center to a shared responsibility model with the cloud services providers creates a wide range of possible solutions [79]. Another division of Cloud Computing resources based on the services delivery type are :

- on-premises resources
- IaaS (Infrastructure as a Service)
- PaaS (Infrastructure as a Service)
- SaaS (Infrastructure as a Service).

Depending on diverse layers of managed resources, covering the hardware or platform layer (runtime) for the applications, the different layer of Cloud Resources architecture can be provided for the final user. That variety of Cloud Resources delivery impacts on the shape how data are processed enhanced by Cloud Computing services. From the Data Warehouse approach, widely used in on-premises facilities [80], to Data Lake concepts with variety of data types handled [81].

Cloud Computing applications are well-known in the mining industry. In [82], a system built with Cloud Computing services is used to monitor the tailings dam in the mines. A novel approach utilizing the virtual reality technology to improve inspection tasks with a cyber-physical system is revealed in [83]. Conceptualization of the future architectures for mining industry is a key part of the paving the way for real use cases. The use of a digital twin approach for mining processes is one of the most suitable examples for cloud services. Hence, the integration of services in the sustainable mining industry can be found in [84]. There are also attempts at experimental application of these for mining machinery [85]. Several mining applications utilize cloud services for visualization and dashboarding purposes to increase safety resilience in the mining industry [86]. Finally, architectures with edge computing patterns are described in [87, 88]. Another use case for cloud services utilization is the integration with miners' equipment such as wearable helmet and additional sensors. In that procedure, wearables represent the data source and based on cloud platform, it is possible to detect human emotions [89].

3.5 Data-driven management systems in mining

The growing development of the computerization of enterprises also includes activities in mining organizations. Computer-aided systems are already widely used to enhance the analysis of mining processes, such as: ventilation of mining excavations [90], orebody modeling [91] or mobile underground machines maintenance [92] to name a few. Nevertheless, creating a system with measuring devices in a mining environment and supervising their work requires an appropriate approach. Setting up an IT system to manage distributed metering equipment, computing modules, and the infrastructure associated with maintaining continuous delivery and deployment operation services, software integration, and data is undoubtedly a major challenge. The volume of data generated by IoT devices is increasing in relation to these technologies and is quite widespread. Services utilization in private or public cloud model can support that process of the management platform creation. Owing that, it is needed to apply best practices in software development workflows in order to deliver software in reliable, repetetive and robust way [93]. As an example provided in [94] for the delivery and processing capabilities of IoT software, several of them are revealed. There are automated Continuous Integration and Continuous Deployment (CICD) pipelines, managed by Infrastructure as Code (IaC) methodology, code linting and static code checks features. Another important parts are containerization of the software application and monitoring abilities of the system. With that common approach, a system maintenance is significantly simpler and with good quality what is essential for IoT systems being mature and scalable.

Considering the utilization of the complex algorithms for reasoning based on the measured data at the edge is necessary, especially for the extended area of mining, hence some enhancements covering the needs of software management for machine learning experiments are enforced. It is where the concept of Machine Learning Operations (MLOps) emerges. Following the literature research and the results of specialist interviews, MLOps is defined as a paradigm of a set of concepts, best practices and development culture aiming to the end-to-end management of machine learning products from conceptualization, through implementation and scalable deployment with monitoring in mind [95]. It extends the principles of the standards from the software development and operations activities in the area of machine learning. There are related to the machine learning workflow orchestration and its ability to reproduce the same results in a given ML experiment. Moreover, worth to mention is the principle of continuous training and evaluation of the models. Based on the use case, it can be performed with ad-hoc, periodic or event-driven (i.e. when a given statistical thresholds of the model metrics is reached) manner. The system observability should be

extended for ML experiment tracking, as well as the model inference monitoring. In the literature, several approaches with usage of open source libraries aiming to provide technical components of MLOps can be found [96–100].

3.6 Cybersecurity in industrial systems

Although there is no single definition of risk [101], the most often term used is taken from PN-ISO 31000 standard [102]. A risk is defined as the effect of uncertainty on objectives. Following [103], the risk assessment is the overall process of risk identification, analysis and evaluation. Hence, cybersecurity, as a part of the organization risk assessment analysis, covers the IT/OT landscape. A literature review of the threat analysis for software systems is presented in [104]. Based on 26 threat analysis approaches covered, the outcome revealed are the lack of quality assurance of outcomes (in the given risk assessment methods), and absence of definition of done when analysis procedures can be stopped. It means that for every architecture used, the separate risk assessment methods should be matched to fulfill all the scenario needs.

The analysis of IT systems should be embedded in the realities of the environment in which it performs its tasks. Following the report [105], the risks related to cyber and digital area of mining activities fell out from top 10 risks for this industry. That change comes from the fact, that the mining organizations intensify their efforts to manage that area and treat it as a business as usual. In 4 years, a significant change in the cybersecurity transformation of mining digitalization has appeared [106]. Nevertheless, the cyber risks has not been disappeared and constantly should be taken into account. The literature has many examples of exploited vulnerabilities dedicated to compomise the existing hardware, software and network layers, commonly used in mining industries [107]. Cybersecurity risk assessment for systems widely used in automation and control systems are analysed in [108]. The constant increase of devices connected to the internet create a need for development of cybersecurity, especially for IoT devices. In [109], a broad survey of techniques enhanced by machine leraning for cybersecurity is presented. Intrusion Detection Systems (IDS) for IoT devices network are revealed in [110]. The several neural networks models are compared to obtain the highest detection scores. The machine learning dataset consists of the many attack records aiming to perform the malicious actions divided into 4 main categories: probe (scan for devices information), DoS (denial of service), U2R (user to root - privileges escalation), and R2L (remote to local - remote access to the compromised device).

The next area of the effort to cover cybersecurity in industrial systems is the integration with cloud services. The cybersecurity posture is heavily embedded within the cloud services utilization. In the scope of the shared responsibility model, the researchers occasionally perform a broaden checks of automated security assessment on selected services supplied by cloud providers. Thanks to that, some open-source tools has been provided for developers to increase the security posture based on configuration evaluation [111]. Another approach to seek out security flaws is to automatically generate attack graphs to perform virtual penetration testing [112]. Especially for architectures with usage of IoT and Cloud Resources it is important to apply cybersecurity and data protection good practise by design [113]. Based on technologies used, some additional techniques can be used to estimate the risk related to IoT firmware version vulnerability analysis [114] or exploit detection in container environments [115].

4 Objects and processes

This section describes all objects and processes that were taken into the author's scope of interest during his research. Object and processes have been selected based on discussion with mining engineers and the importance for mining operations. The examined objects are directly connected with the mining processes in the underground mine. The chosen machines (drilling rigs, bolting rigs), technological processes (ore transportation, rock drilling/bolting), and underground environments (with presence of hazardous gases) are key research areas in mining industry. Each of the subsections include a brief description of the object or the process with experiment details. These research objects introduce the need for the usage of measuring devices for the underground mining, organized as Internet of Things system. Furthermore, to facilitate the usage of above-mentioned IoT devices in those use cases, the cybersecurity resilience approach is also described.

4.1 Drilling rigs

Drilling rig is the common machine used for the preparation of the blasting process in mining facilities. It is the first machine in the technological cycle in mining industry with deposits exploitation based on blasting technology. Hence, the drilling rig performance is crucial in the overall process efficiency in a given mining area.

The drilling rig at the mining face is presented in Fig. 4. As it can be seen, the low profile of the machine is adapted to the corridor shapes existing in room-and-pillar operations. This self-propelled drilling machine comprises key components like operator's cabin, electric cabinet, electric cable reels (for drilling unit), diesel engine (or eletric motor for battery driven drilling rigs), hydraulic system, boom(s), leveling jacks, arm and drill. Alongside drill carriages, some machines also include a miner's platform. Nowadays, this type of the machine is fully adaptable to the specific mining conditions, offering a range of sizes from large models for extensive excavations and tunnel construction to small, compact versions suitable for confined spaces.

This underground drilling vehicle, on arrival at the mining face, connects to the mine's electrical network, since hydraulic pump of drilling rig is powered by electric power. Using an external power supply, machine sets up hydraulic systems, and starts working with rotary-percussive rock drill to create the planned blasting pattern. Depending on the dimensions or underground tunnel type, a single machine possesses one or two booms where the drill feed mechanism is located. The created hole are 3 to 8 meters long (thanks to the extension options of the drill rod) and it is used

Figure 4: Drilling rig at a mining face [116]

for the placement of explosive charge for the blasting procedure for excavating hard rocks. Table 1 shows several parameters of drilling machine.

Nowadays, underground mining machines are equipped with electronic drilling assistance systems [117]. The main characteristic is the recording and visualization of specific parameters of the machine work as well as correct functioning of individual components. In the presented model, Face Master 1.7, the following systems are implemented:

- Basic Monitoring System (BMS) - checks and saves every 30 seconds the operating parameters of the internal combustion engine, drive train, hydraulic oil and supply voltage
- Drilling Monitoring System (DMS) - informs the machine operator about actual events and errors with drilling subsystems. They are divided into several statuses, such as active, non-active, confirmed, and unconfirmed by operator.

Parameter name	Description
Product model	FACE MASTER 1.7
Length	14.4 m
Width	2.4 m
Height	2.2 m
Weight	18500 kg
No. of booms	1
Max coverage [WxH]	9.5x6.3 m
Min. width of heading for tramming 90 °	4.5 m
Rockdrill	Rotary-percussive
Power source tramming /working	Diesel/Electric
Application	Hard rock/Non-flameproof

Table 1: Underground drill rigs specification [116]

These systems help to obtain most of information related to process and accelerate the root-cause analysis during repairing faults or maintenance work. This approach is widely used in the industry for machine park maintenance [118, 119]. Nevertheless, this work focuses on another physical quantity: the current consumption of the drilling machine that is intended to be used for monitoring the operating state. Owing that in next sections, the experiment plan (Section 5.1.1), measurement method (Section 5.2.1), and device description (Section 5.3.1) is presented. Thanks to the proposed data processing methods (Section 6.1), the obtained results (Section 7.1) are explained in more detail.

4.2 Bolting rigs

Bolting rigs (also known as mining bolters - see Fig. 5) play a major role in underground excavations made with room-and-pillar technology. Regarding mechanical parameters of the rock mass and shape of the corridor, several types of rock bolts such as resin, (cement) grouted or expansion bolts, and different technological process of mounting them are used [120]. Depending on the height of the mining bolter, the machine operator can be located in a cabin (for automatic masts) or in a secured cage to mount wire mesh that comes in rolls. In Fig. 6 mining bolter

parameters are presented. These machines have a compact design, because they appear in the mining activities immediately after taking the bulk material by LHD machines, and prepare corridors to be used by other machines and mining workers later. For this reason, some of the machine's design parameters, such as height, turning radius and boom swing angles, are tightly defined, but allow for the performance of excavation safety tasks.

Figure 5: Bolting rig machine [121]

There are many bolting techniques used in the mining industry, for securing the roof and rib for excavations. To make a proper decision regarding the technique to be used, several factors are considered such as geomechanical properites of the rock mass, existence of any local geological disturbances, the function of a given fragment of excavation, and finally the roof class and corridor dimensions. The roof class refers to the local rock stability index [123], what describes the interdependencies of rock strength, degree of fracturing, and stress distribution in the rock mass. Roof bolting is used in high excavations. For excavations with a width of up to 10 meters, the minimum length of the roof bolts is 1.6 meters, whereas for excavations exceeding 10 meters, the minimum length is 2.6 meters. Fig. 7 presents a typical cross-section of the ceiling secured with bolting housing widely used in room-and-pillar system for underground mines. Another important aspect of ensuring the bolting work is done properly is the evaluation of bolting effectiveness. There are several types of measurements performed [124] to estimate it at the time of installation such as:

- measurements of changes in bolt load up to the moment of entry into the workings
- measurements of the restraint (pull-out) of the bolt rocks

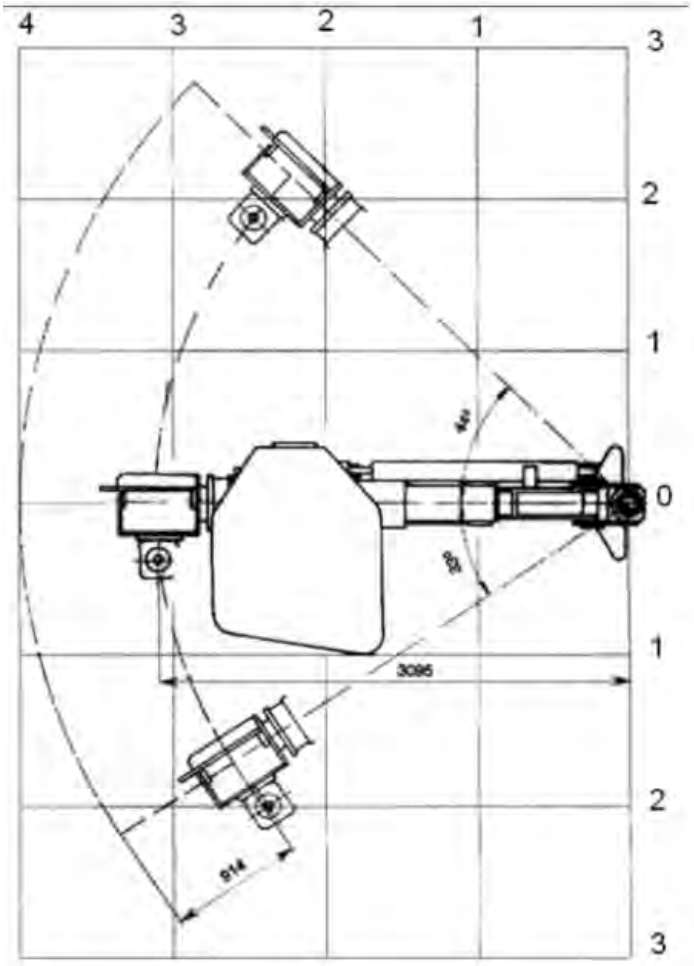

Bolting rig parameters	
Weight	18000 kg
Lenght	10500 mm
Width	2400 mm
Min. Height	1700 mm
Min. seam width	3850 mm
Turning radius	
Outer	6 m
Inner	3.6 m
Grade ability	15°
Cross-grade	8°
Boom extenstion	914 mm
Boom lift	+21/-5°
Boom swing	
left	33°
right	44°
Mast rotation	+/- 90°

Figure 6: Bolting rig machine parameters [122]

- tests of stratification of roof rock in the bolted zone (indirect measurements)

Nowadays, there are many other methods to access the rock bolt condition [125] covering the usage of ultrasonic [126–128], fiber optic [129], piezoelectric [130], and electromagnetic [131].

From an operational perspective, maintenance of the underground machinery fleet is crucial to obtain the valid number of holes created after each shift. Thus, the need for an automated procedure for the prepared holes to secure the ceiling with bolts is essential. Similarly to underground drill rigs, there are two systems for diagnostics and monitoring purposes for mining bolters, namely Basic Monitoring System (described in 4.1) and bolt counting system [117]. It consists of eight pressure sensors connected to input/output pressure modules, Human Machine Interface (HMI) and for communication uses a controller area network (CAN) protocol. The counting algorithm check the correct order of specific parts of the bolting process, and its duration. Only the cycles,

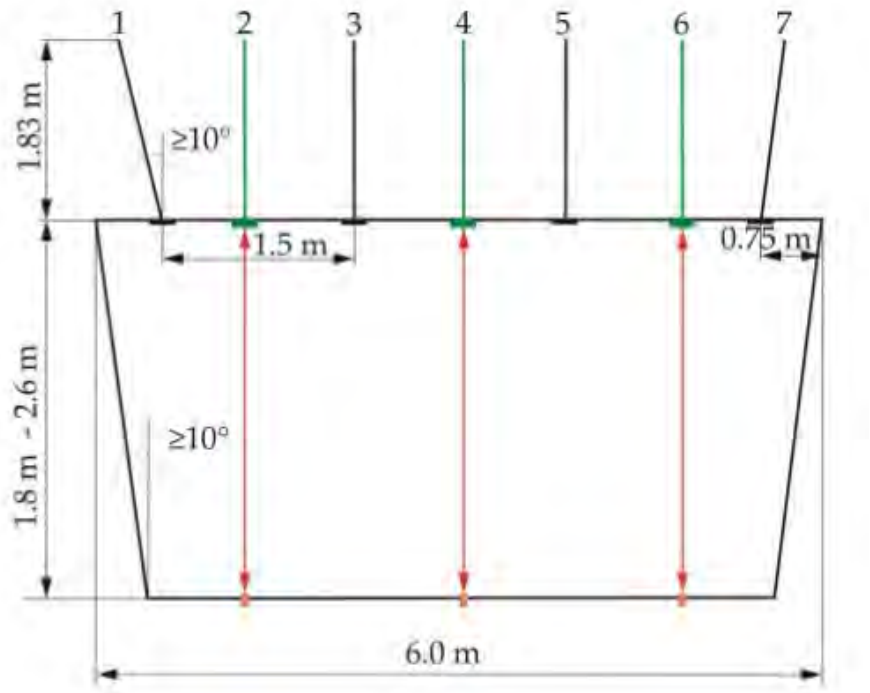

Figure 7: Cross-section of the ceiling secured with bolting housing [132]

which fullfill all bolting instructions, are counted as a correct bolt performed. These cycles are saved and assigned to machine's operator for every shift. In addition to this, the torque tightening of the rock bolt measurement is also saved. There are also applied additional security measures to prevent bypassing the algorithm. Nevertheless, the existing estimations, utilizing data from the machine's on-board monitoring unit (mainly pressure data from drill subsystems) are not accurate. This methodology is highly uncertain for the case of expansion rock bolts mountage in the rock mass. It is characterized by the presence of self-similar subcycles corresponding to the usage of several drill rod extensions and deepening of the hole to the desired depth. To cover this gap, in this thesis, a novel approach for counting the bolting cycles using laser-based measurement system data is presented. The novel approach aims to provide information about the number of installed bolts (number of drilling and bolting cycles) without knowledge related to pressure data. It is described in more detail in Section 5.3.2.

This information is critical for tunnel safety and forms a basis for calculating remuneration for work. Historically, such information has been provided directly by the machine operator (as a declaration). Then, the on-board monitoring system was introduced several years ago. It was based on the flow measurement in the hydraulic system installed in the bolting rig. However, the

system has appeared to be expensive and, due to harsh underground conditions, not reliable enough. This was the motivation for this research to develop an alternative solution, that is, an independent laser-based measuring device and data processing methodology.

The further description of the issue is provided in the following sections: experiment plan (Section 5.1.2), measurement methodology (Section 5.2.2) and device description (Section 5.3.2). It illustrates the general overview of the proposed approach. Following to the data processing methods (Section 6.2), it is possible to get insight into how bolting process behaves (Section 7.2).

4.3 Electric current measurement at a mining section

The power distribution system for underground mines is a complex structure. Today, most technological works in underground copper ore mines require a stable electric power supply to perform the work. The electrical departments execute technological work related to ensuring the supply of electricity for necessary location in the mining divisions [133]. All mining plants possess many electricity substations with additional facilities to enable it. The building of the 110/6kV transformer and distribution station has many 110/6kV transformers with electric network protection facilities to transform the network parameters related to voltage change. With the usage of cable channels, the electric grid is placed closer to the underground mining sections to the next 6/0.5kV electricity substation [134–136]. At that point, the medium voltage level (6kV) is transformed into a low voltage level for the direct usage of machines and appliances. In the polish mining industry, it is a three-phase network with isolated transformer neutral point [137]. The phase-to-phase voltage is 500 V. Electricity with the parameters above is distributed across the mining excavation area.

Following the description above, an important research area is the analysis of the possibility of decomposing the current signal in the electrical cabinet of the mining power supply unit. Signal decomposition refers to the process of division of a complicated signal into independent parts called modes [138]. In this case, from the measured total power consumption, it is viable to obtain parts of the signal related to electric power consumption divided into a specific group of receivers. To do that, current measurements can be taken at the output of the transformer to access the current consumption of all the devices working in the mining area. The scheme of underground transformer station is presented in Fig. 8. The three main groups of electrical receivers can be distinguished:

- wheeled mining machines (temporarily connected to a given mining area)
- air conditioning devices

- mine drainage devices.

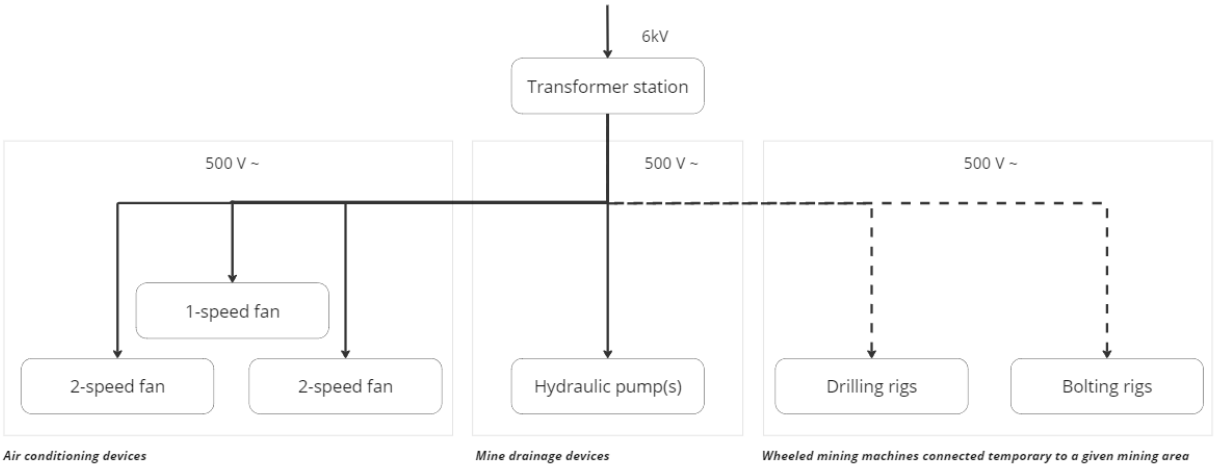

Figure 8: Underground transformer station electric scheme with possible receivers

Most self-propelled mining machines, mainly drilling and bolting rigs, used for work at the mining face are connected to the mine's power supply during drilling. Within a mining area, according to the extraction plan, a fleet of bolting and drilling rigs are used. Their number and work duration can vary. A second group of electric power receivers is the air conditioning and ventilation devices. The last group of devices are mine drainage devices such as hydraulic pumps, which ensure proper water management in a mining division. The last two groups are permamently connected to the electric grid (continuous line in Fig. 8) on the contrary to wheeled mining machines (dashed line). Nevertheless, above-mentioned groups of receivers are not the only ones connected to a mining network of power supply. There are also other machines and devices using electric power. They deal with other activities of ore extraction (e.g., construction of technical infrastructure, horizontal transportation) in the given mining division. To facilitate data acquisition in subsequent steps, mining areas were selected where only drilling and bolting rigs and other necessary receivers were operating. The purpose of this approach is to gain a new source of data regarding reporting purposes for cost management as well as new source of data related to mining machine cycles detection.

The continuation of this topic is presented as follows: experiment plan (Section 5.1.3), measurement method (Section 5.2.3), and detailed device description (Section 5.3.3) are provided. Thanks to data processing methods proposed (Section 6.3), the final results obtained from electric current measurement at a mining section (Section 7.3) are revealed.

4.4 Gas hazards

Ensuring safe working conditions is a key aspect during mining operations. There are many factors that should be taken into account to assess the risk for underground mining operations. Among them, an important one is an air quality assessment [139]. The main emphasis is on maintaining safe air parameters in the mining departments where people work. The air pollution in underground mines can come from two major sources: natural and human-made [140]. Altogether with underground deposits of copper ore resources, there are gas hazards present, that originate from the natural emisson from the rock mass. There are methane (CH_4) and hydrogen sulphide (H_2S). However, the methane presence is occasional and in a small quantities, what implies that underground copper ore mines are classified as non-methane [141]. Nevertheless, mining works are subject to preventive measures dictated by appropriate regulations.

Second group of hazardous gases are technological gases, generated by mining activities. They are mainly formed by self-propeled wheeled mining machines, as well as mining blasting operations. These gases are mainly nitrogen (NO) and carbon (CO) oxides. The main means of reducing the concentrations of hazardous gases in underground mining is proper ventilation. Another solution for improving air quality in mining excavations is e.g. an upgrade of diesel engine with eletronically controlled injection system or additional equipment with a Diesel particulate filter (DPF). Some of the improvements enable the digital control of machine subsystems (hydraulic, gearbox). Another approach can be the usage of specific physical / chemical processes, such as the photocatalysis process [142]. Today, even the usage of electric machines is possible for the maintenance of the underground machine park [143].

Undoubtedly, the highest priority for mining work is to ensure the safety of underground workers. Especially for deep underground mines, it is complicated to inlet enough fresh air in corridors. Because of this, there is a need for portable personal devices for miners to inform them in real time that a gas hazard is on the way. Existing, widely-used approaches for preserving workers from a polluted air are measurements in a schedule manner. Taking only these results into consideration, there is only the possibility to use model predictions from offline data. Following that way, it cannot be enough to properly manage and prevent the gas hazard accidents in real-time. In this regard, an approach with portable hazardous gas sensor with smartphone visualization layer is presented to cover that gap.

In this thesis, the main consideration is taken for hydrogen sulfide and carbon monoxide. It comes from the fact that the exposure the mining workers on them implies many health effects depending on concentration values. In case of H_2S for concentrations up to 5 Parts Per Million

(PPM) human bodies react with headaches, nausea or eye irritation. For the scope of 5-50 PPM, conjunctivitis may happen, up to 100 PPM olfactory disorder is possible. At values of about 200-750 PPM respiratory disorders in the form of pulmonary edema and apnea emerge. 1000 PPM concentration induce immediate respiratory paralysis and death [144–146].

The next analysed gas is carbon monoxide (CO). It is one of the most hazardous gases in underground mines, because is a highly toxic, colorless, odorless, and tasteless gas. Exposure at a concentration of 35 PPM, can be visible even after 6-8h as a headache. The next level of 100-200 PPM concentration induces symptoms after 2 hours, and 400 PPM after 1 hour. The fatal dose of 1600 PPM with approximate exposure of 2 hour as well as 12,800 PPM with 3 minutes of exposure implies the death [147, 148]. Owing that in next sections, the methodology (Section 5.3.4), experiment plan (Section 5.1.4) and finally the obtained results (Section 7.4) for CO and H_2S measurements are presented.

4.5 Robotic inspection for transportation systems maintenance

Scheme of belt conveyor describing the main components is presented in Fig. 10. This type of an extensive underground infrastructure needs to be inspected on a periodic basis. Some working parameters of the standard belt conveyor used in copper ore transportation are given in Table 2. The length of the belt conveyors vary, following to the installation place and technological limitations, but a single conveyor length is within the range of 0.5-2km [149].

The fragment of the transportation system chosen for robotic inspection is placed between the two drive units: head and tail pulleys. This structure has multiple idlers that support the moving belt with material along the way. These rotating elements include a shaft, two bearings, and specific coating material. Taking into account the large-scale infrastructure, it requires an extensive monitoring for diagnostics. The standard approach with human inspection is impossible for such an extensive infrastructure (see Fig. 9).

In consequence, as part of the dissertation work, the automated robotic inspection approach is considered as an equivalent to manual supervision. For that reason, the robot should be equipped with measuring devices to further diagnose the idlers.

In Fig. 11, an example of underground transportation system for copper ore mine is presented. With blue lines, there are visualized the belt conveyors, which transport the ore material from dropping point (red dots) to mining carts unloading station (cyan dots). On the way, there are

Table 2: Belt conveyor parameters [150]

Conveyor belt width	1000 mm
Conveyor belt length	1500 m
Conveyor belt velocity	2-2.5 $\frac{m}{s}$
Efficiency	1100 $\frac{Mg}{h}$
Belt conveyor slope	$\pm 5°$
Power of the drive station	2-3 x 110kW

Figure 9: Belt conveyor human inspection [151]

many weights (green) and discharge points (small triangles with black edges), before ore material is moved by railroad (orange lines).

Transportation system of copper ore in underground mining stands for a crucial part of the technological processes. Any bottlenecks generated by out of the order the mechanical or the electrical part of the system above make significant and costly delays [152]. Following that, keeping the belts conveyors in a prosperous state is essential from the mining company perspective. Unfortunately, due to limitations from a such intrastructure of significant size, the occasional unplanned breakdowns happen. For that reason, several trials are investigated to use an inspection robots for these repetitive tasks. Instead of insufficiently frequent (or ad-hoc) inspections of belt conveyors performed by underground workers, this process can be automated in a constant manner.

From the maintenance point of view there are three major inspection tasks suitable for inspection robots [149]:

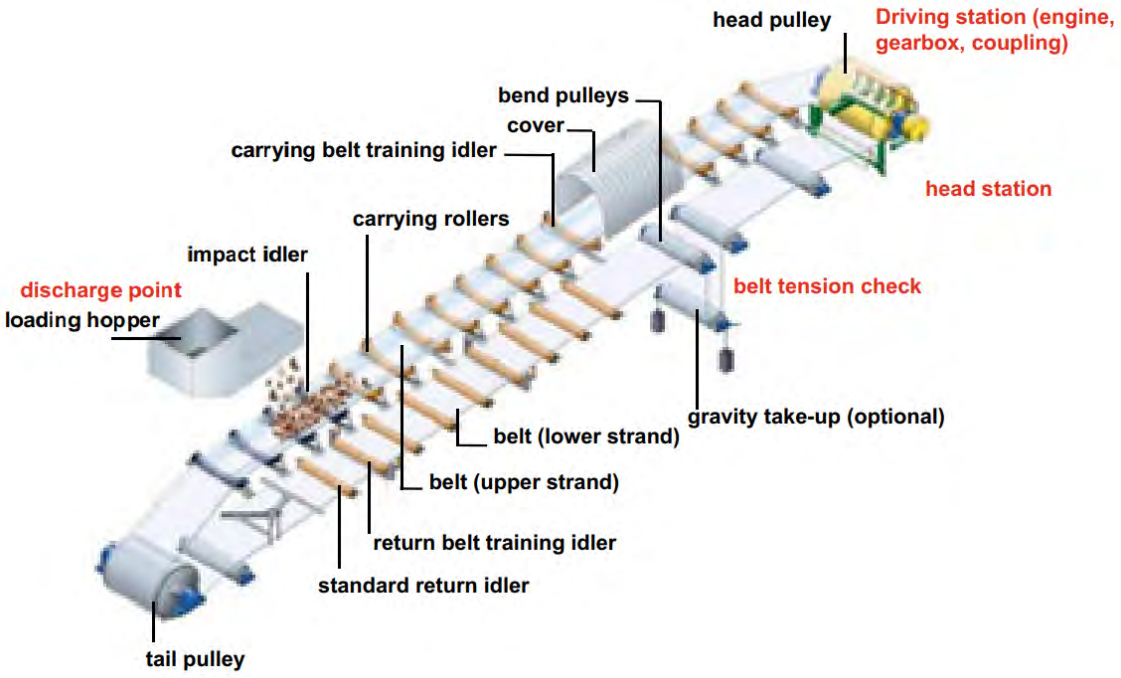

Figure 10: Belt conveyor scheme with idlers [50]

- condition monitoring for idlers
- condition monitoring for conveyor belt
- condition monitoring for drive unit

The first two inspection tasks are considerably more difficult to carry out due to the extensive inspection area and the number of components to be monitored [154]. In addition, the number of electric drives is significantly smaller compared to the number of idlers. This makes it possible to prepare stationary measuring systems for the motors to assess their condition, which is not a trivial task for the first two inspection tasks. For that reason, limitations in the ability to assess the condition of the infrastucture can be overcome by using inspection robots. There are many types of robot widely adapted in numerous industries used for inspection or monitoring task such as: Unmanned Aerial Vehicle (UAV), Unmanned Ground Vehicles (UGV), wall-climbing robots, cable-crawling robots, marine robots, and legged robots [155]. The most suitable construction for harsh environment from underground mining conditions are wheeled UGV [151, 156] and legged robots [149, 157]. In Fig. 12 and 13 there are presented the inspection robot types broadly used in underground mining asset monitoring. Using measurement devices such as cameras (RGB, depth,

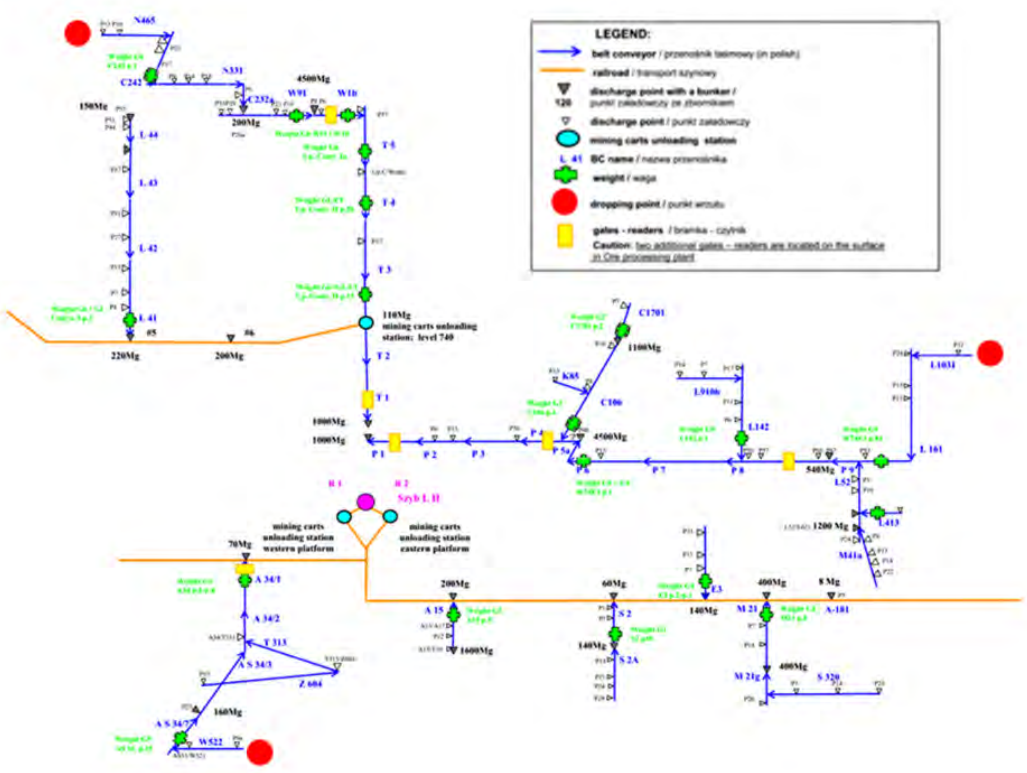

Figure 11: The underground transportation system [153]

infrared) or vibro-acoustic sensors, it is possible to automate the inspection of belt conveyors. These sensors replace the senses of the underground worker, who carries out the inspection.

Figure 12: Wheeled robot for belt conveyor inspection [52]

Figure 13: Legged robot for underground asset inspection [149]

In addition to the sensors mentioned above, it is also important to use sensors that enable the robot to traverse the mining environment. Simultaneous localization and mapping (SLAM) is used

for this task [158]. LiDARs, depth cameras and IMUs are used for this purpose widely in condition monitoring in underground mines [159, 160].

In order to increase the quality of the resulting map and enable the robot path be more complex, many improvements are made in terms of more accurate measuring devices or data processing techniques. In this dissertation, the implementation of a mechatronic system in the form of a 3D housing (for equipment protection in harsh mining environment) is presented altogether with the servo drive that enables the rotation of the LiDAR mounted within it. The necessity of the precise map creation of an unstructured environment, such as mining excavations, results in new measurement methods using a LiDAR sensor. In addition to this, precise data that describe the interior of excavations can be valuable for infrastructure diagnostics. For example, laser outputs from rotating LiDAR can be used to scan the surface and edges of conveyor belt as well as determination of idler-belt contact. The creation of the servo communication software was integrated into the ROS system.

The rest of the inspection robot work is presented as follows: experiment plan (Section 5.1.5), sensor integration methods (Section 5.2.5), and inspection robot description (Section 5.3.5) can be found. Finally, the data integration of the rotary LiDAR and results are described in more details in Sections 5.3.5 and 7.5.

4.6 Cybersecurity risk assessment of IT infrastructure

All the above-mentioned sections describe the objects and processes where their measurement units have the ability to be connected within the Local Area Network (LAN). If the system architecture will allow these devices to be connected to Wide Area Network (WAN) and then to the global Internet directly, it would affect enormously the state of the cybersecurity of the assets. With that in mind, it is reasonable to manage the risk where the current state of the digital affairs and future technological developments may lead to. The advanced automation and robotization of processes in mines represents the next phase of the digital revolution for mining companies. IoT devices in key mining areas, described in this section, will exemplify the fundamentals for data sources to manage, plan, and control machines and devices remotely.

As a natural consequence of the increasing use of digital solutions for control engineering, process automation, and measurement devices, the cyber threats arise notably. These processes upgrades bring a lot of benefits to the organization, among other things, ensuring better working conditions for the staff. Instead of manual measurements, the digital layer of sensors can be

visualized using, for example, the SCADA system, widely used approach to manage state of the processes (see Fig. 14). The digital transformation is accelerating and taking place in many industries as well as in the mining industry. The integration of technological processes with complex measurement systems, communicating on a common network, opens up new possibilities for using the collected data and making the best decisions based on real-time data. Although not all elements of the IT infrastructure, often including critical ones, are connected to the Internet, but this may change in the future. Many activities are performed remotely nowadays, thus the proper risk assessment should be taken into account. Ultimately, technological developments will allow partial or full autonomy of work in mining, especially underground, where working conditions are extremely difficult. Today, with closed systems, fully managed by the organization's IT department, cyber threats can also take place. There is the possibility that bad actors will break or bypass security and can take control of the IT infrastructure and, by extension, the physical infrastructure that manages technological processes. For this reason, this dissertation attempts to perform a threat risk analysis focused on the specifics of a mining company.

Figure 14: Control room of technological process with SCADA system at ZWR District [161]

According to the risk terminology from Cybersecurity and Infrastructure Security Agency (CISA), the following are distinguished [162]:

- **Threat**: A circumstance or event that has or indicates the potential to exploit vulnerabilities and to adversely impact organizational operations, assets, individuals, other organizations, or society
- **Vulnerabilities**: A characteristic or specific weakness that renders an organization or asset open to exploitation by a given threat
- **Likehood**: Refers to the probability that a risk scenario could occur
- **Risk**: The potential for an unwanted or adverse outcome resulting from an incident, event, or occurrence, as determined by the likelihood that a particular threat will exploit a particular vulnerability, with the associated consequences

The initial steps to establish cyber risk assessment are identification and creation of backlog of all IT components. Based on that, it is possible to generate cyber threads using open vulnerabilities catalogs to list all possible scenarios where assets are susceptible to. Many organizations, mainly government, produce and manage cyber threat reports [163–165]. The next phase is documentation of selected threats and cyber breach common indications. They can come from external as well as internal origins, in regards to misconfiguration, internal bad actors, etc. By combining all of the above, a cyber incident response plan can be created to mitigate possible systems breaches. Knowledge of mostly all possible exploits allows one to identify the consequences that potentially can impact on an investigated system. At this stage, the proper risk analysis is performed considering all threats, possible vulnerabilities, and likehood. Finally, for all studied risks, the prioritization for specifc risk responses is viable now. The prepared procedures in that way help to respond for any cyber incident taken into consideration.

Nevertheless, the early adoption of new digital technologies is often problematic for many companies. It is necessary to carry out any digital enhancements with strong technical skills to architecture digital assets along with industry know-how. Especially for the demanding work environment in the mining sector where every mistake could cost a lot.

In Information and Communications Technology (ICT), most projects are managed with agile methodologies, where the most impactful risk factors are quality of the delivered solution and overrun of the project's time & budget [167]. As this dissertation states, an example of digital transformation in mining industry and its next level of automation needs to comply with risk assessment. It can be mitigated by cyber-atacks risk analysis based on fuzzy theory.

Figure 15: Switchboard with devices for controlling electrical network parameters as an example of binding the digital and physical assets [166]

For this particular reason, mining operations processes can be handled to estimate the risk taking into account the level of mining automation levels. The risk assessment consists of differentation of cyber-attack targets based on mining procedures computerization. The next factor relies on the identification of cyber-attack techniques. Based on in-depth understanding of the mining sector, the consequences can be defined. Finally, the risk ratio assessment can be estimated and proceeded with expert knowledge.

Building modern solutions enabling data-driven decision making can be difficult not only in the design stage but also in the operation phase. To ensure a stable environment for any robust digital assets, it is needed to consider several factors to keep the operation viable. Ensuring cybersecurity

in that case is not an ad hoc action. It is a well-suited set of rules that allows companies to retain their digital assets safe [168]. Especially for cloud-managed infrastructure, where several aspects are needed for it. Owing that, the following part of software delivery should be applied to have an ability to have cyber-resilient in mind :

- CICD automation
- Unit tests of software logic
- Static code checks
- Container images scanning
- Repository artifacts scanning
- Private / Hybrid / Cloud infrastructure configuration compliance

All aspects enumerated above states for the parts of digital intrastructure which should be taken into account for ensuring cybersecurity. In Section 8, these perspectives are described in more detail to present the impact these have on the overall system architecture. Nevertheless, the present approach above, represents only a limited scope of IT/OT landscape of mining companies infrastructure. Fortunately, the industry awareness is getting rising, thanks to numerous dissemination activities during industrial congresses as well as the plan for national cybersecurity centre of excellence especially for mining industry [169, 170].

The continuation of topic is described as follows: Section 6.6 describes the details of usage the fuzzy logic to assess the risk and Section 7.6 shows the risk analysis of cyber threat for a mining company.

5 Experimental works and measurement methods

In this section, the measurements methods for the chosen objects and processes presented in this dissertation are described in more detail. A comprehensive technical description is provided for each device, including the hardware specifications and the dedicated software developed to perform the data acquisition tasks. In addition to that, some enhancements for manageable scaling out the hardware and software solutions for distributed architectures with usage of cloud services are proposed. Finally, the measurement methodology is presented, taking into account environmental, technological and equipment limitations.

5.1 Measurement experiment plans

In this chapter, for each objects or processes, a detailed description related to experiment plans is presented. Many different aspects of mining processes can be taken into account; however, the research was limited to specific use cases for underground copper ore mines. As described in the following, the experiments were carried out in cooperation with the mining company as part of research projects at the university. The description of the experimental research carried out is limited to 5 cases, for which solutions were developed or co-created to measure various physical quantities characterizing the selected mining processes described in more detail in Section 4.1 - 4.5.

5.1.1 Current consumption assessment for drilling rig machine

The drilling of blast holes is one of the first technological operations in the copper ore mining process. Performing mining operations in a room-and-pillar mining system enables many drilling rigs working at the same time. In Fig. 16 it is presented above-mentioned mining system with dozen of mining faces (black icons). They proceed according to the direction of mining. Each machine drills the blast holes at the mining face in accordance with a blasting pattern.

An example of the pattern is presented in Fig. 17. Each circle corresponds to a drilled hole and its color indicates the mass of the explosive (blue and orange, 3.5 and 2.5 kg, respectively). The red numbers indicate the delay of every hole detonation [ms]. As one can see from the top view (bottom part of the drawing), these holes are not parallel to each other. This arrangement makes it possible to optimize the number and length of holes drilled for each rock mass burst. However, the distribution of boreholes depends on the parameters of the rock mass in a given location.

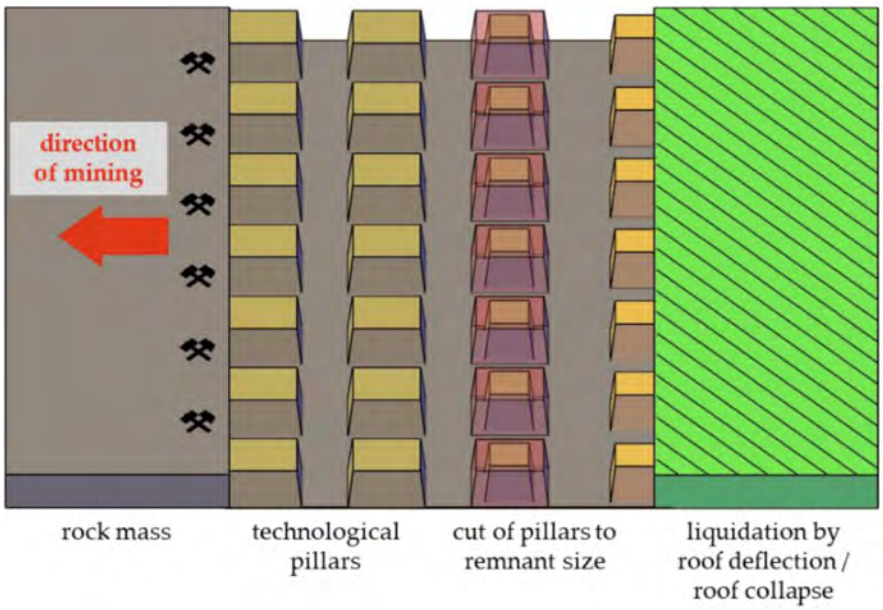

Figure 16: Mining front with room-and-pillar technology for copper ore mines [171]

The drilling rig experiment relies on current measurement in the machine's power cord to estimate the work regime. The test rig was placed at the mining machines manufacturer test site. A test holes was performed on the rock surface, as can be seen in Figure 18. Underground drilling rigs have an electrical cabinet mounted closely to the rear part of the machine. Within this unit, a three-phase electrical power from the underground electricity network is connected to the machinery. To measure instantaneous current consumption, on one power cord, the Fluke current clamp (i400s) is mounted as can be seen in the Fig. 28. The signal has the shape of a sinusoidally alternating voltage signal modulated in amplitude by a current value in the range of -400 + 400 mV. The data acquisition card cDAQ-9171 USB converts the signal using a built-in analog-to-digital converter (ADC) module with a frequency of 2000 Hz. The collected signal provides information on the drilling process that corresponds to the creation of dozens of drill holes in the rock that has physical parameters similar to the underground copper rock deposits. The experiment was carried out during tests at a mining machinery manufacturer.

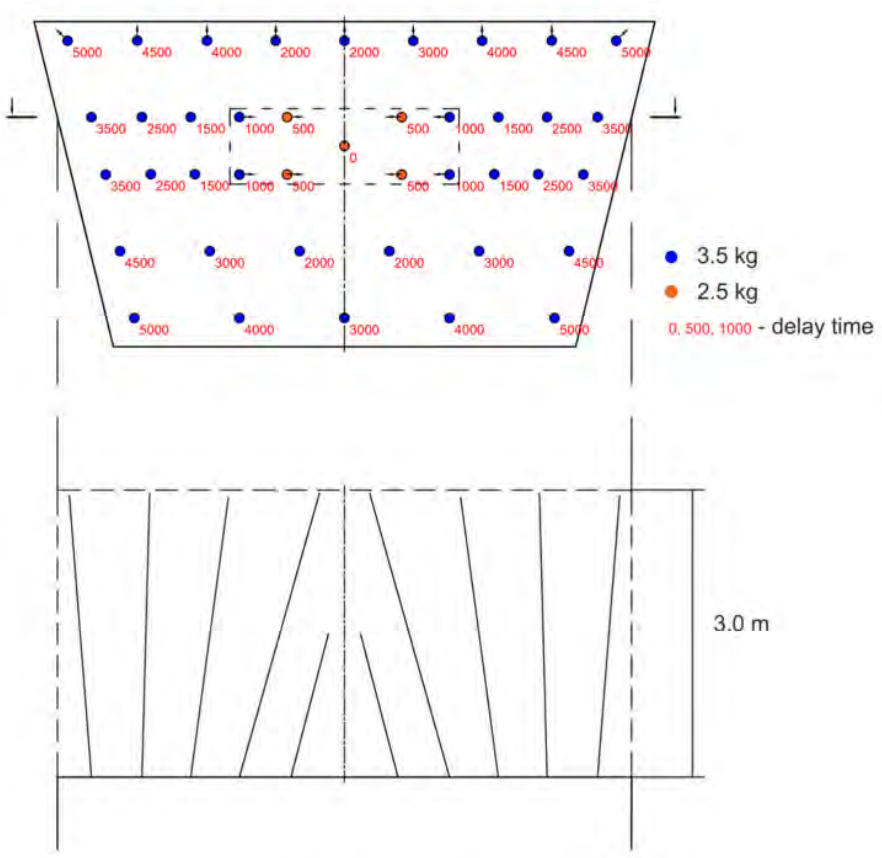

Figure 17: Drilling face blasting pattern: cross-section (upper), topside view (lower) [172]

Figure 18: Test site of drilling rig machine experiment [173]

5.1.2 Bolting progression monitoring experiment

There are many techniques for installing ceiling support bolts in the room-and-pillar system. To simplify the measurement unit construction and further data analysis from the process, the mounting of expansion rock bolts is only considered during the experiment. This is the most popular technology used to secure the ceiling of the corridor for underground copper mines in Poland. Measurement device, described in more detail in Section 6.2, includes a laser rangefinder. It estimates the drilling progress on the basis of an indirect method. The distance between the ceiling and the mountage point on the mining bolter's boom is measured. Taking into account the harsh underground environment, particularly the high dustiness, several mounting places were tested to eliminate as much as possible the impact of the dust on the laser beam. The final placement of the measurement device on the bolting rig is presented in Fig. 19. Dataset analysed in this

Table 3: Bolting rig machine working parameters

Metrics Name	**Value**
Corridor height	2-2.5 m
Bolt rod length	1 m
Laser mouting point	0.3 m

dissertation consists of 11 days of the measurement with at least one working shift quantified. In the first place, the quality of the measured laser data was taken into consideration. Other factors such as access to the validation data (from another sources), trouble-free bolting progress (lack of bit jamming in the rock), and finally preserved the shape of the cycles without additional drilling were used for final dataset collection. In Table 3, the selected process-related parameters are presented. These values are related to the dimensions of the machine, the type of bolting process and the location of the measurement device from the head of the drilling tool of the machine. The measurement frequency is 8Hz, because the laser rangefinder can work with such repeatability at most.

Figure 19: Laser rangefinder mounted on mining bolter boom [174]

5.1.3 Experiment of electric current measurement at the mining section

As a continuation of the experiment from Section 5.1.1, the new approach is proposed to measure an instantaneous electric current consumption. As compared with the previous manner, when current measurement takes place in one of the drilling machine's power cord supply phase using a current clamp, the measurement device remains the same. Measurements are performed at an electrical switchboard output power cord, in which electric power is distributed across the mining section for many devices and machines. That approach is selected in order to limit possible measurement

disruption, which can occur at the mining face. Current measurement unit, described in 5.3.3, logged data during a month in an uninterrupted manner in total with a 2000 Hz frequency.

In the first phase of experiment preparation, electric devices switching tests are performed. A table 5 describes all types of machines and devices with corresponding current consumption. The purpose of that is to have valid datasets corresponding to each device working under mining division. Moreover, the second part of the experiment handles cases where overlapping of receiver groups is considered in order to unambiguously identify them during standard working shifts. Measurement in a mining section covers the sum of current consumption of all devices and machines connected to the electric grid at a given time. During that period, they can simultaneously work with several different machines. However, it is possible to interpret unambiguously only some moments when, for example: only one mining machine is working. This is evident from the shape of the envelope of the current signal. There are four regimes of operation connected to the underground mine electrical network:

- constant working regime - after startup, some of the devices characterize with a nearly constant current consumption in time. The current level can be estimated based on the power rating (Fig. 20). This regime can be interpreted as the work of hydraulic or ventilation devices within the given mining area.

- drilling rig regime - in the current envelope it can be possible to see the cyclic changes corresponding to drilling holes at the mining face. There are 4 distinguishable phases of drilling rig work: idle gear, manoeuvring, drilling, and run-up peaks. (Fig. 21).

- bolting rig regime - after run-up peaks (occured after machine plug-in to electric grid), there are idle gear, bolting, and characteristic rock bolt tightening peaks levels. (Fig. 22).

- others - combination of work of many different machines and devices working in parallel

The last phase of the experiment manages the measurement in different mining areas to cover all possible scenarios of underground machines works. In Fig. 23 it is presented a view from the drilling machine operator's cabin during the experiment.

Using current consumption measurements in a given mining area, it can be interpreted as a record of operating events. Handling the above-mentioned knowledge of the group of devices and duration of individual current levels described in this section draws a broader perspective on how electric devices work overall in mining section. Based on the methodology described above and the information obtained from the electric devices switching test, it is possible to identify

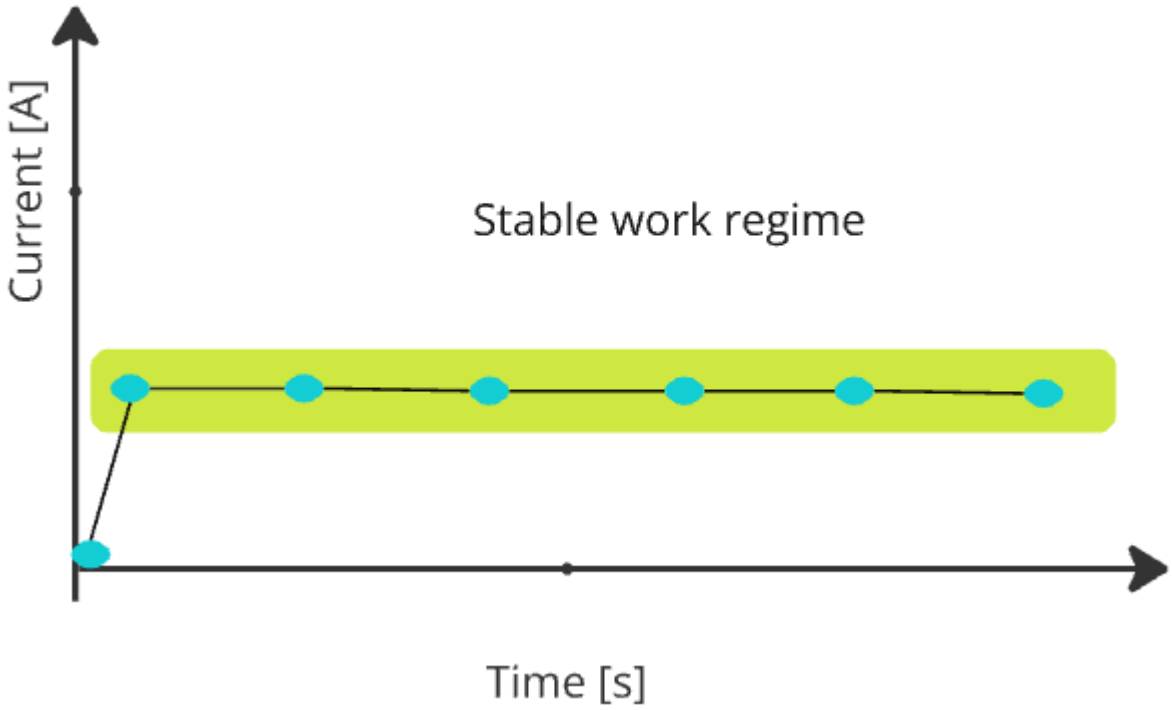

Figure 20: Stable working regime pattern

several parameters of the electric devices and machines that work within the given mining area. Some of these are:

- an average work time of the specific device/machine in a selected mining localization
- an estimate of the energy consumption rate of a particular machine or group of machines
- start and end of the wheeled mining machines work
- wheeled mining machines cycles idenfitication (when just the one machine works in the given area).

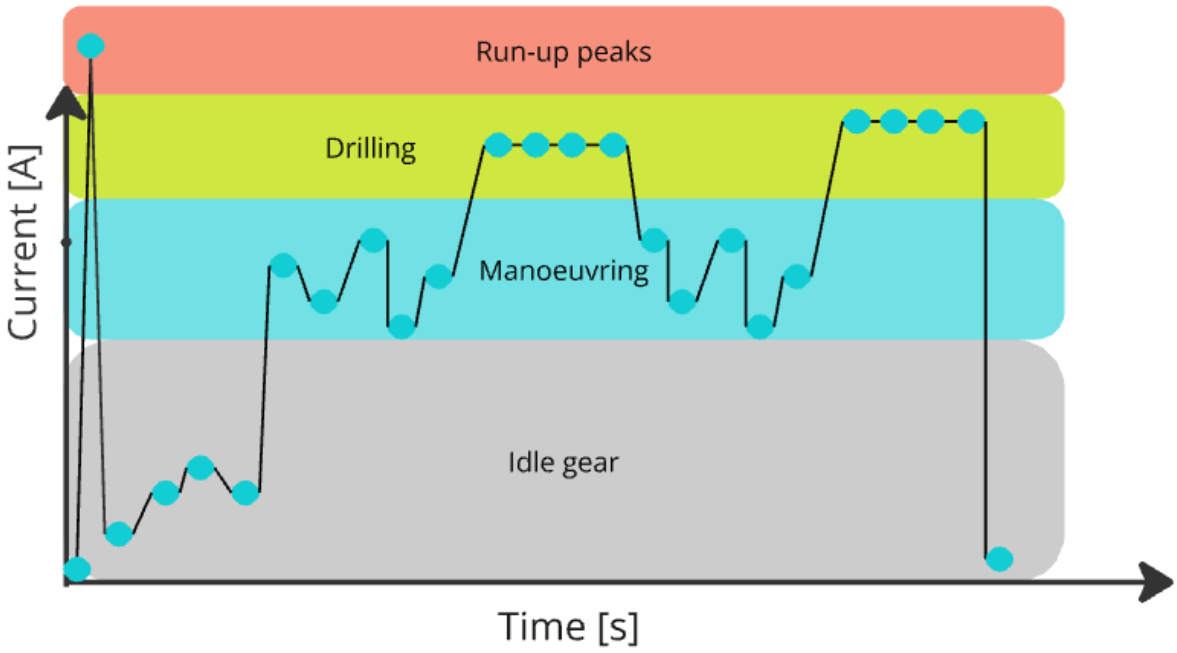

Figure 21: Drilling rig regime pattern

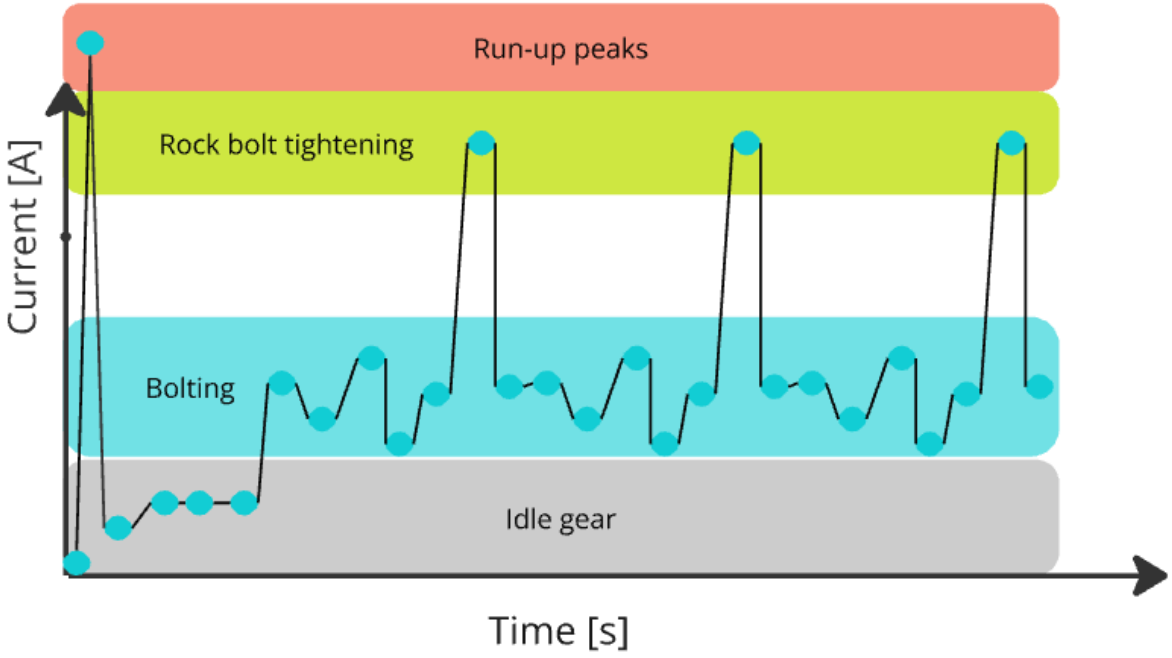

Figure 22: Bolting rig regime pattern

Figure 23: View from the cabin of a drilling rig operator during drilling blast holes

5.1.4 Plan for hazardous gases measurement

The hazardous gases present in an underground copper ore mines are H_2S and CO as the main concern. The purpose of the experiment is to validate in real working condition the hardware & software of the personal gas measurement unit for the mine workers. Prior work for system check was verified in the lab and in the mine. Indirect sensor software-based validation used in this case is a more convenient way to calibrate the linear sensor output with certified portable sensors managed by the mine ventilation crew. The second part of experiment is the measurement session undertaken in an underground mine in several places, where natural or man-made sources of hazardous gases existed. In the map shown in Fig. 24 the masurement points (green cirles with number of 1 and 2 respectively) and air flow directions (red arrows) are presented. The measurement device described in 5.3.4, has the direct connection with smartphone. Thanks to the usage of custom application it is possible to present on-line measurement results with frequency refresh of 1Hz. Within the application, several alarms were designed to inform mining workers in a clear way about the possibility of gas hazard based on the thresholding of gas concentration.

Figure 24: The map of the measurement experiment in an underground mine with sensors location and fresh and used air stream flow [175]

5.1.5 3D scan optimization experiment using inspection robot

The inspection robot, developed by the research group from our faculty, was equipped with many sensors for environmental parameters analysis as well as for surface 3D reconstruction. During the experiments, the necessity of precise map creation was revealed. Such mapping solution can be used for navigation as well as diagnostics purposes [176, 177]. The precision improvement was achieved by the development of lidar movement mechanism. In this study, the main emphasis is taken on robot's equipment devices such as lidar enabling robot neighborhood mapping. The mobile robot during belt conveyor inspection is presented in Fig. 25 (open-pit case) and Fig. 26 (underground mine case). The detailed description of the robot setup with the above appliances is described in Section 5.2.5. Moreover, in this dissertation, only the way how devices are assembled and configured in the robot operating system is applicable. Techniques related to point-cloud analysis and additional data processing are outside the scope of this thesis.

Experiments can be divided into two major parts. Measurements were taken in two different environments. The first was a measurement on a belt conveyor located in the production hall, on which bulk materials was transported. The second part took place in an underground mine during the transport of copper ore. Each experiment involves driving a robot along a belt conveyor with set of sensors presented in Fig. 27. The device used is 16-line Velodyne VLP-16 lidar. Nevertheless, there are other sensors mounted on the robot mast, namely: Depth camera Intel

Figure 25: An automated idlers acoustic inspection with robot (Source: AMICOS project)

Figure 26: Robot during inspection in a mine (Source: AMICOS Project)

Realsense D455, ELP RGB camera, FLIR IR camera, and CCLD Microphone Preamplifier Bröel and Kjær 4189-A-021 with type 2671 preamplifier. During this work, the only lidar output is considered.

Parameter name	Description
Robot type	Skid steering, wheeled mobile platform
Control mode	Teleoperation / autonomy
Weight	65 kg
Maximum payload	75 kg
Height	400 mm
Length	867 mm
Width	655 mm
Mast height (upper part)	1400 mm
Mast width (upper part)	150 mm
Mast length (bottom part)	360 mm
Mast width (bottom part)	400 mm

Table 4: Wheeled robot platform parameters

Figure 27: The view on robotic inspection sensors suite

When the measurement equipment is in motion, data is collected and recorded using ROS protocols enabling data exchange. The data frames are sent from lidar with 10 Hz frequency and

stored in raw data format as *.rosbag* files. All files possess a timestamp for synchronization with other processes of robot operating system, i.e. for navigation purposes. This feature helps to process data offline.

5.2 Measurement methods

In this chapter, author presents the measurement methods used to gather data necessary to enhance the processes-related knowledge of the mining machine operations and improve the safety of miners. In next paragraphs, the key factors that helped to obtain the durable data sources are explained as best as possible, describing the various mining processes dealing with the complexity of mining activities. Taking into account that the presented measurement methods or sensors used are well-known in other industries, the crucial part of the work is to propose the adjustments making these data sources reliable and one of the pioneer usages in mining science.

5.2.1 Drilling rig electric current consumption measurements

It is assumed that based on direct electric energy consumption featured by current measurement, it is feasible to identify the mining machines work cycles. Many sensors used for measuring current in the automation industry rely on in-circuit measurement techniques. This form of interference with the machine system needs to be integrated at the machine design stage. To satisfy the limitation above, the usage of non-invasive method of the mining machine's workload assessment with the current measurement for instantaneous energy consumption is presented. Current clamps offer a more convenient solution, as they allow current measurement without altering the machine's electrical circuits. The key factor of usage of current transformers is a galvanic separation from the controlled circuit. Among from the well-known current transformers types, the current clamps with Rogowski coils is more suitable for mining usage than the optical or hallotron transformers due to their structure and range of operating parameters.

Underground drill rigs, to support the main drilling operations, use an external eletric power supply from underground mine infrastructure. A diesel engine only powers the driving systems and a small hydraulic pump mounted there because of incomparably greater power consumption from drilling subsystems.

Therefore, in these devices, the hydraulic system for drilling was powered by an external three-phase AC voltage of 500 V or 1000 V at a frequency of 50 Hz. An external electrical source was linked to the machine's electrical cabinet. The power supply was symmetrical, and as a result,

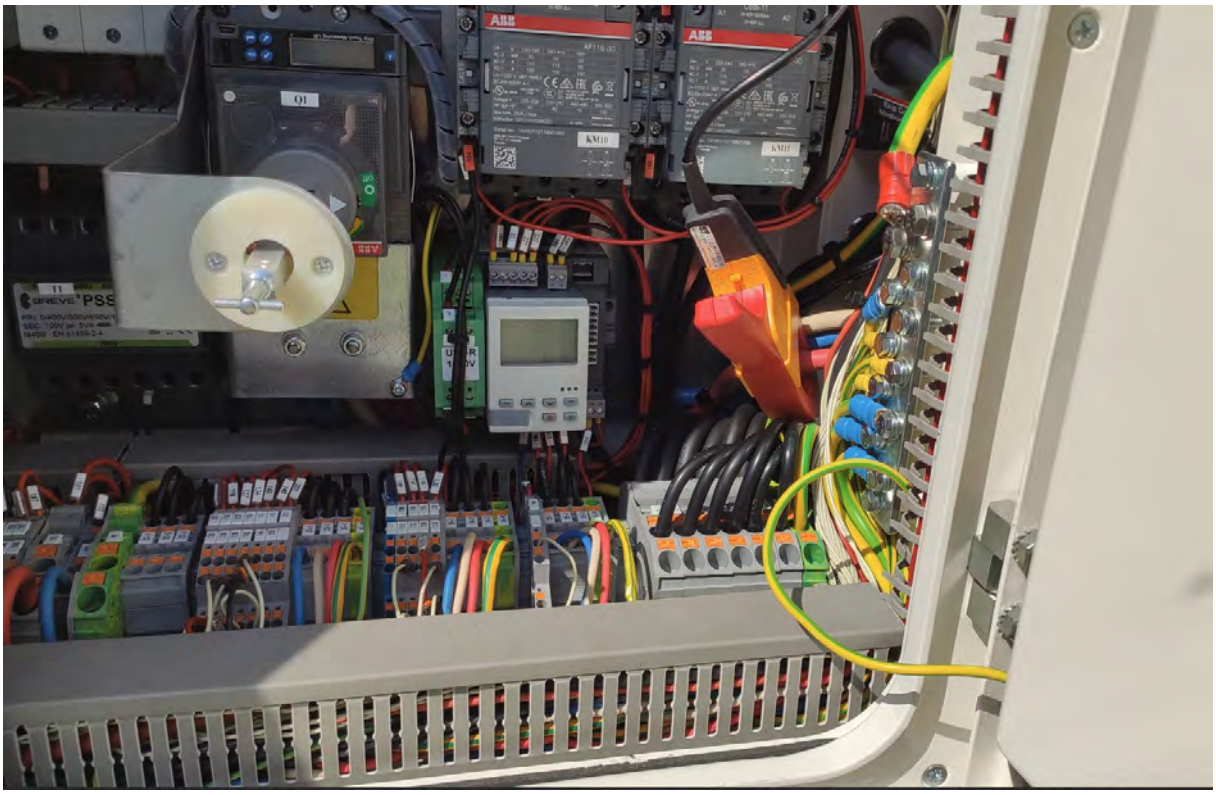

Figure 28: Current clamp mountage point on the drilling rig [173]

a current clamp can be installed on any conductor of the supply line. The assembly of measurement system is rather simple where the center of the measured conductor is installed in the current clamp jaw. Moreover, it is important to mount the clamp perpendicularly to the power wire for correct results. The current clamp mountage point assembled on the drilling rig is presented in Fig. 28.

It is crucial to note that the energy consumption levels for the machine's other subsystems, excluding the drilling system, remained relatively stable during the drilling process. This stability in energy consumption, observed during measurement session, allowed to derive insights into the changes in the drilling process directly from the current measurements.

5.2.2 Bolting progress measurement

There are plenty of machine equipment settings and different techniques for excavation roof support with usage of bolting rigs. The most prevalent procedures utilize the steel joints and expansion rock bolts. The correct process execution to strengthen the corridor ceiling relies mostly on the bolt type used. It is mainly the results of rock mass physical properties and finally the internal procedures to follow.

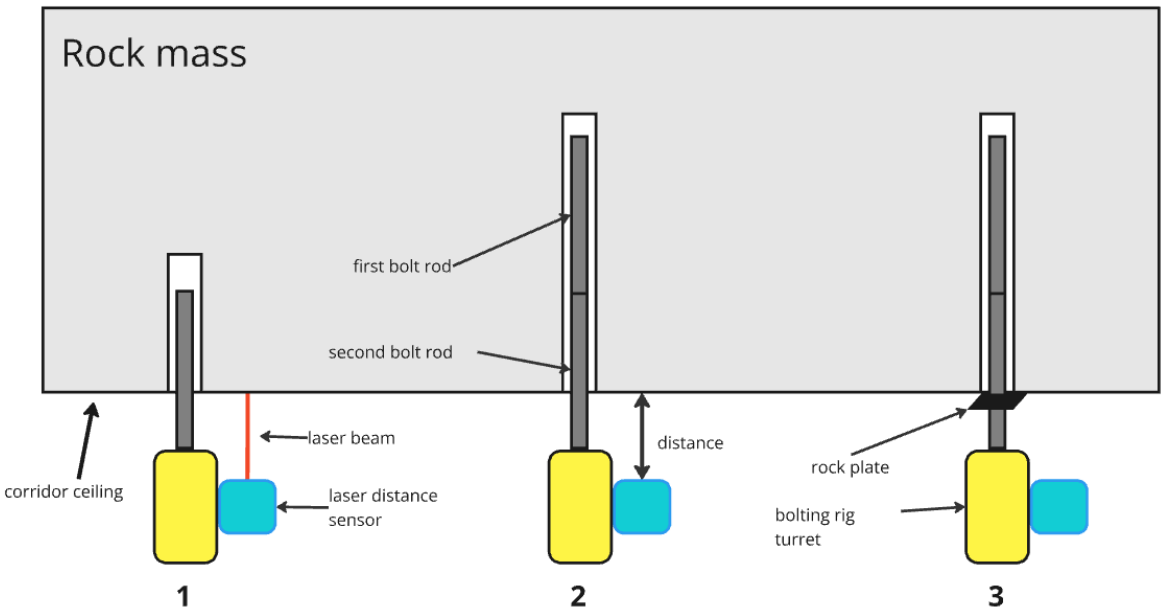

Figure 29: Scheme of the bolting process [174]

The process of preparing ceiling protection using expansion rock bolts is selected for examination due to its repeatability. The above process is illustrated in Fig. 29. Firstly, it involves creating bolt holes by placing the rod into the drill socket and drilling the hole along the rod's entire length (step 1). Following this, the tool is brought back to the starting position, where an additional rod is attached, and the hole is drilled deeper to the required depth (step 2). The final step involves returning to the initial position once more to insert the rock bolt and blowing out the hole in parallel. This step is marked by a quick change in distance over time and the application of tightening torque. At this moment, a rock plate is added to properly fix the end of the rod on the ceiling (step 3). These holes form a grid with distances in the range of 1-1.5 m between each other, but could vary depending on the local geological parameter of the orebody [178].

The performance of a drill hole to secure the roof of the corridor with rock bolts consists of 2 drilling subprocesses (the geometry of the tunnel makes it impossible to drill an appropriate hole without such a division into 2 phases) and the bolt installation process. There are also many auxiliary movements of the bolt during the installation of a single bolt.

During several measurement sessions, where the subject measurement unit was mounted on the machine during its standard work regime, a few mountage options for laser system were tested to resolve the problem of the most appropriate laser placement. Some of them, like mounting closely to the ceiling roof, or on movable parts of drilling rig turret were tested. It helped to estimate the

overall quality of the data obtained from laser rangefinder and achieve as smallest as possible the impact of dustiness from the drilled ceiling or from the ground, or rock crumbs crossing the laser measuring path and finally the vibrations what could damage the device.

5.2.3 Electric current measurement at the mining section

Based on the methodology proposed in Section 5.2.1 it is likely to assess the work of specific mining machines using noninvasive current measurement. To extend that approach in this paragraph, the identification of machine's work is presented taking measurements on transformer station output. It is a place in electric power supply network, where the medium voltage of 6 kV is transformed to low voltage level 500 V and parametrized for a direct use for mining machines and applicanes (e.g. ventilation, lighting etc.). That network is distributed accros the excavation mining area. There are three main groups of devices connected to the underground transformer station output network: air conditioning devices, mine drainage devices, and wheeled mining machines connected temporarily to a given mining area. The work of these first two groups tends to be cyclical, mainly on the basis of extraction work and daily cycles related to the ventilation and drainage needs of the mining area in question. The last group, mining machines, operate acyclically, mainly based on the mining plan for a given mining division, and only then are connected to the electrical network in the area specified.

Device name	Nominal current [A]	Start-up current [A]	Additional information
Undefined	<1	-	Lighting / other receivers
1-speed fan	15	110	Single motor switching
2-speed fan	35	110	Dual motor switching
Hydraulic pump	5-6	56	Hydraulic pump work
Drilling rig	55	>200	50A - idle gear, 60-100A - standard drilling
Bolting rig	30-45 (based on the type)	>150	30/45A - bolting, >80A - auxiliary movements (Tightening the rock bolt)

Table 5: Result of a electric devices switching test within eletric network after transformer station

In order to explicitly identify the characteristic parameters for individual groups of receivers, a electric devices switching test was carried out. The greatest emphasis was placed on finding out the current consumption values at start-up and during each cycle of operation of the individual devices and machines. The result of a switching test is presented in Table 5.

5.2.4 Hazardous gases measurement

The conventional method for validating sensors in industrial applications requires specialized calibration equipment. These instruments come with necessary certifications and attestations that verify their functionality and operational dependability. This is the standard procedure for calibrating any industrial device in a certified lab. However, this process is time-consuming and costly. For the portable environmental measurement unit considered in this thesis, a different approach is suggested. Based on readings from devices commonly used by the mine ventilation team, calibration is performed. Following software calibration, described in more details in Section 6.4, the data from certified portable sensors and prototypes align. This method, similar to the entire proposed solution, is cost-effective, quick, and maintains similar accuracy. Moreover, with the advancements in technology and the Internet of Things, this unique software and measurement system can be effortlessly adapted to evaluate the conditions of various other gases such as NOx, SOx, CH4 in the same manner.

It is worth to mention of the several pitfalls of the proposed method used, which are not handled there. For example, the impact of gas sensor cross-sensitivity is unknown after calibration method proposed. The linear output interpolation from calibration sensor has a form of convolution on two cross-sensitivity functions, which gases sensors reactiveness used in measurement unit is unknown what implies the same for output function. It is suggested to work in this area in more details to remove the signal noise and uncertainty in the exact gas concentration estimation, but it would demand an additional overhead for consequentive calibration. Nevertheless, the received sensor output is acceptable bearing in mind a significal cost reduction for usage at scale.

5.2.5 Measurement for transportation system inspection using mobile robot

During mobile robot inspections, several sensors and data sources are used to complete the entire investigation of the transportation system. As described in Section 5.3.5, to obtain the 3D point clouds from a single scan, a Velodyne VLP-16 lidar is used. This configuration has options to generate cloud points retrieved from rotating or statically mounted lidar. In addition to the lidar

data to be gathered, there are other data needed for the correct configuration and interpretation of the dataset for inspection of transportation systems. One of them is an IMU sensor data (ROS output topic) to correctly calculate the displacements of the robot in space. Another data source comes from the custom driver from the servo that controls the lidar movement and returns the actual angular position. In Table 6 the selected range of data collected by the robot is presented.

As mentioned before, ROS uses publisher - subscriber messaging pattern, where every device, sensor, actuator etc. stands for a ROS node and transmits data into the operating system as a publisher. In this mode, a topic and message type are provided to be used by other ROS nodes working in a subscriber mode. It could be another sensor (using data from different device), a process (triggered by a separate script), or a custom software for calculation or data visualization purposes. In this case, topics listed in Table 6 along with their formats are handled by rosbag tool (ROS command line utility) to save all data in .bag file format for future use. All data frames are wrapped with the actual timestamp. As a result, data can be filtered using the same rosbag utility. For better storage performance, it is proposed to use LZ4/BZ2 compression formats. During the tests, the size reduction was approximately 50-60%.

With usage of data above, during data acquisition from transportation systems inspection, a tablet interface was used to control it in real-time. Fig. 30 presents the data visualized on a tablet, which greatly impacts the quality of inspection. To realize it, the topics generated by the sensors are also subscribed to Rviz software to generate visualizations and send the data to be presented on the tablet [180]. In the center of the figure there is displayed the stereo camera output with horizontal stripes from lidar data. All around this view, there are other camera outputs presented, but camera data are beyond the scope of this thesis.

Table 6: Rosbag file structure description

Sensor Type	Topic name	Format	Description	Sensor driver
Point clouds	/velodyne_packets	velodyne_msgs/VelodyneScan	Raw data transferred by UDP from lidar	Velodyne ROS driver [179]
	/velodyne_points	sensor_msgs/PointCloud2	Structured full point cloud data	
	/scan	sensor_msgs/LaserScan	Structured single scan data	
IMU	/IMU	sensor_msgs/IMU	All data in standard ROS IMU format	Custom ngimu driver
	/ngimu/ngimu/earthAccel	geometry_msgs/Vector3Stamped	Acceleration vectors	
	/ngimu/ngimu/euler	geometry_msgs/Vector3Stamped	Angular data as Euler angles	
	/ngimu/ngimu/quaternion	geometry_msgs/QuaternionStamped	Angular data as quaternions	
Rotating lidar	/dynamixel	std_msgs/Float32	Current angle of Velodyne actuator inclination	Custom driver for dynamixel, but output data is standard Float32

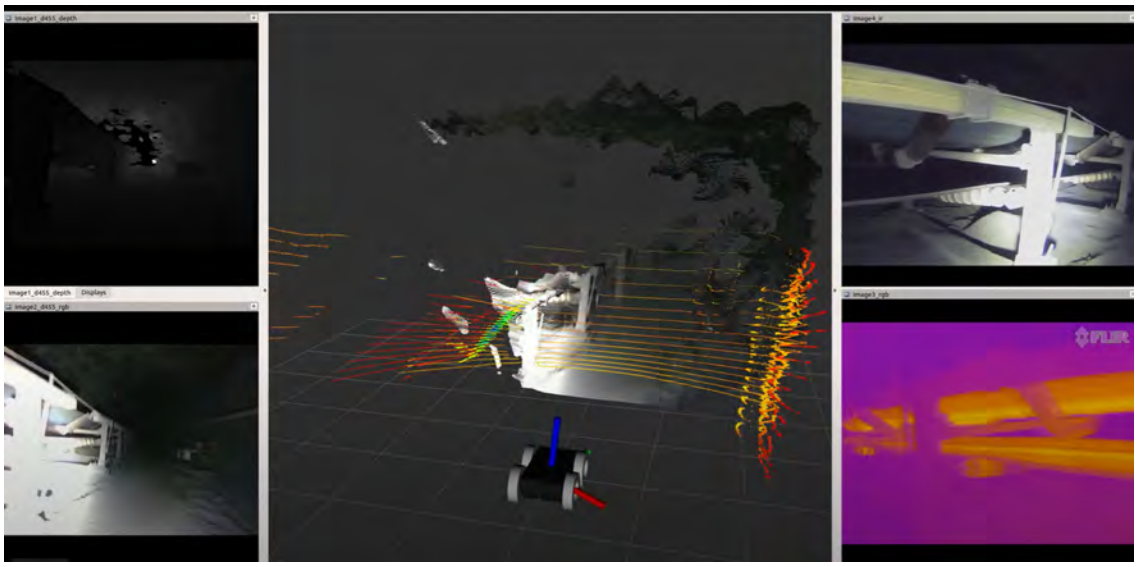

Figure 30: Online visualization panel view from belt conveyor inspection (Source: AMICOS project)

5.3 Measurement devices

Measurement system developed for mining environment or processes consists of hardware and software. The selected hardware components used in the systems are off-the-shelf chips available on the market. Their selection is dictated by the following key aspects such as:

- Motherboards with Linux-based operating system / open-source compilers applied
- Open-source libraries (written in c/c++/python programming languages) used for communication with the on-board hardware
- Chips with ready-to-use GPIO for connection to the measurement system
- Sensors have sufficient capabilities to achieve experiments objectives
- DC power supply (5/12/24 V DC applicable)
- Cost effectiveness

This approach is proposed with bearing in mind that easy solution adoption is mostly applicable when there is a reduced supply chain that effects the cost the most [181]. For majority of cases, the dedicated hardware components, will behave better and in a predictable way rather than off-the-shelf chips, but the cost of final solution would be significantly higher. Moreover,

the adoption time would typically increase. Finally, the adoption strategy of such extended IoT solutions should be managed by mining company respectively concerning all prons and cons, and risk management in particular.

5.3.1 Device for drilling rig electric current consumption measurements

The main goal of the measurement device is to determine the variability of the current consumption level for the drilling process with a wheeled drilling rig. Two data acquisition approaches were used during the measurements. First concept stands for utilization of laboratory class equipment for data acquisition. For this purpose, a National Instruments cDAQ-9171 acquisition card has been selected. The cDAQ-9171 chassis with DAQ measurement card has four programmable channels for connection analog or digital sensors. In this case, one of the channel is used as input host for Fluke i400s current clamp sensor with configured 2000 Hz frequency measurement as it can be seen in Fig. 31. With usage of manufacturer software Signal Express™ it is possible to run the measurements and store data on the laptop connected to the equipment. The view of the test rig is presented in Figure 32.

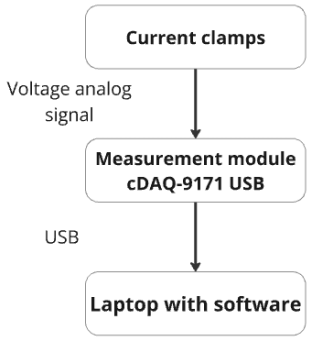

Figure 31: Standard current measurement setup

The second approach is to create a stand-alone measurement device that allows the connection of additional sensors needed to register relevant data. The proposed device block diagram is presented in Fig. 33. Microcontroller used is Arduino M0 Pro motherboard with ATSAMD21G18 chip. Current clamps voltage analog signal in the scope of -400 + 400 mV is transformed using Analog-To-Digital (ADC) converter. The output of the conventer is connected via I2C protocol and saves the status information on the pin as soon as the new value appears. In addition, Real-Time Counter (RTC) connected via I2C protocol is also applied. Using USB cable, a power source of 5 V DC is plugged using a portable powerbank. Finally, software application is written in C language

Figure 32: Standard current measurement setup during drilling rig work

for sensors & measurement management. It enables to store data and saves it in .txt format on an SD card. The obtained measurement frequency was about 150 Hz, what states for inssufficient value, in particular for analysis in frequency domain. Owing that, the device design is upgraded, mainly focusing on replacement of microcontroller with more efficient single-board computer. The detailed description is provided in Section 5.3.3.

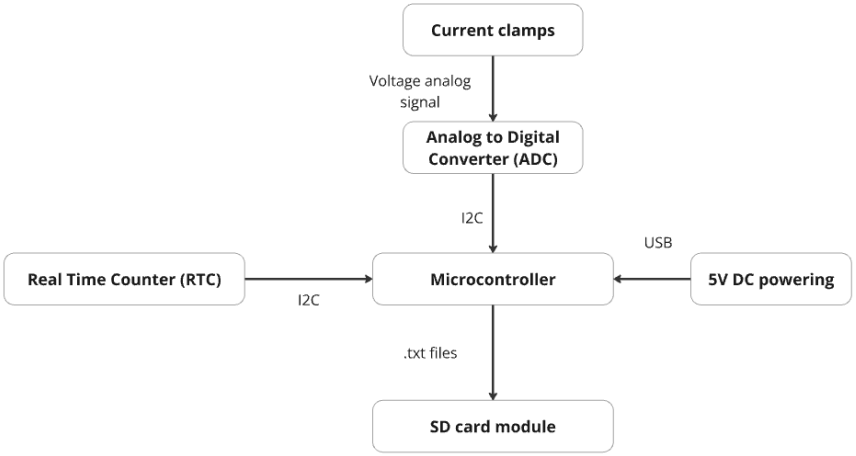

Figure 33: Microcontroller-based current measurement device

5.3.2 Device for laser-based measurements for bolting operations

This section presents the laser-based system for drilling and bolting operations monitoring module. This device, mounted on the bolting rig allows acquiring data during normal operation of the machine. It collects distance data taken between the mounting place on the working arm (mining bolter boom) and the ceiling of the mining tunnel. The main measuring component is a Laser Distance Module (LDM) M703A model produced by JRT Meter Technology. Laser sensor and its parameter is described in more details in Table 7. High measurement accuracy with a relatively high data collection frequency and a favourable price is a key factor of this sensor. It should be noted that sensors with higher measurement frequencies are available on the market, but their accuracy is at a much lower level or the cost of the sensors is significantly higher.

Table 7: Laser distance sensor parameters

Accuracy	$\pm$ 1 mm
Measuring range	0.03 - 40 m
Laser class	Class II
Laser type	635 nm, < 1 mW
Supply voltage	2.0 - 3.3 V
Frequency	8 Hz
Working temperature	0 - 40 °C

System components are listed in Table 8. The laser is placed in dust-proof housing altogether with IMU sensor to provide additional information related to vibration during the drilling in the ceiling. The IMU sensor is integrated in the measurement module and its communication with the microcomputer takes place via the I2C bus. In addition to this, with usage of the Serial Communication Port (UART), the data frame is sent from laser to the microcomputer. In parallel, handling the outputs from real-time counter (RTC) enrich each distance measurement with information about timestamp and acceleration and angular velocity accordingly. Communication between all sensors and microcomputer is presented in Fig. 34. An user interface on the device states for two LED (green/red) displaying the actual status of measurements and buttons for turning on/off device. All components of the system were placed inside the housing with the power module and assembled on the mounting plate. The plate was attached to the mining bolter head using vibration isolators, as can be seen in Fig. 19. Preservation of laser sensor against the mechanical

Table 8: Components of bolting roof measurement system

Microcomputer	Raspberry Pi 3B+
IMU	MPU 6050
Real-time clock (RTC)	DFRobot DS3231M
Laser Distance Module	M703A (JRT Meter Technology)
User Interface	Switch (ON/OFF), LED (green & red)
Power Supply	Powerbank (output: 5V 2A)

damage by rock crumbs is satisfied by usage of additional glass cover. It is made of non-interfering material with the laser beam and mounted on the housing surface.

As a main microcomputer, the Raspberry Pi 3B + is used with a Raspian Pi OS 5.10.92-v7+ version. Created software written in Python 3.8.5 version uses also libraries provided by producers of ready-to-use RTC and IMU modules [182, 183]. Managing threads by integrating the aforementioned sensor output and user feedback provided by LED indicators relies on the Python subprocess library. It handles the hardware interface through GPIO (General Purpose Input/Output) pins using bash scripts for optimized code performance. Each sensor output iteration is performed based on eventual consistency, triggered only when laser data is required. When the memory buffer is nearing capacity, the data is written to a text file and stored in the system memory. This method allows for achieving the highest possible data frequency, with a maximum rate equivalent to the laser rangefinder output on the serial port at 8 Hz.

The data displayed were collected during the process of mounting expansion rock bolts with a bolting rig. All captured data were logged throughout the operation. Information obtained from the measurement unit, which runs on a Linux-based operating system, was sourced from multiple sensors linked to the Raspberry PI 4 board via RPIO pins. The collected measurements were stored in .csv files, which were subsequently transferred to external media using a designated USB port on the case (with a circular rubber cover, see Fig. 19).

Every file name with data saved contains information on the start of the measurement in the format YYYY-MM-DD hh-MM-SS am/pm generated from a real-time clock. The measurement is performed at a constant frequency of 8 Hz and has the following columns:

- distance [m] - laser sensor distance measured

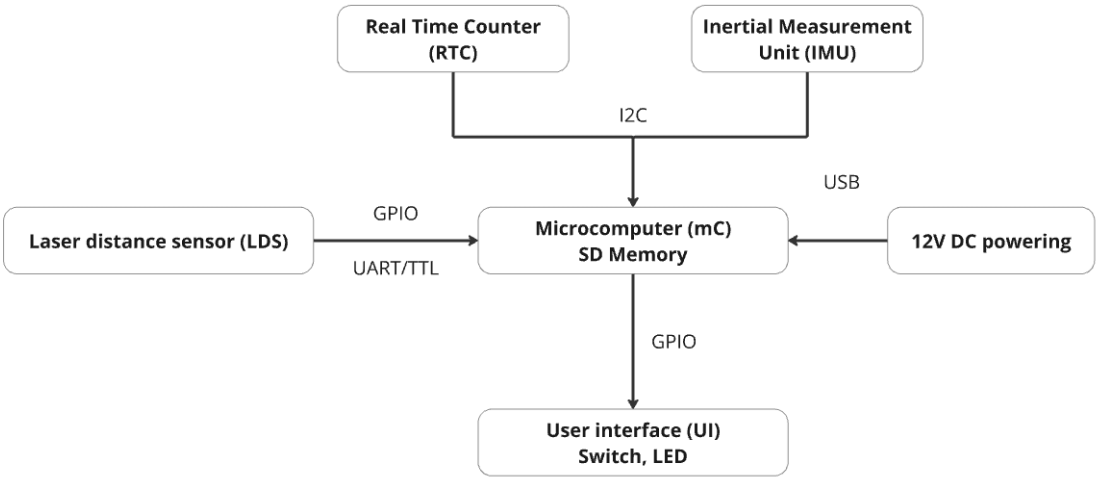

Figure 34: Block diagram of the measuring module

- accuracy [0-2500]- measurement quality of the received distance (built into standard laser sensor payload, provided by the device manufacturer).
- accx, accy, accz [G, m/s2]- 3 axes of the accelerometer
- gyrox, gyroy, gyroz [rad/s] - 3 axes of gyroscope

5.3.3 Device for measurement of energy consumption by electrical receivers

In this section, a new developed current measurement device is described. The specification below is designed to measure the current level on the electrical switchboard outlets for corresponding underground mining area. The placement of the measurement unit inside electrical cabinet is depicted in Fig. 35. It is an improved form of the device described in section 5.3.1. For that reason, several enhancements are proposed to allow identifying energy streams associated with the operation of specific machines and equipment: e.g. self-propelled drilling rigs, self-propelled bolting rigs, fans, pumps, and air conditioning equipment under real conditions.

The block diagram of the updated current measurement module is presented in Fig. 36. Instead of using microcontroller as computing power for measurement devices, Raspberry Pi 3B+ microcomputer with a Raspian Pi OS 5.10.92-v7+ version is used. A selected device possesses Broadcom BCM2711 64-bit processor chipset with four Quad-Core ARM Cortex-A72 cores and 2 GB LPDDR4 memory. System components are described in more detail in Table 9.

Figure 35: Mountage place in electrical cabinet in the mining area

Table 9: Current measurement system components

Microcomputer	Raspberry Pi 3B+
RTC	DFRobot DS3231M
Analog-to-digital converter	ADS1x15
Current clamp	Fluke i400 AC Current Clamp
User Interface	Switch (ON/OFF), LED (green & red)
Power Supply	Battery (output: 5V 3A, 20000 mAh)
SD Card	Kingston 256 GB Endurance

The device interface is presented in Fig. 37. The Fluke i400s current clamps are mounted on a given outlet in the electrical switchboard of the of the selected operating mining area. The sensor wire is connected by BNC connector on the housing of the appliance (Fig. 37 reference number: 5). Analog signal from BNC connector is wired with input of Analog to Digital Converter (ADC). Following that, using I2C communication protocol data is sent to microcomputer input, where recording on the internal flash memory is placed. Data recording also uses information about the

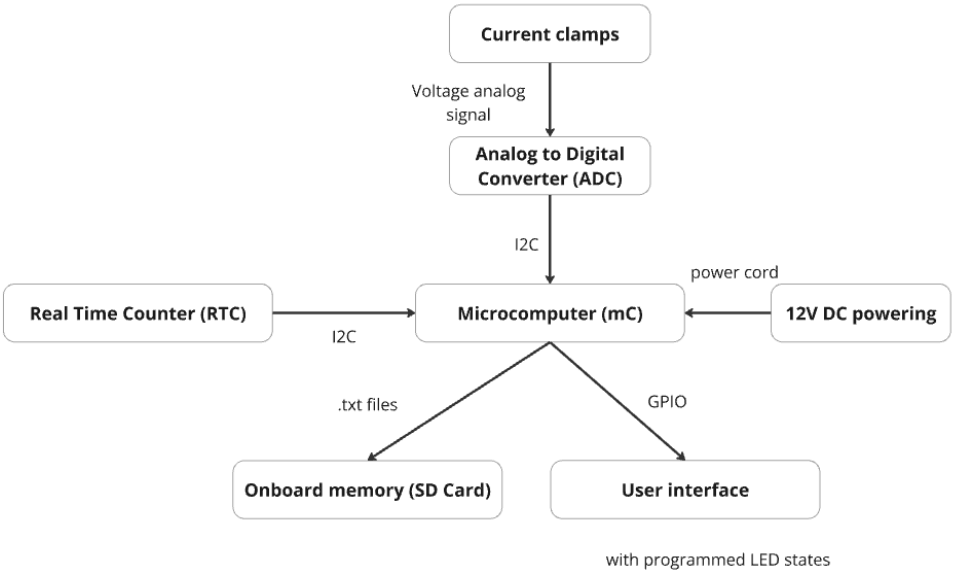

Figure 36: Block diagram of the measuring module

actual date and time, provided by the RTC module communicated using I2C protocol. At this stage of processing the data are combined, a time vector is added, as indicated by the real-time clock from the measurement device. The data thus prepared is then ready for further analyses and reports required in further stages of the work. The correct work of the device signalizes the green LED diode (2). The copying of data to an external USB memory device takes place automatically after inserting the storage medium in the connector on the housing (4). Copying process is visualized using the red diode (3). The device is also equipped with a push button for start-up (1) and an external power connector (6) for 12V DC power (if applicable).

Data acquisition software is written in Python 3.8.5 version with RTC producers library to handle clock output. LED interface and data sending protocol is coded in Bash to handle the hardware interrupts and correctly manage the microcomputer workflow. Every file with measurement data stored has 1 milion rows taken from 16-bit analog-to-digital converter in a raw format to enable the quickest data acquisition. This analog signal, which is the current clamp output for values corresponding to a range of +/- 1.024 V, can be converted to values of the instantaneous current consumption. Data are not processed on the measurement device in order to minimise a computional workload. It helps increasing the signal sampling rate and the file size optimization (saving int instead of float values). In each of the measurement files the first line contains the time stamp used in subsequent steps to create the time vector. The following lines contain individual values in the range $\pm$ 65535 ($2^{16} - 1$) corresponding to the values of the analogue signal $\pm$ 1.024V.

The source is a sinusoidally alternating signal with a frequency of 50 Hz. The signal is sampled with a frequency of approximately 2000 Hz. The measuring range of the instrument is 5-400 A and resolution of 0.03125 A with measurement accuracy of 2% + 0.04 A [184].

Figure 37: Current measurement device interface with a memory connected to data transfer

5.3.4 Device for hazardous gases measurement

The device prepared for measuring hazardous gases in underground mining is described in this section. The concentrations of hydrogen sulfide (H_2S) and carbon monoxide gases (CO) are considered. The main idea is to support works of ventilation crew during the periodic inspections by handling several measurements in an automated way and visualize them using smartphone. The architecture of this accessory can be divided into three main layers:

- Sensor layer
  - CO Gas Sensor
  - H2S Gas Sensor
  - Temperature sensor
  - Pressure sensor

  - Humidity sensor

- Microcontroller layer
  - Data acquisition
  - Data storage
  - Data transmission to receiver

- Analyzer layer
  - Visualization mode
  - Data management / persistent storage
  - User interface

The presented gas measurement device consists of several components. The main parts are gas concentration sensors, namely MQ-9 sensor for CO concentration and ZE03-H2S & MQ-136 for H_2S accumulation [185, 186]. Sensor changes its conductivity thanks to usage of tin dioxide (SnO_2) as responsive material. Changes in resistance are tranformed to the voltage output of the sensor and based on that the concentration of gases mentioned above is determined. In addition, DHT-22 temperature & humidity sensor is used for estimation of the value of temperature in range $-40°C$ to $80°C$ and humidity from 0% to 100% $\pm$ 1% (see table 10). Sensors are connected directly to Arduino M0 Pro with 32-bit ARM Cortex M0 processor with clocking of 48 MHz and 32kB SRAM memory. Sensors described above are connected to analog pins. Other devices, such as HC06 Bluetooth module [187], SD card reader use UART & SPI protocols. System is powered with stable 5 V DC from RAXFLY 10,000 mAh powerbank. Environmental conditions are measured at a frequency of 1 Hz. Then, PPM values are computed, and the data frame is transmitted to the smartphone via Bluetooth. To protect against data corruption in the extremely harsh and variable mine environment, the entire file with measurements is sent to the smartphone every 5 minutes for redundancy.

Smartphone with the dedicated application states for a medium to visualize data online for the mining crew. The screenshoot of the crafted application for Android operating system is presented in Fig. 39a. The UI displays gas concentrations and archive data on smartphone storage using Bluetooth connection [188]. In addition to this, some smartphone built-in sensors are also used to enhance the dataset. IMU sensor with information about acceleration, velocity is managed with 10 Hz of measurement frequency. An application has some functionality created for handling gas

Table 10: Gas measurement system components [175]

Component	**Role**
Arduino M0 Pro	Board
MQ9-Sensor	CO concentration
MQ136-Sensor	H_2S concentration
ZE03-H2S	H_2S concentration
DHT 22	Temperature
	Humidity
HC06	Bluetooth controller
Polulu SD Card Reader	SD data acquisition

concentration thresholds. In the case of the emergency state and hazardous gases increases above the permissible values, the app makes a phone vibrating and the background start blinking red.

Fast prototyping of measurement units is not only related to the usage of custom electronic devices with the dedicated software. It includes technologies for rapid manufacturing, i.e. printing custom case for on-board computer. To achieve that, 3D printing technology is used to prepare a casing to protect all measurement system components from harsh mining environmnent as well as enable the environmental sensors to operate correctly. For that case, a 70 × 75 × 67 mm 3D-printed container with holes for sensors and diodes is created as can be seen in Fig. 38. Polyactic acid (PLA) as a core material is used, because it has mechanical properties suitable for use in the mine area. Nevertheless, it is worth mentioning that PLA is a biodegradable plastic with an exemplary physical parameters for thermoplastic forming process [189, 190]. In accordance with the Regulation of the Ministtry of Energy of 23 November 2016 (Chapter VI), the degree of protection of the device must not be less than IP 54 [191].

Software for Arduino board is written in C language using the integrated development environment (IDE) for embedded project, namely platformio.org to increase capabilities and manage the software project in more efficient way [192]. This IDE, as an add-on for Visual Studio Code, enables rapid application development with a variety of boards and microcontroller models. Moreover, it helps with smart features to maintain libraries and perform code completions to gain the overall software project maintenance. Second part of the created software is an application for

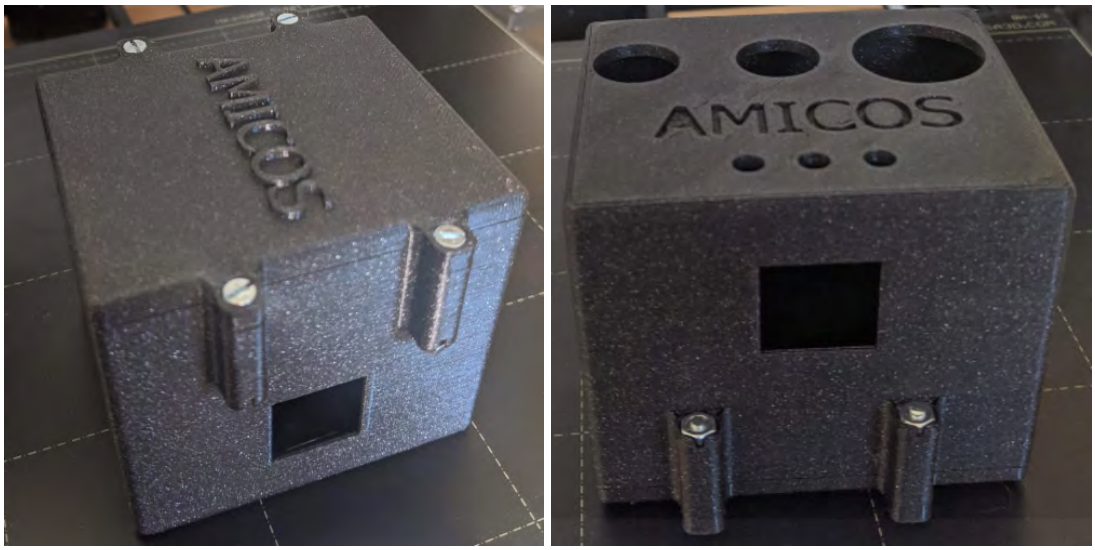

Figure 38: Bottom and top side of 3D printed case for the gas measurement unit [175]

data visualization and logging. Owing the fact that more than 70% of mobile phones use Android operating system, this system is chosen for the dedicated application [193]. This approach allows for unlimited opportunities to manage information to other applications, such as cloud provider storages (see Fig. 39a, 39b). To achieve this, the MIT App Inventor, a block-based coding platform for mobile app development, was utilized. It allows for the rapid creation of mobile applications. Within the MIT App Inventor, blocks of code for Bluetooth connectivity and data acquisition from IMU sensors were added. When a new data frame from a microcontroller is sent, data visualization occurs immediately. In the background, the app records the current values from sensors and smartphone's sensors: acceleration and velocity every 100 milliseconds. Other key features of the application include measurement data management, basic visualization in a text field, and data plotting.

(a) Android application for data visualization.

(b) General scheme of the system.

Figure 39: Example of using the smartphone application for underground gas measuring system [175]

5.3.5 Prototype of rotating lidar mechanism for an inspection robot

In this section, the mechanism of rotating lidar for the usage on the wheeled robot for mining machinery inspection is presented. The most emphasis is set to connect the hardware, namely the lidar and integrate it into Robot Operating System (ROS) [194]. In this work, two main robot application cases for the mining industry are considered: mapping system generation for the robot's locomotion purposes and mining transportation systems autonomous inspection. Owing that, the precise map of the surroundings is necessary and for that purpose the prototyped lidar mechanism is revealed.

First approach includes an adjustable mapping system with the usage of additional, controlled rotation of the lidar device around its longitudinal axis (see Θ_2 axis in Fig. 40). In standard working operations a lidar uses beam rotation around Θ_1 axis. Thanks to that additional movement, fully controlled by operator (using frontend on tablet or parametrizing the script with specific value), it is possible to increase the effective field of view (FoV) closely up to the point of full-spherical FoV. The work uses a 16-line Velodyne VLP-16 lidar and its rotational movement is executed by Robotis Dynamixel AX-12A servo drive. Assembly method is presented in Fig. 41a. Lidar is attached on 3D-printed stand, which is press-fit mounted on a drive pin. On the rear side of the grip joined with 5 screws, the servo drive is placed and this part of the case is mounted on rail with 4 screws to aluminium profile on the inspection robot's mast. The achieved movement resolution is 0.29° [195]. Owing the fact of mounting method limitation, the rotation scope is limited from -90° to $+90^\circ$, where 0° stands for the horizontal position. The voltage supply is separated from robot power system to 19V (for PC) and 12V (for Lidar and other sensors) levels. It is achieved thanks to the usage of DC/DC step-down converter and power supply coming from 24 V DC power mounted inside the inspection robot chamber.

The lidar data reading system structure is shown in Fig. 41b. Lidar data is sent via Ethernet cable using the user datagram protocol (UDP). This approach helps to receive the highest data transmission possible. In parallel process, the current inclination angle from the actuator is transmitted via USB port with usage of half-duplex UART converter. Procedures described above are orchestrated by ROS and uses the control software written in Python programming language with some extents to bash snippets of code and XML notations for process management within the operating system. Moreover, the software allows to setup configuration parameters from the set value sensor position to aregular spinning around the Θ_1 axis. The current angular position feedback is utilized to dynamically create the rigid body transformation between the lidar and the robot's base reference frame. It enables mapping within the robot frame and offers an initial

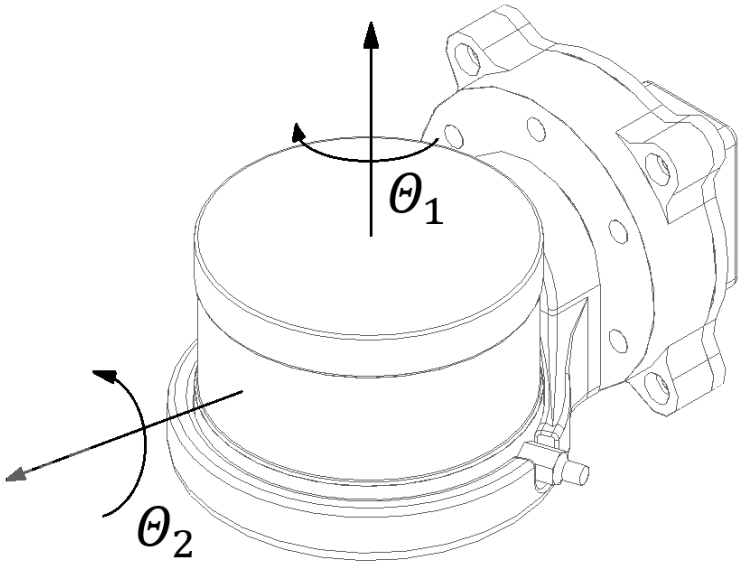

Figure 40: Lidar rotation axes diagram [196]

approximation for transformations between successive lidar positions in a global reference frame, as calculated by the SLAM algorithm.

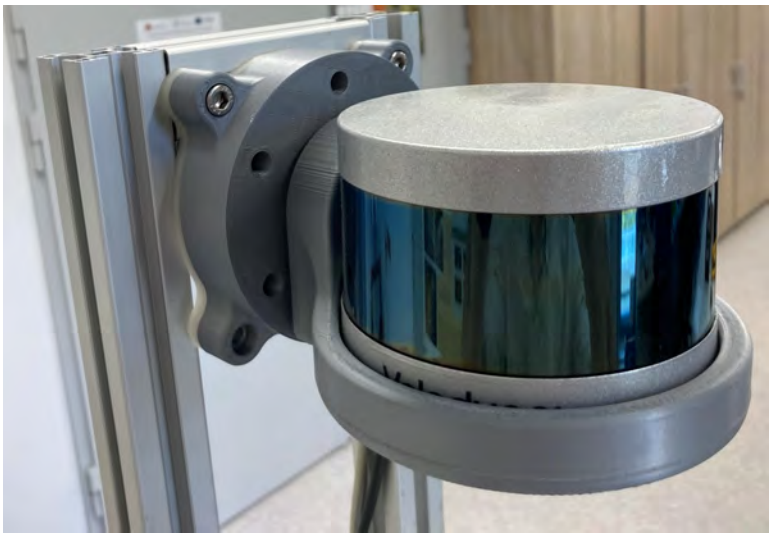

(a) Lidar with 3D printed grip mounted on the robot

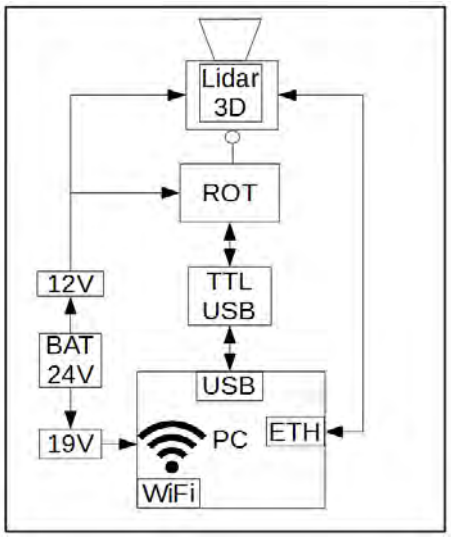

(b) Lidar data reading system structure

Figure 41: Lidar usage on inspection robot [196]

6 Data processing methods

In this section, the data processing steps for the selected use cases are presented. Data transformation involves raw data handling, the initial analysis of the dataset as well as the required steps to achieve the results described in Section 7.

6.1 Electric current consumption data processing for drilling machine

Data for drilling rig machine is measured on one machine's power supply conductor. Current measuring clamps sends the voltage signal to measuring device to the ADC converter. Next to this, the device converts the measured voltage data to digital voltage representation and saves in .csv files with timestamp headers. Electric current consumption data processing flowchart is presented in Fig. 42. The source signal is modulated sine signal. The carrier sine wave is defined as in the following equation:

$$y(t) = \mathbf{A}\sin(\omega t + \phi), \tag{1}$$

where $\mathbf{A}$ is a signal amplitude, $\omega = 2\pi f_c$ is the angular frequency, and $\mathbf{f_c}$ is a sine signal frequency expressed in Hertz. Following that, the amplitude-modulated signal $\mathbf{x(t)}$ using a carrier $\mathbf{y(t)}$ and modulating signal $\mathbf{m(t)}$ is represented as:

$$\mathbf{x(t)} = (\mathbf{A} + \mathbf{m(t)}) \cdot \sin(\omega t + \phi). \tag{2}$$

Finally, the carrier frequency is $\mathbf{f}_c = 50Hz$, and amplitude value $\mathbf{A}$ can be transformed to current consumption via root mean square (RMS) signal value calculation.

Owing that, the demodulation of the measured discrete signal $\mathbf{X}$ is obtained thanks to upper envelope calculation using Hilbert transform [197].

$$Env(X) = abs(\mathcal{H}(X)). \tag{3}$$

The next phase of the data processing flow is thresholding the signal based on its density distribution estimation. With usage of Gaussian Kernel Density Estimator (KDE), the empirical probability density function for a random variable can be assessed :

$$\hat{f}(x) = \frac{1}{\mathbf{nh}} \sum_{i=1}^{n} \mathbf{K}\left(\frac{x - x_i}{\mathbf{h}}\right), \tag{4}$$

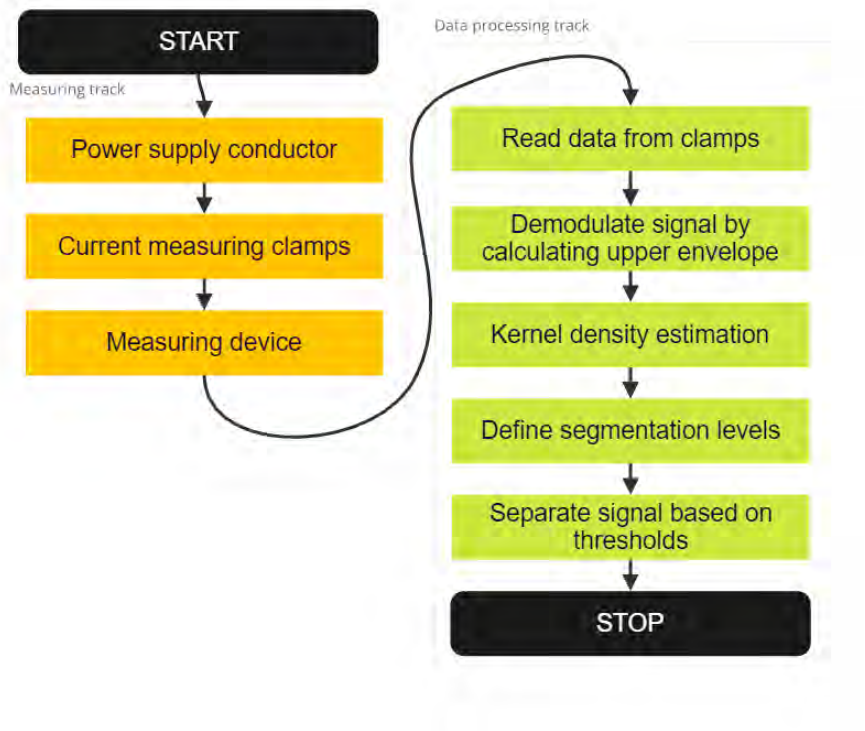

Figure 42: Current measurement and data processing flowchart

where $\mathbf{K}(\cdot)$ is kernel smoothing function, $\mathbf{n}$ is vector length, and $\mathbf{h}$ stands for the bandwidth [198]. $\mathbf{h}$ bandwith is calculated following the Silverman's rule of thumb for Gaussian-like signal distribution [199]:

$$h = (\frac{4\hat{\sigma}^5}{3n})^{\frac{1}{5}} \approx 1.06\hat{\sigma}n^{-1/5}, \tag{5}$$

where $\hat{\sigma}$ is samples standard deviation, and n number of samples.

It has been observed that during execution of the consistent task, the overall value of current consumption signal for a given machine remains at relatively constant level. Hence, signal segmentation is performed with usage of thresholds between different levels of the signal. These thresholds are calculated as local minima of the signal distribution function. Considering the drilling rig machine, the pattern of operation can be divided into three regimes: idle, pre-drilling and drilling state.

For the given signal (Equation 2) and two thresholds T_1 and T_2 (with $T_1 < T_2$), the threshold-based classification of current consumption into 3 classess can be defined as:

$$\mathbf{C} = \begin{cases} c_0 & \text{if } x_i < T_1 \\ c_1 & \text{if } T_1 \leq x_i < T_2 \\ c_2 & \text{if } x_i \geq T_2 \end{cases}. \tag{6}$$

With the classess determined, a new vector $C = \{c_1, \ldots, c_N\}$ for every sample of the signal holds class indicator. After this step, the segmentation is performed by localizing of moments in time, where the value of class indicator changes. In particular, moments where $\frac{dC}{dx} \neq 0$ indicate the changes of work regime.

6.2 Procedure of data analysis of laser-based roof bolting

In this chapter, the end-to-end approach to transform raw laser data from indirect distance measasurement method to detect and interpret the bolting cycles is presented. The data processing workflow consists of 9 steps, where step 0 is only needed once during new machine onboarding. The data processing workflow is presented in Fig. 43.

Step 0: Load pressure data from the machine

Within this preliminary step, pressure data $P = \{p_1, ..., p_p\}$ of length of p from the on-board monitoring system are loaded together with timestamps every 1 second. At this step, the loaded machine data are upsampled to be consistent with f_L=8 Hz sampled laser data. Upsampled points are populated with usage of linear interpolation. This step is only needed to compare the machine's operating parameters with the new laser readings. For the next iterations it can be omitted.

Step 1: Load raw laser data

Data stored on the designed measurement device is loaded in the form of .csv files. The laser signal $\mathbf{L}$ of the length of l with corresponding timestamps is described in Equation 7 . The detailed files and data description can be found in Section 5.3.2. The subsequent stage in preparing raw data involves data cleaning and transformation to address the characteristics of real data. In Fig. 44, the raw data taken from laser measurement unit is presented.

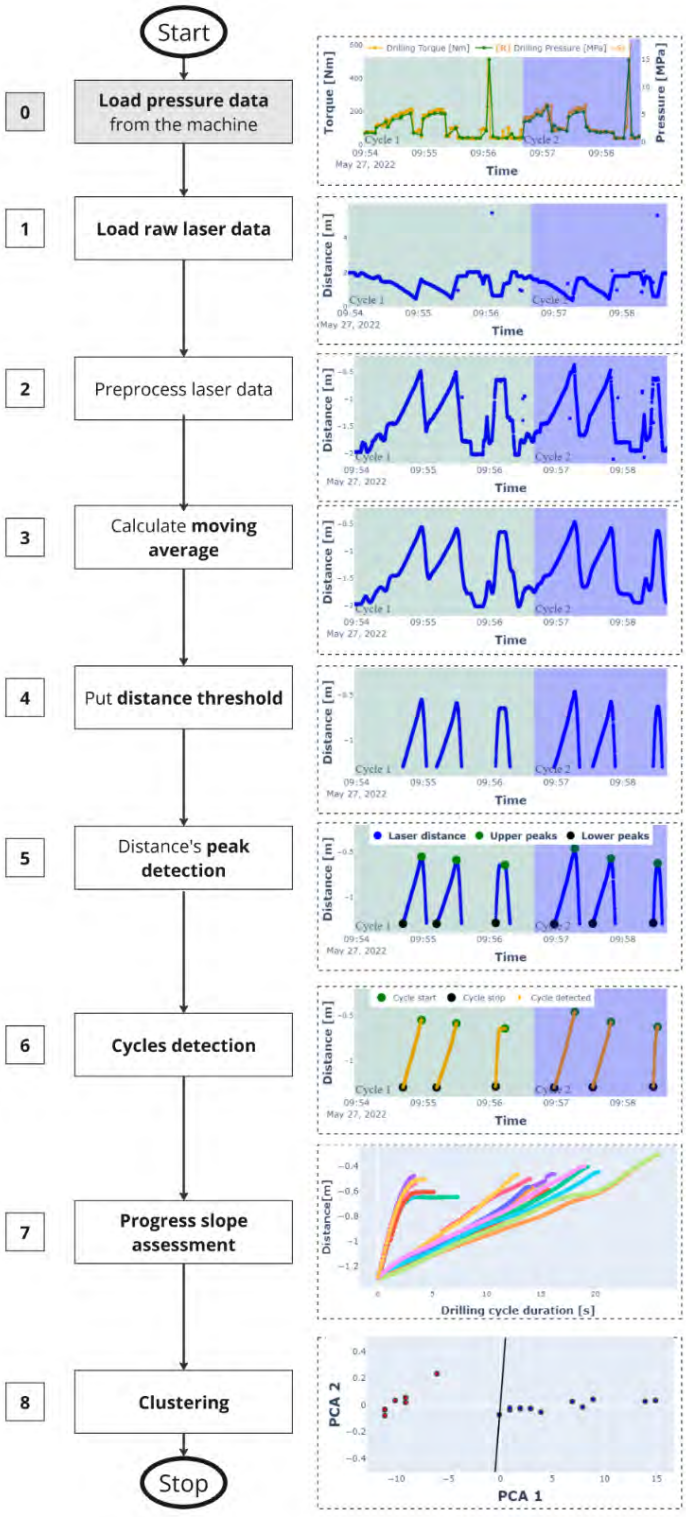

Figure 43: Laser distance measurement data processing [174]

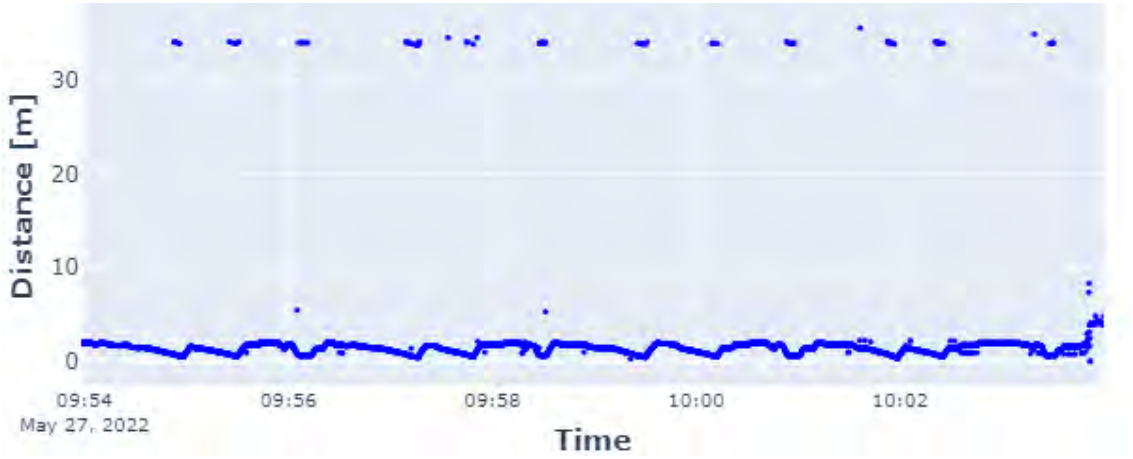

Figure 44: Fragment of raw laser data [174]

$$\mathbf{L(t)} = \begin{bmatrix} (L(t_1), t_1) \\ (L(t_2), t_2) \\ (L(t_3), t_3) \\ \vdots \\ (L(t_l), t_l) \end{bmatrix}. \tag{7}$$

Step 2: Preprocess laser data

The first step of data processing is to handle incorrect data (i.e. NaN or outliers). When the laser measurement route is disturbed by the presence of the dust, or the bolting rig turret is not pointed at the ceiling, it is needed to remove these points. Moreover, during the measasurement, the laser is headed towards the corridor' ceiling. Owing that, the outliers are found when the distance indicate the value higher than $\mathbf{y_{max}} = 4m$. To interpret data fusion with the machine's on-boarding monitoring system correctly, it is necessary to handle outliers in machine data either. For that reason, an additional step is performed to alter data outside the valid scope (following technical description of the machine) and replace it with maximum value. Thanks to that, data connected to temporal overloads of machine are handled, what improve the overall cycles interpretation significantly. The final phase of this data processing step is the upsampling of machine data. The data acquisition occurs at different frequencies — 8 Hz for laser data and 1 Hz for machine data

— linear interpolation is used to synchronize timestamps and values. Newly added data points are calculated on the basis of linear interpolation of the values of intermediate points, enabling the merged data to be uniformly sampled at 8 Hz. All steps described above are displayed in the form of pseudo-code snippet in Algorithm 1.

Algorithm 1: Preprocess laser data

for *n* ***in*** *1:N* **do**
  `/* for each data file... */`
  for *k* ***in*** *1:K+1* **do**
    `/* for each sample greater than thresholds... */`
    if $\mathbf{L_k} > max(\mathbf{L_k})$ **then**
      `/* Assign value to max value */`
      $\mathbf{L_k} = max(\mathbf{L_k})$
    `/* Change reference point as ceiling level */`
    $\mathbf{L_k} = -1 * max(\mathbf{L_k})$
    `/* Insert linear interpolation */`
    $\mathbf{L_k} = L_{k-1} + \frac{(t_k - t_{k-1}) * (L_{k-1} - L_k)}{t_k - t_{k-1}}, for \quad \mathbf{L_k} = None$

Step 3: Calculate moving average

To mitigate the influence of outliers, a moving average is calculated on the laser data to eliminate individual laser points affected by i.e. dust or other local process disturbances. The value of $\mathbf{W_1}$ (length of moving average window) is aligned with the shortest data interval in regard to the shortest drilling subprocess to be identified, ensuring it is practical from a process perspective.

$$SMA(l) = \frac{1}{W_1} \sum_{i=l-W_1+1}^{l} L(i), \tag{8}$$

where $L(t) = [L(t_1), ...L(t_l)]$ is a vector of preprocessed laser data and i is the iterator over the samples within the window.

Step 4: Setting of the distance threshold

Following the bolting process parametrization, the range of interest is defined as $T_R = range(D, E)$. That range corresponds to distance between the laser mountage point and the mine roof. Variable D references to the minimum, and variable E to the maximum penetration of the

bolt drill bit. These fixed values result from the machine's dimensions as well as mountage point in relation to tool front (see Table 3). Furthermore, the individual bolting rod can extend to a length of R meters, thereby providing this range.

$$L_2(t) = \begin{cases} SMA(t), & \text{if } D \leq SMA(t) < E \quad \& \quad |D - E| < r \\ \varnothing, & \text{otherwise} \end{cases}, \tag{9}$$

where L_2 is a vector of laser signal with thresholding applied, $SMA(t)$ is laser signal with moving average applied, D - lower distance threshold, E - upper distance threshold, r - bolting rod length, and $\varnothing$ is defined as an empty set.

Step 5: Distances' peak detection

In this step, the position of the start of the segment (PL) and peak value of the segment (PU) are determined. Peak value PU is found as a maximum value of the segment. Therefore, the maximum drilling duration is limited by $\Delta t = t_{i+W_2} - t_i$ seconds, what corresponds to the longest one hole drilling duration detected. In a similar way, the lower peaks PL are calculated as the smallest distance from A lower threshold every W_3 points (see Fig. 45). It is defined as follows:

$$[PU(c), \quad C_E(c)] = \max(L_2(t_i), L_2(t_{i+1}), \cdots, L_2(t_{i+W_2})), \tag{10}$$

$$[PL(c), \quad C_B(c)] = \min(L_2(t_i), L_2(t_{i+1}), \cdots, L_2(t_{i+W_3})), \tag{11}$$

where c is index of the cycle, PU is vector of upper peaks identified, PL is vector of lower peaks identified, $L_2(t)$ is vector of laser data with thresholding applied (Step 4), W_2 is a length of peak detection window (number of samples for upper peaks), and W_3 for lower peaks. Following formulas 10 and 11, where $\min()$ and $\max()$ returns a timestamps of corresponding values of PL and PU, the values of C_E and C_B are obtained automatically.

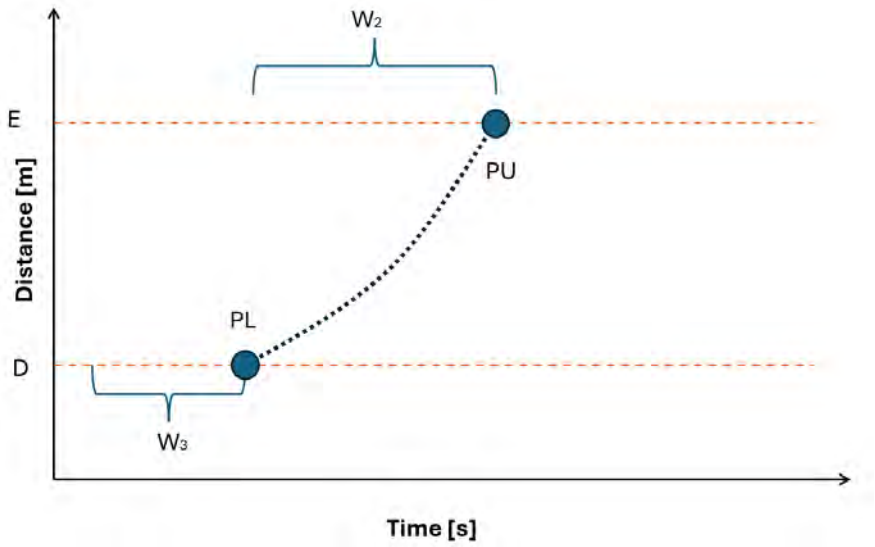

Figure 45: Parametrization of peak detection

Step 6: Drilling cycles detection

Subsequently, after collecting the results from Step 5 it is possible to obtain all points for each cycle $C(c)$ based on values extraction between D (lower threshold) and E (upper threshold) using Formula 12:

$$\mathbf{C(c)} = \{t \in (\mathbf{C_B}(c), \mathbf{C_E}(c))\}, \tag{12}$$

where c is index of cycles identified.

Step 7: Drilling progress slope assessment

Each cycle C interpretation becomes straightforward thanks to linear interpolation using least-squares regression of Formula 13.

$$\widehat{y}(t) = \beta(c) + \alpha(c)t, \tag{13}$$

where t is defined in $C(c)$, y is a part of L_2 segmented for a given $C(c)$, $\hat{y}$ is the linear function estimated for y, $\beta(c)$ is a intercept point, and $\alpha(c)$ is an estimated drilling progress slope.

As an additional parameters describing each cycle determined, the Pearson correlation coefficient (Formula 14) and the duration of cycles (Formula 15) are calculated [200].

$$\mathbf{PCC(c)} = \frac{\sum_{k=1}^{n(c)}(y(k)-\overline{y})(\widehat{y}(k)-\overline{\widehat{y}})}{\sqrt{\sum_{k=1}^{n(c)}(y(k)-\overline{y})^2 \sum_{k=1}^{n(c)}(\widehat{y}(k)-\overline{\widehat{y}})^2}}, \tag{14}$$

$$n_L(c) = f_L * (C_E(c) - C_B(c)), \tag{15}$$

where $\hat{y}$ is the estimator of y, $\bar{(\cdot)}$ indicates the mean value, c is index of the cycle, f_L is frequency of laser signal, and $n_L(c)$ is the length of the c^{th} cycle.

The final assessment is built upon the following parameter calculation for each cycle determined: α, β, PCC, n_L.

Step 8: Clustering of regression results

At this stage, for clustering purposes, the slope parameters from Step 7 are used. The next part of data preparation is usage of min-max method to normalize coefficients [201]. Additionally, a Principal Component Analysis (PCA) is calculated within data processing pipeline for 4 input parameters: α, β, r, n_L [202]. Finally, K-means clustering, an unsupervised clustering algorithm, has been selected. The number of clusters is configured $k = 2$ to appropriately differentiate between the subcycles of bolting operations, specifically the drilling of the first or second bolt rod and the tightening of the rock bolt. The obtained clustering labels are treated as a subcycles detection labels.

As a result of the above data processing steps and with the usage of the unsupervised learning technique, it is applicable to enable the automated clustering dataflow for drilling regimes of bolting rigs working under real mine conditions.

6.3 Data processing method for electric current measurement at the mining section

In this section, data processing methods for electric current measurement at the mining section are revealed. As compared with Section 6.1, sensor, measurement unit, and initial data processing steps remain unchanged. Owing that, the raw data transformation is covered by Formulas 1, 2, and 3. The next data processing steps covering raw current signal handling aiming to perform analysis in frequency domain is represented in the form of flowchart in Fig. 46.

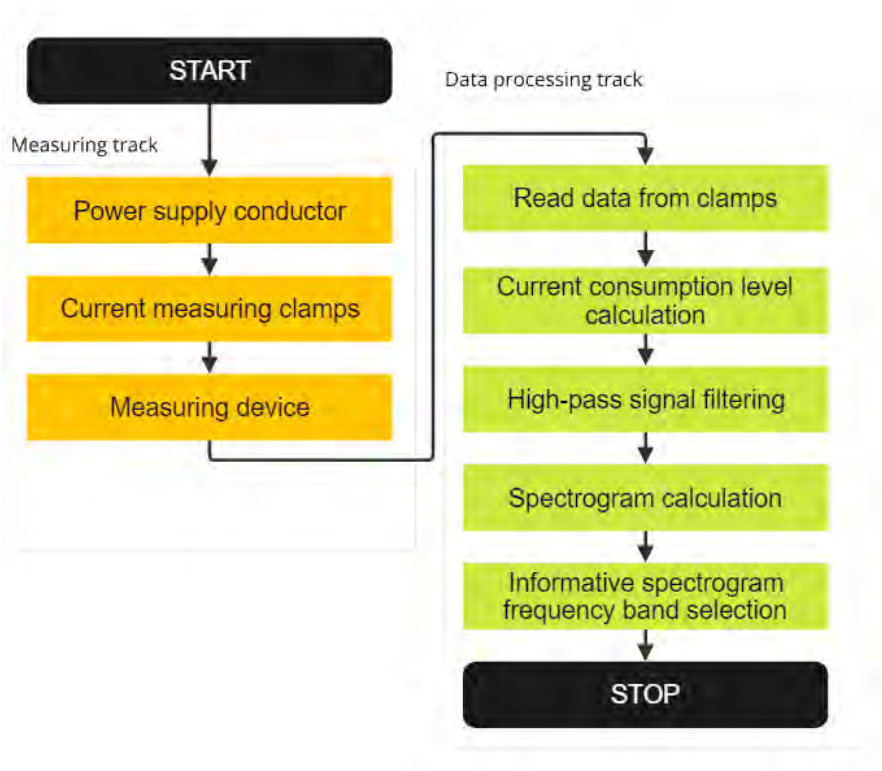

Figure 46: Current measurement and data processing flowchart

Before starting analysis in frequency domain it is necessary to apply digital filter in order to limit the impact of the signal carrier frequency f_c in further analysis. For that purpose, Chebyshev Type II filter is selected. The transfer function $H(z)$ for the filter given is [203]:

$$H(z) = \frac{b_0 + b_1 z^{-1} + b_2 z^{-2} + \cdots + b_d z^{-(g-1)}}{a_0 + a_1 z^{-1} + a_2 z^{-2} + \cdots + a_d z^{-(g-1)}}, \tag{16}$$

where: z is a complex number, $a = [a_0, a_1, a_2, \ldots, a_r]$ and $b = [b_0, b_1, b_2, \ldots, b_r]$ are row vectors of coefficients, $d = e + 1$ is number of samples, and g is filter order.

Data analysis in frequency domain starts with Short-Time Fourier transform (STFT) calculation [204]. For dicrete signal X it is defined as:

$$STFT(t_P, f) = \sum_{i=1}^{n_w} X[\tau + i] w[i] e^{\frac{2j\pi fi}{N}}, \tag{17}$$

where w is the Hamming window, n_w is length of the window, i is the iterator index, L is number of signal points, j is an imaginary unit, $t_P = [1, \ldots, T_P]$ is vector of time points, and $f_c = [1, \ldots, F]$ is the frequency bin.

Hence, the output of spectrogram matrix has the following form:

$$\text{Spec} = |STFT|. \tag{18}$$

In order to keep only the columns corresponding to frequencies f_{lim}, the limited spectrogram is defined as:

$$\mathbf{Spec}(t_P, f_{lim}), \quad f_{lim} \in (f_{bc}, f_{\max}), \tag{19}$$

where $\mathbf{Spec}$ is the original spectrogram matrix, f_{bc} is the band cutoff frequency, and f_{max} is maximum frequency from Nyquist criterion.

Data prepared with the manner above are directly used as dataset for machine learning experiments. Based on the final model (group of models) used, there are needed additional data transformations to cover specific model's implementations needs. They may lead to i.e. converting datatypes to specific ones, updating the column names etc. Nevertheless, these transformations do not change the dataset itself and thus are not covered in this section. Hence, transformation pipeline for classification dataset (see Fig. 75) is treated separately.

6.4 The data processing methodology for hazardous gases measurement

For this particular dataset, the data processing methodology is divided into two major parts. Firstly, the most emphasis is to set up a software calibration of gas sensors. Secondly, there are presented several steps to handle IMU data. Following results obtained in Section 7.4, these steps can be processed at a smartphone application runtime to separate more demanding calculation from IoT device.

Gas sensors return voltage signals, which vary during the changeable gas concentration given. According to sensor documentation, its output is linear, but, as with every gas sensor, additional calibration is required with the use of certified gases under controlled conditions. In this case, a software-based calibration is made. As a ground truth, the output of calibrated gas sensors used by the ventilation mine crew is utilized.

The estimated output of gas concentration GC for a given raw digital output O based on calibrated gas sensor reference V is calculated using the following Formula:

$$GC(i) = V_{min} + \left(\frac{O(i) - O_{\text{min}}}{O_{\text{max}} - O_{\text{min}}} \right) (V_{max} - V_{min}) \,, \tag{20}$$

where:

- O is the given raw digital output from the sensor,
- O_{min} is the minimum raw digital output value,
- O_{max} is the maximum raw digital output value,
- V is the reference from calibrated sensor,
- V_{min} is the minimum reference value,
- V_{max} is the maximum reference value,
- GC is the estimated sensor output.

For every gas sensors, namely CO and H_2S, reference values are obtained from the dataset during the experiment. Data transformed in this manner is later visualized on smartphone application. The advantage and limitations of the proposed calibration procedure are described in more detail in Section 5.2.4.

Second part of data transformation is a distance calculation covered by miners during the shift. Data source is an Inertial Measurement Unit (IMU) sensor from smartphone. To calculate the estimated step length, the empirical relationship with vertical acceleration is used [205, 206]:

$$s = U \cdot \sqrt[4]{a_{\max_{v_i}} - a_{\min_{v_i}}}, \tag{21}$$

where s is an estimated step length, $a_{\min_{v_i}}$ and $a_{\max_{v_i}}$ are vertical acceleration values during $i - th$ step, and constant U from calibration of the given user. Information about every step is taken from Android operating system $TYPE\_STEP\_DETECTOR$ variable. Following that it is possible to calculate the distance covered using smartphone IMU sensors.

As a matter of fact, this section describes the overall data processing steps of received data. There is no data analysis performed. In fact, the main aim of receiving new data has been done. Subsequent to the example described in this section, the next steps can be performed to enable data storage on Cloud Resources. The implementation can be established within the scope of the smartphone application for visualization. Data synchronization with a remote data repository can

take place, for example, after each work shift when the phone has access to the network and further data transmission is possible.

6.5 Methods of processing of data from the integrated sensors of the inspection robot for mining transportation systems

In this section, data processing methods related to the integration of sensors with a Robot Operating System (ROS) are presented. This hardware integration and low-level system programming was necessary to make data acquisition from rotating lidar possible. As an outcome, the result obtained by research team based on the proposed integrations are described in Section 7.5. Fig. 47 provides a general overview of the steps corresponding to the unification of the data with common ROS utilities.

In the ROS ecosystem, every sensor is connected to the host as a ROS node. Usually, sensors are set as `publisher` and transmit data to the operating system. In this case, LiDAR and servo are connected to the main computer via USB/UART and publish data frames. Firstly, the direct sensor communication and format of date frames is configured within the driver for lidar movement. It handles several hardware tasks such as starting the communication, maintaining it, configuring sensor operating parameters, etc. These scripts are mostly written in Python / c (c++) languages to enable low-level communication with the given hardware. The next step is to start up the sensors with ROS. It is handled by `roslaunch` ROS system utility. `roslaunch` program creates a configuration list with arguments and paths with driver codes to run multiple ROS nodes at the same time [207]. The next step is configuring the `rosbag` tool to record messages between nodes. It generates one binary large object in `.bag` format of significant size per robot experiment run. At this stage, especially under real working conditions, sensors can occasionally become unresponsive, which causes in breaking the files. Thus, it is necessary to reconstruct the `.bag` files with `rosbag fix` tool. Having said that, it is worth adding this step to the automated data processing workflow, also. Finally, for further usage of the specified sensor output, the data extraction step can be performed to receive data in the different file formats [176].

Listing 1: .launch file example

```
<launch>
<arg name="rpm" default="600.0" />
<arg name="laserscan_resolution" default="0.001" />
<node pkg="rotating_velo" type="dynamixel_tf.py"
name="dynamixel_tf"/>
<node pkg="rotating_velo" type="dynamic_velo.py"
name="dynamic_velo"  output="screen"/>
</launch>
```

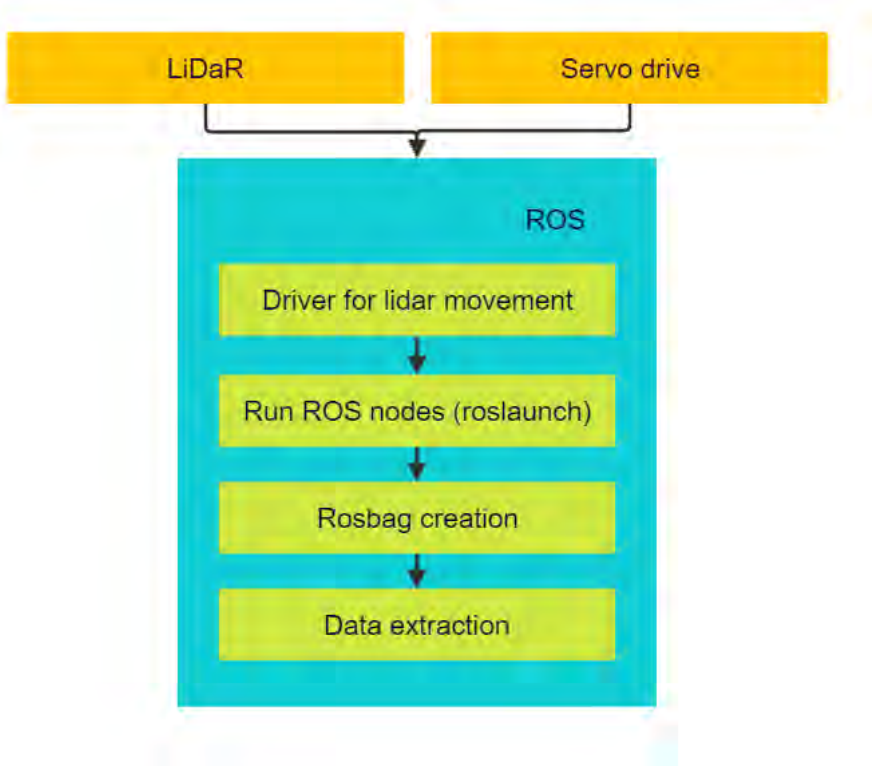

Figure 47: Sensor integration with ROS workflow

After the steps defined above, the actual data processing is performed on the LiDAR data. Based on that approach, data is available together with timestamp and synchronized with other sensor's output. Because of this, the selected methods of actuated LiDAR system utilization to perform 3D reconstruction can be used to perform more advanced data processing [208].

6.6 Cybersecurity risk assessment methodology for a mining company

Together with the enormous growth of computer science and its usage in applications in a wide variety of industries, awareness of cybersecurity arises likewise. Today, the scope of securing the digital infrastructure is often at the same stage as the physical infrastructure of the company. These changes also apply to the mining industry. The information system would never be fully resilient to cyber threats. However, the most cuminative approach is to mitigate risk and ensure the security of the core components with appropriate techniques [209]. To accomplish this, an approach to assess the risk should be noted. For that reason, in this thesis, a novel cybersecurity risk assessment methodology based on fuzzy theory is presented.

In this section the qualitative analysis of cyber threats and possible outcomes is outlined based on several levels of mining processes automation. To manage risk, the risk analysis procedure is proposed for a mining company. Using Kaplan and Garrick's approach [210] for risk assessment with fuzzy theory use and expert knowledge related to mining industry, the several cyber threats can be exemplified. Following the above, cyberattack risk analysis can be represented as follows:

$$R = \{S(i), P_S(i), M_C(i)\},\ i = 1, 2, \ldots, \Omega, \tag{22}$$

where:
R — risk,
S — a scenario (undesirable event) description,
P_S — the probability of a scenario,
M_C — the measure of consequences caused by a scenario,
Ω — the number of possible scenarios.

The risk analysis procedure suggested for a mining company is presented in Fig. 48. It consists of 3 main phases of handling the qualitative analysis of problem definition. At this point, the definition of mine automation levels with possible cyberattack scenarios and affected objects and processes is created. The next phase, the quantitative analysis, represents the core of the risk analysis procedure. Based on the expert's opinion collection, it is possible to determine the probability of a given scenario occurrence and hypothetical outcomes covering the mining company activities. The next stage of the procedure is fuzzification of risk parameters to use them for the proposed rule-based fuzzy interference system. Finally, risk score obtained related to a

given scenario is defuzzified (using the Mamdami fuzzy model [211]). The last phase, the output phase rationalization, interprets the results received and supports the management of risk decisions.

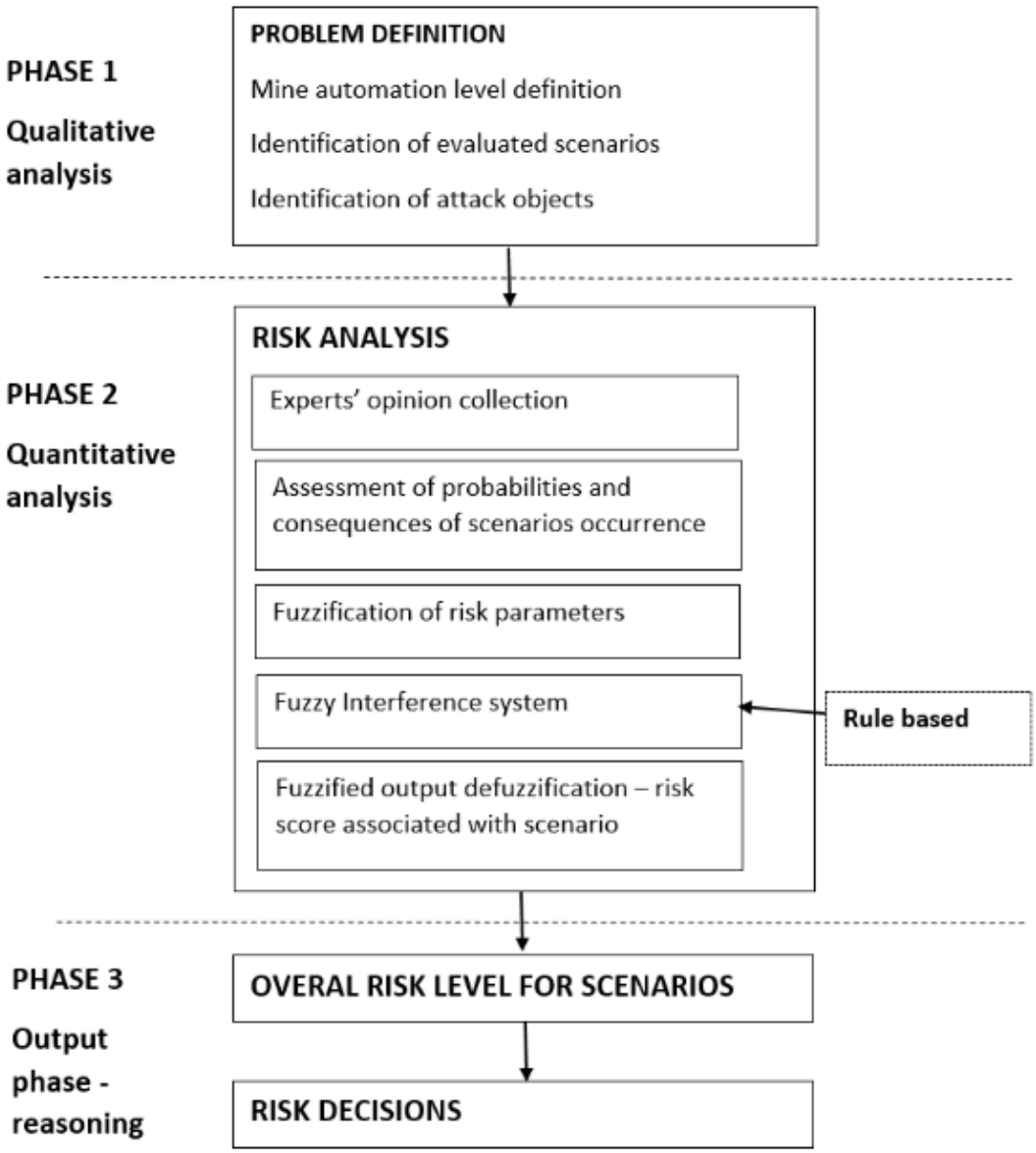

Figure 48: Cybersecurity risk analysis procedure for usage in a mining company [212]

The key part of the proposed methodology utilizes the development of mine automation levels and places greater emphasis on the digitalization of production processes. Owing that and following the literature review [213–215], the Table 11 presents a characteristics of the mine automation levels with three levels highlighted. The main features describing the realization of mining processes

are: mechanization and mining automation levels, the ability of machinery and automation control systems to communicate, and the role of the miner. Based on a mining development scenario created above, seven techniques are presented that can be used to affect the network and mining company computer systems. The attack techniques and their short description are presented in Table 12.

Following Formula 22, it is necessary to prepare a measure of probability of a scenario occurrence (Table 13) and a description of the consequences (Table 14). For scenarios probabilities and consequences, fuzzy values are presented using fuzzy set theory. It is used to perform expert evaluation on direct triangular fuzzy numbers (FN) [216]. The final risk level is specified with the usage of trapezoidal fuzzy numbers.

A triangular FN is defined as $A_z = (a, b, c)$ with a membership function of $\mu_1(\phi)$ in the formula 23.

$$\mu_1(\phi) = \begin{cases} 0 \rightarrow \phi < a \\ \frac{\phi - a}{b - a} \rightarrow a \leq \phi \leq b \\ \frac{c - \phi}{c - b} \rightarrow b \leq \phi \leq c \\ 1 \rightarrow \phi > a \end{cases} . \tag{23}$$

A trapezoidal FN is defined as $A_z = (a, b, c, d)$ with membership function of $\mu_2(\phi)$ in Formula 24.

$$\mu_2(\phi) = \begin{cases} 0 \rightarrow \phi < a \\ \frac{\phi - a}{b - a} \rightarrow a \leq \phi \leq b \\ 1 \rightarrow b \leq \phi \leq c \\ \frac{d - \phi}{d - c} \rightarrow c \leq \phi \leq d \\ 0 \rightarrow \phi > d \end{cases} . \tag{24}$$

Finally, in Table 15 a proposed risk rating category is presented with the corresponding risk to the impact of a cyber threat on the operation of a mining company versus the likelihood of an event occurring. Fuzzy values are quantified using trapezoidal FN of Formula 24.

Consequently, the usage of above-mentioned methodology is achievable to assess the risk based on the transformation of the knowledge from experts. Without a doubt, technology and all that it brings the front lines of a cyber attack would evolve and every mining company could have different

Table 11: Mine levels of automation proposed [212]

Level	Name	Description
L1	**Modern mine**	1. Limited machines and people localization possibilities. 2. Miner as an in-situ mobile machinery operator and supervisor. 3. The lack of underground communication infrastructure, process-oriented data tracking in batches (i.e. every shift). **Selected characteristics**: mining processes mechanization, computer-aided planning and maintenance, semi-automated procedures, cyclical risk and resources analysis, constant output analysis.
L2	**Real-time mine**	1. Real-time machines and people localization possibilities. 2. Miner as decision-maker supervisor. 3. An underground communication infrastructure allowing to real-time tracking. **Selected characteristics**: mining processes automatization, process-oriented with non-human maintenance production, real-time risk and resources analysis.
L3	**Intelligent mine**	1. Fully controlling system and with a partial supervison of production based on analysing the outputs of its past actions. 2. Human role is analysing data, software and intrastructure maintenance, most of the work can be performed automatically. 3. Communication between software management layer of the separate mining processes is possible and it results in an adaptative work based on a changeable input parameters. **Selected characteristics**: fully automated mining processes, only autonomous and ex situ process control, an advanced risk and resources analysis.

requirements for risk assessment. Despite the above obstacles, a risk analysis method using fuzzy logic theory can be a good starting point.

Table 12: Chosen cyber attack scenarios analysed [212]

No. Scenario	Attack technique	Description
S1	Phishing and social engineering attacks	Employing tailor-made emails or efficient social-engineering tactics to obtain confidential data
S2	Watering hole attacks (phishing)	A targeted attack on a particular group, such as employees of a specific department, resulting in the attacker interception of credentials to websites used by the team regularly uses in their work.
S3	Malvertising	Inserting harmful or malware-infected ads into reputable online networks and websites
S4	Vulnerability exploitation	Usage of the software bugs to perform control overtake by crafted program, undetectable by user or operating system
S5	System misconfiguration exploitation	Finding vulnerabilities in software that has not been patched yet and using those to breach the operating system
S6	3rd party vendors (backdoor)	Access to the internal, corporate network via backdoors - functions or programmable implemented features within devices connected to the company LAN
S7	Man-in-the-Middle (network spoofing)	Interception of communication between two nodes (usually: user and an application), by usage of prepared data reminiscent of normal communication

Table 13: Scenario occurrence probability [212]

Rating Category	Description	Fuzzy Value
P_{S1} - RARE	Could happen but probably never will	[0, 1, 2]
P_{S2} - UNLIKELY	Not likely to occur in normal circumstances	[1.5, 2.5, 4]
P_{S3} - POSSIBLE	Potential occurrence at some time in the future	[3.5, 4.5, 6]
P_{S4} - VERY LIKELY	Expected occurrence at some time in the future	[5.5, 6.5, 8)
P_{S5} - CERTAIN	Expected to happen regularly under normal circumstances	[7.5, 8.5, 10]

Table 14: Scenario consequences [212]

Rating Category	Description	Fuzzy Value
M_{C1} - NEGLIGIBLE	Minor injury, insignificant property or equipment damage	[0, 0.5, 1]
M_{C2} - MINOR	Non-reportable injury, minor loss of process, or slight property damage	[1, 2.5, 4]
M_{C3} - MODERATE	Reportable injury, moderate loss of process, limited property damage	[3, 4.5, 6]
M_{C4} - HIGH	Major injury, a single fatality, critical process loss, critical property damage	[3, 4.5, 6]
M_{C5} - CATASTROPHIC	Multiple fatalities, catastrophic business loss	[3, 4.5, 6]

Table 15: Fuzzified risk level [212]

Rating Category	Description	Fuzzy Value
R1 - LOW	The consequences are negligible within the rare or unlikely occurrence	[0, 10, 20, 30)
R2 - MINOR	Not significant consequences altogether with possible event occurrence	[20, 30, 40, 50]
R3 - MEDIUM	The probability of an event materialization is almost certain, and the consequences are minor or unimportant, OR the consequences are high, but the event is unlikely to occur	[40, 50, 60, 70]
R4 - MEDIUM HIGH	An almost certain or certain event that occurs with minor consequences or the unlikely event that may have critical consequences	[60, 70, 80, 90]
R5 - HIGH	Consequences are catastrophic or high with undoubted occurrence or almost certainly in the future	[80, 90, 100 100]

7 Results

This section presents the results obtained from experiments carried out on selected facilities and processes for underground mining. Data comes from real mining processes. Following the data processing methodologies from Section 6, there are presented results from the chosen mining processes.

7.1 Results for drilling rig electric current consumption analysis

Following the proposed measurement method (Section 5.2.1) with usage of measurement device (Section 5.3.1) in this paragraph the results obtained from the experiment (described in Section 5.1.1) are presented. A raw electric current signal taken from a drilling machine during drilling the holes is presented in Fig. 49. Raw data is the amplitude-modulated sine signal with actual current level amplitude with a carrier frequency of 50 Hz. On the graph, one can see a characteristic peak when the machine starts up, with an instantaneous current draw of around 120 A. Then, we see a section with a pulse value of about 40 A, which corresponds to the machine running at idle gear. These ripples come from the cyclic activation of the hydraulic systems that maintain constant hydraulic pressure in the i.e. drill mechanism on the drill rig. In the following sections of the diagram, it is possible to see the characteristic patterns matching to the blast holes being drilled and grouped together. The fragment of the drilling cycle corresponding to the actual drilling of the borehole is approximately 85A. Between these fragments, a so-called pre-drilling regime is evident with levels in the 60-70A range. It is related to the instantaneous current consumption associated with performing the auxiliary movements of the machine in order to drill the next hole correctly. These movements include moving the tip of the working organ by a given distance (according to e.g. blasting pattern). Moreover, this regime also includes the initial stage of hole drilling, when the drill has not penetrated the rock, and spot drilling is performed. In addition to this, at 11:30 on the graph, tool jamming in the rock was simulated, which is a common problem during drilling.

The output of signal demodulation is shown in more details in Fig. 50. Current consumption is calculated from the raw signal directly taken from Fluke's current clamp voltage output based on Root Mean Square (RMS) convertion. Blue trace corresponds to a raw sine-shaped signal, and red values are calculated using the Hilbert transform (see Section 6.1). To visually validate results, the data has been ploted together. It is presented in Fig. 51 where processed signal is compared with data from the machine on-board system.

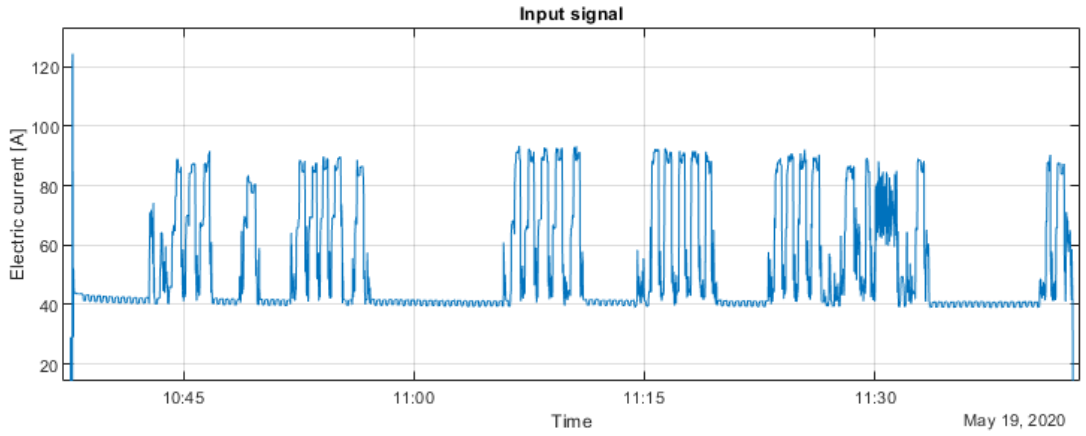

Figure 49: Electric current signal of drilling machine [173]

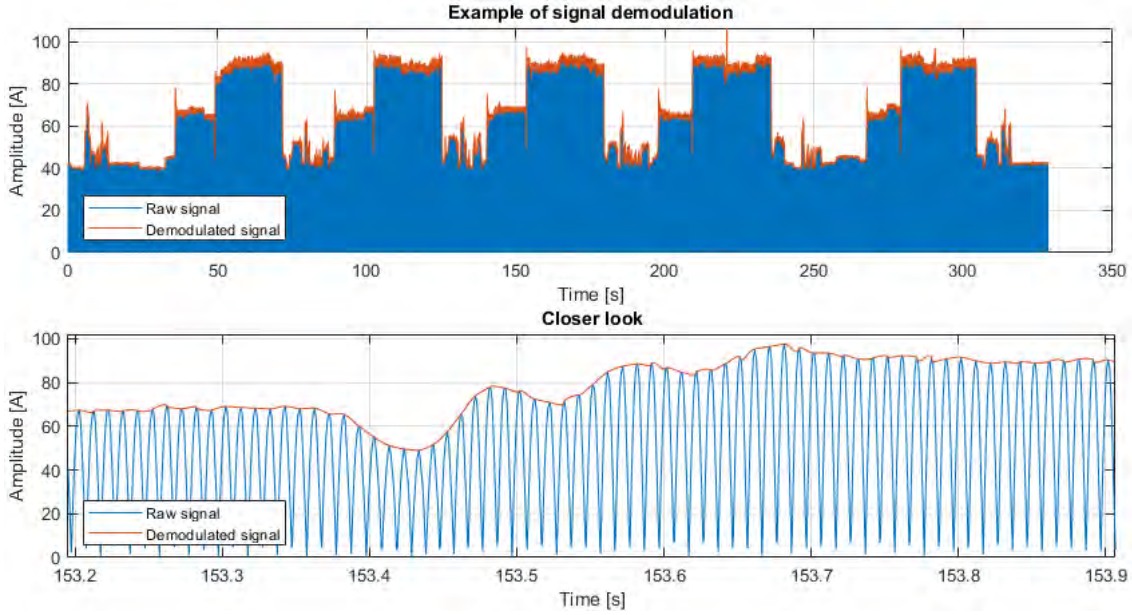

Figure 50: Electric current signal demodulation [173]

Next steps is to divide the current signal to the regimes corresponding to work regimes of underground drill rig. There are indentified three phases of the machine states during the work, namely: idle, pre-drilling, and drilling. For automated thresholding detection, the Kernel Density Estimator (KDE) is used. In Fig. 52 on y-axis can be seen the determined distribution frequency of the demodulated current signal. There are visible three modes, correlated to three machine's regimes. With two red dots, there are marked the resolved thresholds to divide these regimes. The values are of 59 A and 75 A respectively.

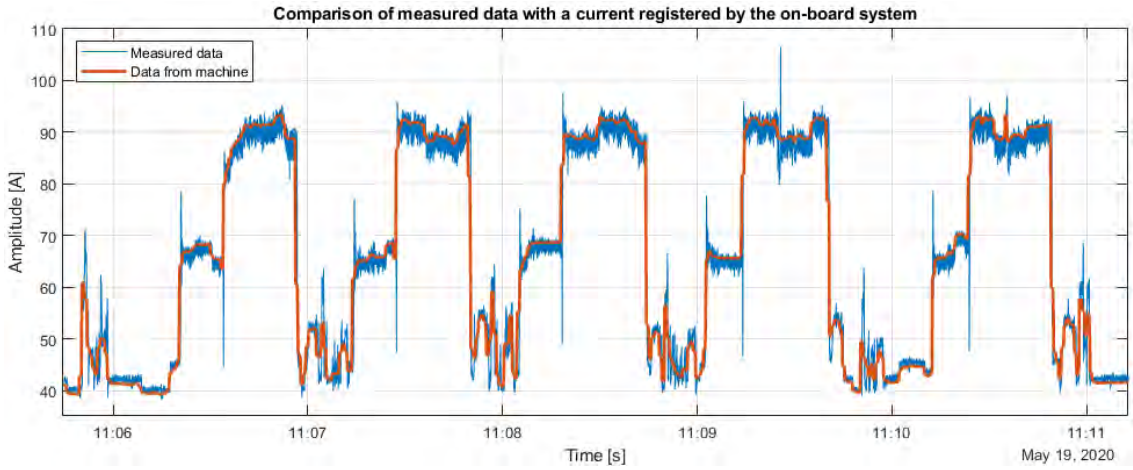

Figure 51: Electric current signal comparison with drilling rig on-board monitoring unit data [173]

Following the results above, the next step of drilling machine work assessment with usage of current measurement can be performed. An automatic regimes identification based on the calculated thresholds is completed, and its results can be seen in Fig. 53. Finally, the number of identified boreholes is estimated, in this case, 28.

The additional analysis regarding the drilling quality has been achieved. The first 14 holes (before 11:15 time on the chart's x-axis) are made with the phase of initial spot drilling performed. It is visualized as a thin blue stripes before green parts of the bottom subplot. In comparison to this, the next 5 holes are prepared without this step (it was omitted in the process on purpose). The next 4 cycles (after 11:20) are performed with very short (nearly noticeable) pre-drilling phase, what induces the longer actual drilling (green stripes). The rest of the holes completed by the machine operator are random: some of them are completed with pre-drilling phase, some not. Moreover, some duration of the holes preparation is longer or shorter than usual (managed by changeable feed power used) to cover the most possibilities of deviation feasible in underground conditions.

Finally, summarizing the obtained results, it can be viable to divide drilling rig regimes with some statistical metrics such as mean and standard deviation following the usage of KDE thresholds. In Table 16 specific metrics values are presented. These stipulated values can be reused for drilling rig work assessment during a current measurement at a mining section. This aspect is described in more details in Section 7.3.

The results of these analyses are described in detail in the article [173] as a part of the work supported by EIT Raw Materials GmbH under the Framework Partnership Agreement no. 19036 (SAFEME4MINE. Preventive maintenance system on safety devices of mining machinery).

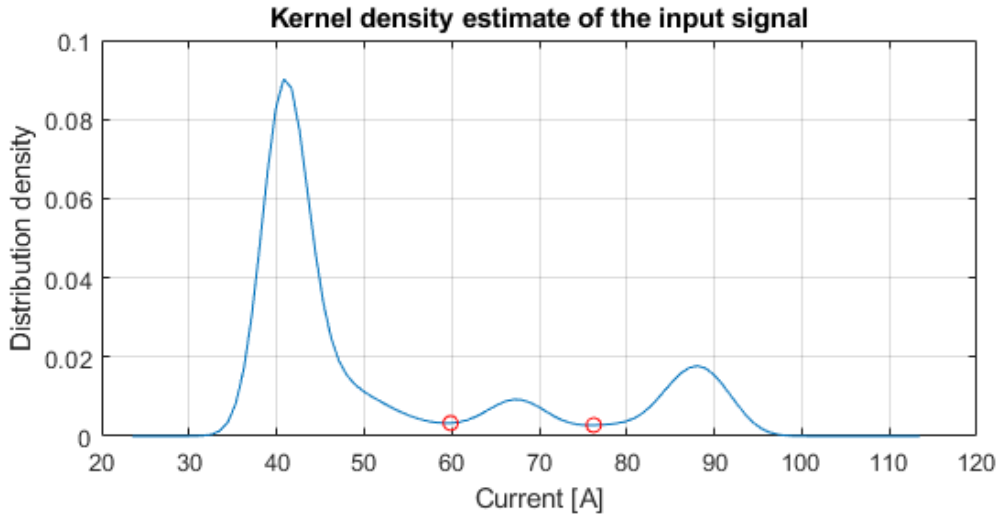

Figure 52: Results of Kernel Density Estimation of electic current signal [173]

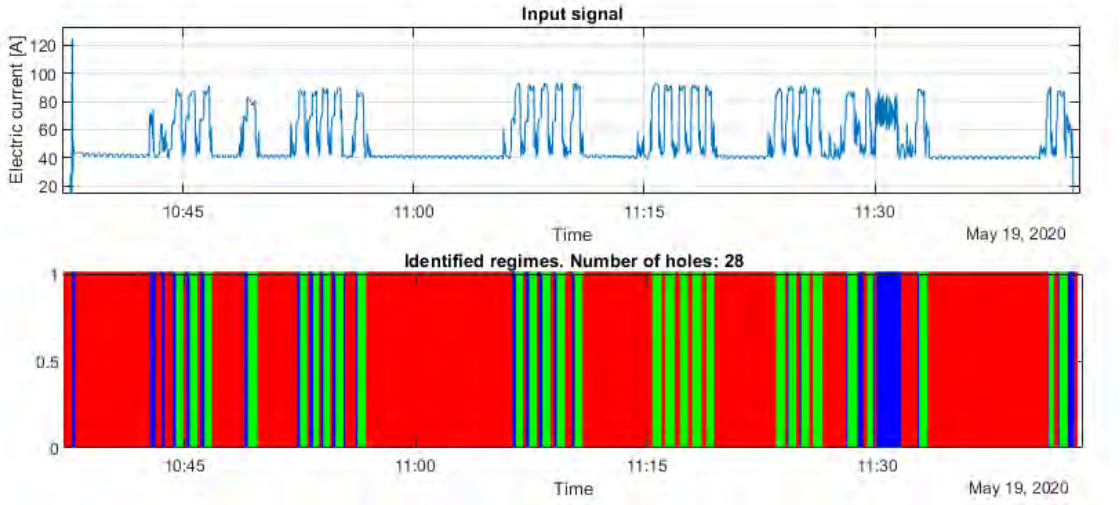

Figure 53: Current signal divided into segments following to KDE values [173]

Table 16: Statistics of the identified drilling regimes [173]

Regime	**Mean**	**Standard deviation**
Idle	43.4	6.91
Pre-drilling	67.8	5.15
Drilling	86.5	6.26

7.2 Results of analysis the laser-based roof bolting

This section describes and examines results obtained through the data processing methodology (see Section 6.2) for laser-based measurement data. There are multiple combinations of laser measurement unit mounting points tested, varying bolting rig system settings, different machine subtypes, and types of bolting processes. The most consistent and repetitive data are gathered for configurations where the laser is mounted near the bolting turret at the drill bit and the laser beam is directed towards the ceiling. This segment of the dataset, which includes 7 complete bolting cycles, is submitted further in this section.

Firstly, as an initial step (Step 0 - Fig. 43), it is needed to load pressure data from machine's measurement on-board system. It is just a preliminary step needed to verify the data correctness obtained from laser measurements as well as a reference setting for further analysis. This step is not necessary with the deployment of the laser device for the same type of bolting machine. For future usage with the same roof bolting operation scheme and type of the machine used, it can be omitted. The next step is loading and preprocessing distance measurement from laser unit. As a reference point (0 value), the ceiling level is set, and laser data is inverted to make the drilling progress more interpretable (the distance grows from negative values to values close to 0). Laser mountage point is placed $0.3m$ from the drill face, thus the highest values obtained are close to $-0.3m$ following the transformation above. The next stage is to filter out irrelevant data larger than $|y_{max}| < 4$ meters, which corresponds to the moments, when the laser beam is not pointed out on the ceiling roof, or another measurement disorders happened. Knowledge about the bolting process helps to establish correct scope of the measurement related to drilling hole preparation. Thus, $r = 1\ m$ is a drill rod length, and following the process limitation above, the cycles scope is $D = -1.3\ m$ and $E = -0.3\ m$.

An additional step is made by covering the data unification with machine measurement unit as well as an additional source - the video footage from the given process. The result of the data integration from 3 sources is presented in Figures 54 and 55. There are two traces visualized: laser distance, with changeable color following the laser measurement quality values (see horizontal legend) and orange trace of tightening torque. The measurement quality describes how the light beam if reflected back to the laser rangefinder optics. As a background color, every cycle is distinguished with the number of cycles being recorded from the video footage (text description located at the bottom).

The full bolting cycle consists of three substantial parts: two 30-seconds part of drilling the hole for one drill rod length each, and the last phase corresponding to 10-second fragment of final

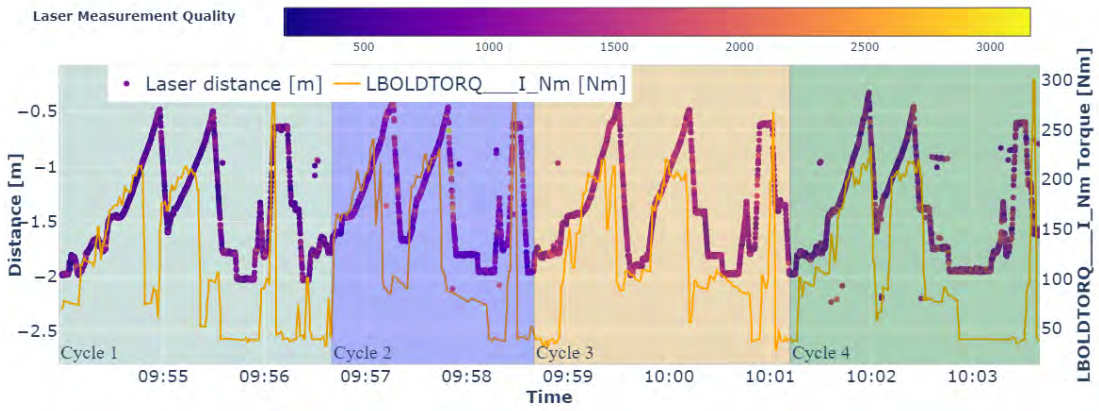

Figure 54: Cycles identification from video recording - part 1 [174]

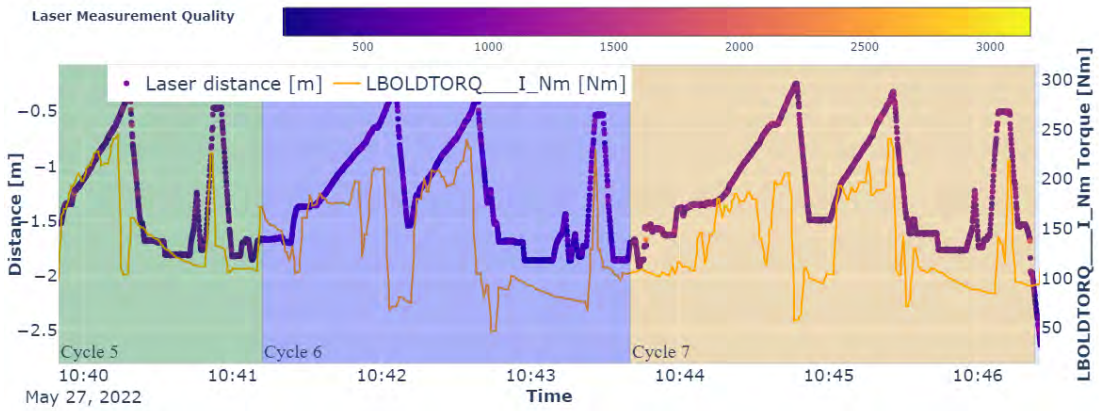

Figure 55: Cycles identification from video recording - part 2 [174]

hole deepening and tightening the rock bolt. Some swift movement between -2 and -1.7 meters to the ceiling is associated with the preparatory actions of the mining bolter's drilling turret. The largest variation in measurement quality (higher values and warmer colors) is observed during drill withdrawal and when the turret maneuvers near the corridor surface, probably due to increased dust in the laser beam's path.

In these figures, some values appear in unexpected locations because of environmental interference with the laser beam. Furthermore, the yellow trace represents the torque applied to tighten the rock bolt. Some of the peaks reaching close to the maximum 300 Nm are not significantly different from the usual torque range used for drilling and countersinking holes for bolt protection. It appears that identifying the specific step of rock bolt tightening in the process is not straightforward utilizing only machine-sourced data.

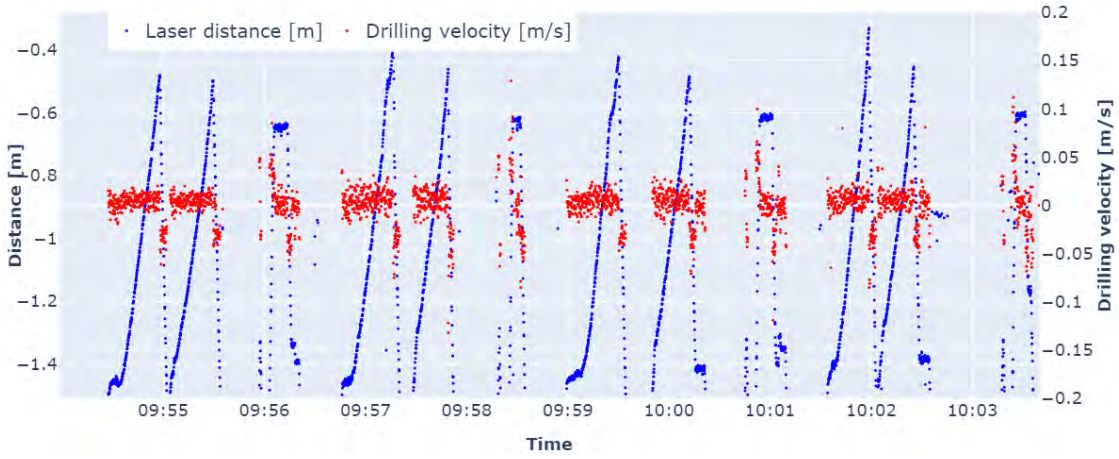

Figure 56: Bolting process distance measurement with limits applied [174]

In accordance to data validation presented above, there is a strong reason that the displacement of the bolter turret can be useful for drilling cycles identification. The measured variation in distance from the ceiling coincides with the variation in the parameter related to the tightening of the bolts. Knowing that, it may be possible to replace the usage of standard parameters such as pressure from drilling subsystems or torque data to detect bolting rig drilling cycles.

To achieve this goal, there are the next steps of the proposed data processing algorithm performed. In Fig. 56 laser data is truncated to the measurement scope related to bolt rod dimensions: $T_R = (D, E), D = -1.3\ m, E = -0.3\ m$. The time-based displacement of the bolting rig represents a sawtooth-shaped pattern. Each segment marks the process of drilling a hole corresponding to the length of the first or second rod. Although the velocity distribution (represented by the differential of the drilling progress visualized in the red trace) is examined, automatic cycle detection remains unfeasible. This difficulty arises from the variations in each trial, which depend on the rock mass characteristics and the operator's way of working. This stage could be utilized for other techniques, such as identifying rock mass discontinuities, which is beyond the scope of this work.

The next step of the proposed solution is to calculate the laser data moving average with $W_1 = 32$ samples (while the signal is being collected with f_L =8 Hz frequency). This value was determined through experimentation, bearing in mind that rock bolt tightening phase requires a maximum of 10 seconds. This method allows for the observation of characteristic inflection points in the drilling speed, as shown in Fig. 57. Subsequently, the PU detection is performed based on the preprocessed dataset using data transformed in the manner above. For that step, the $W_2 = 70$ is also experimentally determined as a maximum window size for detection of the drilling

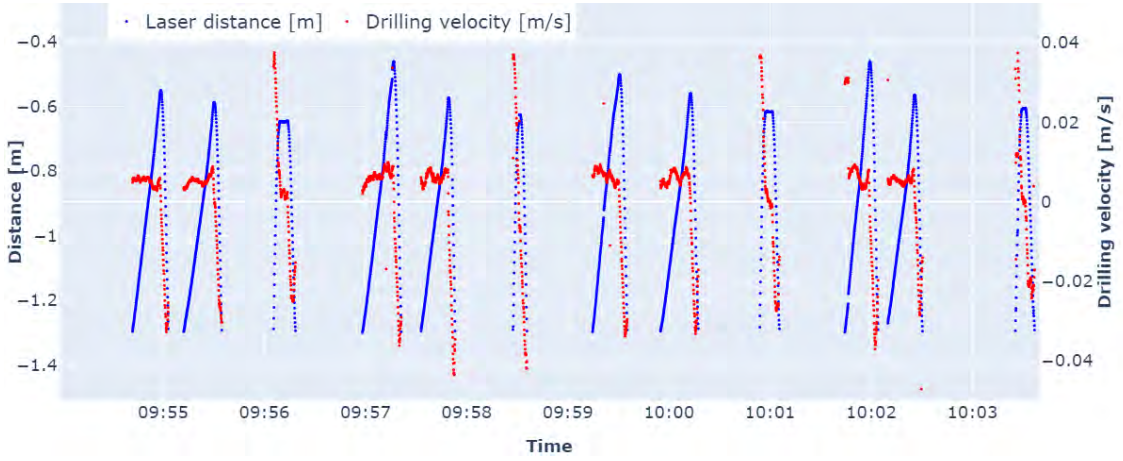

Figure 57: Data smoothing with rolling mean of 32 points [174]

cycle-ending peaks. These peaks are marked with green dots in Fig. 58. For detecting the starting point of the drill cycle (PL), a different approach has been proposed: namely completion of two conditions: the drilling progress must be greater than $D = -1.3$ m and the smallest distance from lower threshold D every W_3 is taken.

As a black dots, the beginning of the every cycle is presented in Fig. 58. Following the proposed steps, the drilling cycles are identified between the points corresponding to the lower and upper peaks for each subcycle and presents as an orange part of the traces. These established principles make possible to automatically detect cycles, previously validated by video footage.

Using one common x-axis representation of all detected drilling subcycles are presented in Fig. 59. It is viable to determine a clear differentaion: there are two visible subgroup related to drilling first or second hole for the rock bolt, and the final tightening the rock bolt. The length and maximum depth observed in drilling cycles can fluctuate, and this irregularity is another challenging aspect that can influence the detection process. The aforementioned calculations, from a monitoring standpoint, are a crucial parameters taken from the analysis. Supplementary metrics are considered for further examination, such as the α slope and β intercept parameter of linear interpolation for each identified cycle, PCC as Pearson correlation coefficient, and the duration of the drilling (represented as n_L parameter). Given these values, there is a necessity for the automatic identification of these cycles and the counts for each segment of the bolting process. To accomplish this, an experiment with unsupervised machine learning utilizing clustering algorithms is necessary.

The proposed machine learning experiment uses the data describing every detected drilling subcycles, following the Step 8 of the proposed algorithm. Prior to clustering, a Principal Component Analysis (PCA) step was introduced to the data processing pipeline to reduce the

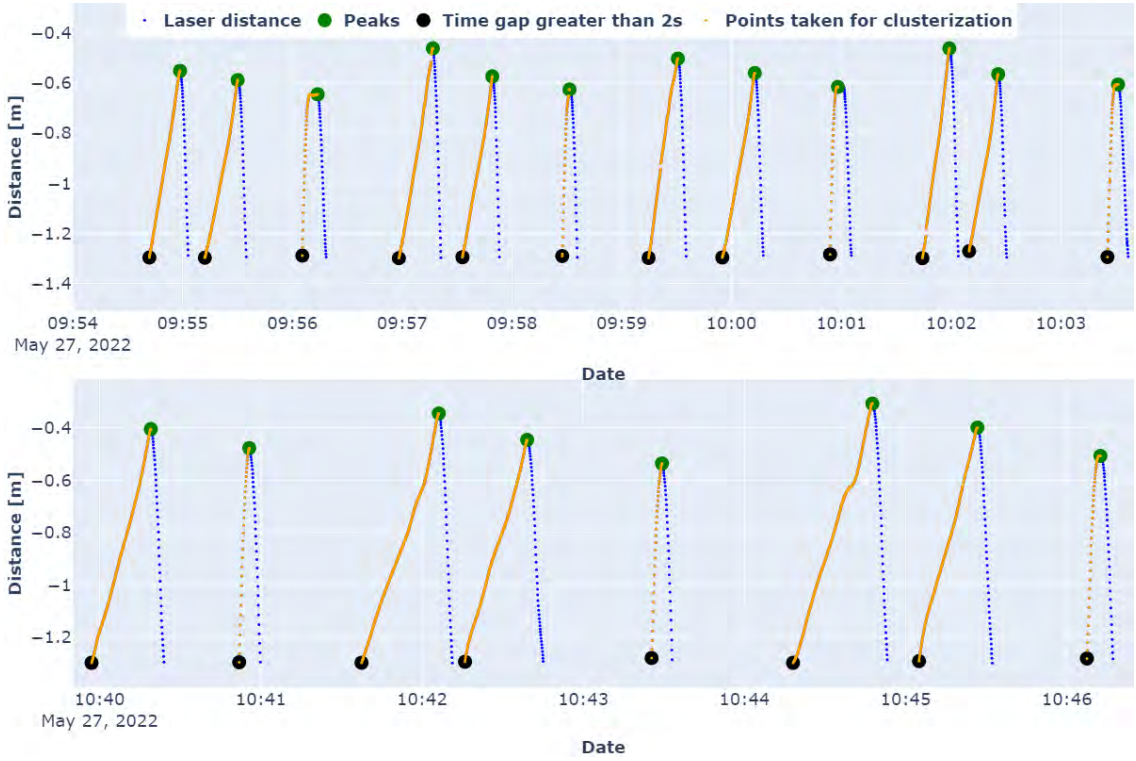

Figure 58: Drilling cycles with the start and end points detected [174]

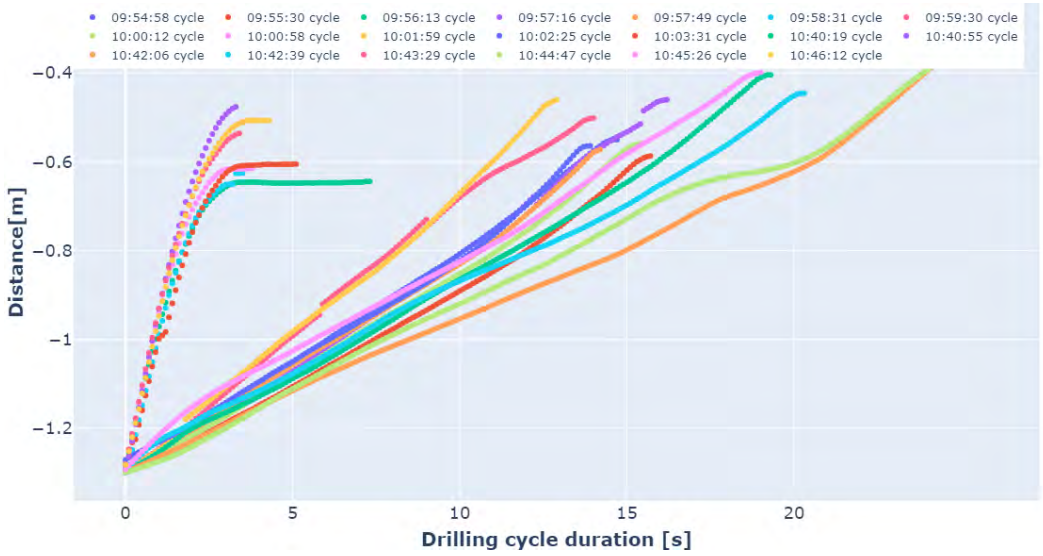

Figure 59: Summary of the extracted drilling cycles [174]

Figure 60: Results of clusterisation with the KMeans algorithm [174]

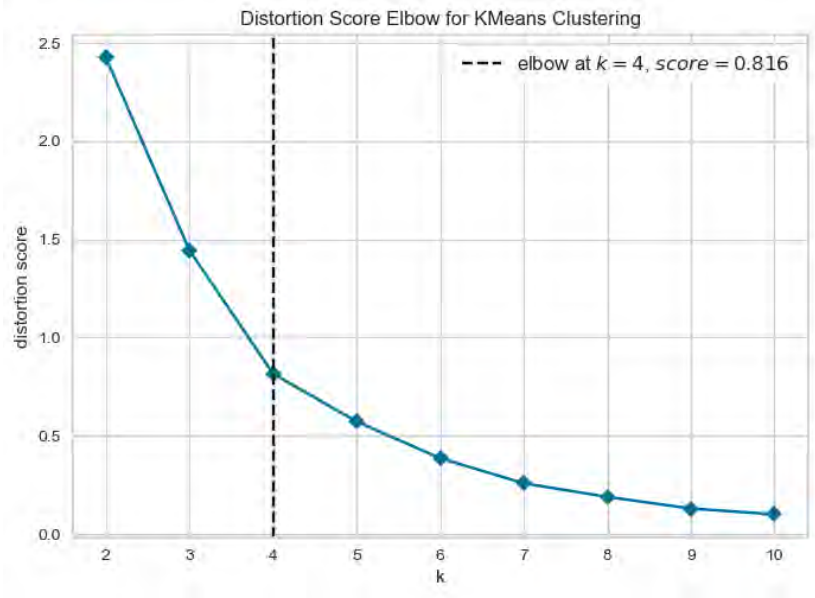

Figure 61: Distortion score elbow plot [174]

data dimensionality and enable visual validation, utilizing four parameters: α, β, PCC, n_L as an input data. The principal components are used in the clustering process to distinguish between sub-processes (drilling versus bolting). K-means clustering algorithm is selected to make an automatic cluster labeling in an unsupervised manner. To perform it, the sklearn Python library is used [217], where as a final number of clusters for drilling cycles labeling $k = 2$ is applied. The obtained labeling outputs is presented in Fig. 60. The model above correctly covers all cycles, where the first two phases are the drilling of the hole and the next is the tightening of the rock bolt (except for cycle 13 starting at 10:40:55, where the drilling of only one hole was correctly measured). To follow this, the elbow plot and silhouette score are used to validate the model correctness.

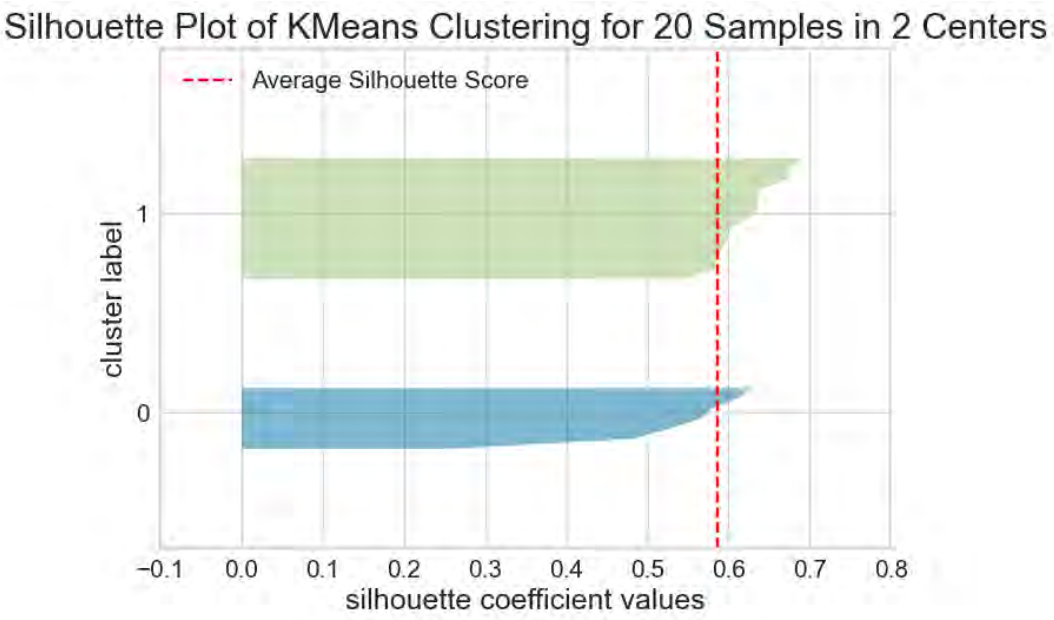

Figure 62: Silhouette score for the clustering experiment [174]

First of all, the elbow plot (see Fig. 61) is generated to assess the correct number of clusters being separated. It implies that $k = 4$ with score of 0.816 stands for the best dataset ditribution [218]. However, the Silhouette score for $k = 2$ presented in Fig. 62 shows that each cluster has this metric above the average. It indicates that a heterogeneous distribution of clusters is achieved. For $k = 3$, one of the class is significantly overrepresented and for $k = 4$ exists a class with Silhouette score below the average value.

The aforementioned results indicate that the approach presented here can be used for a starting point for the automatic procedure for bolting rig machine cycles detection. Instead of using complex pressure data from mining bolters, the new source of data from laser measurements delivers the satisfactory results with robust algoritm presented here. For scalling up this solution, a machine's on-board computer can serve predictions in real-time about the bolting cycles being processed based on laser data. Furthermore, the cycle count and duration can be effectively assessed using data from the laser distance measurements. This is feasible by querying the data at the transition to or from the one cluster, which indicates the start or end of the critical bolting process, namely hole drilling. These time points facilitate the calculation of the drilling scope from the data, resulting in a precise identification of the number of cycles.

The results of these analyses are described in detail in the article [174].

7.3 Results of electric current measurement at a mining section analysis

In this section, the results from electric current measurement at a mining section are presented. The analysis consists of three main parts. The first part corresponds to preliminary results from electric devices switching test, where several devices and machines types are selected in order to make them working and measure the simultaneous current level taken by these appliances. The next step, frequency domain analysis, describes the methods of signal frequency analysis performed. In that part, the results consist of the raw signal filtering with high-pass filter and the spectrogram parametrization description. The last part defines the classification experiment analysis. Within that part, the training dataset is presented in order to transform the raw measured signal into a valuable description of the objects. The detailed characterization of the automated machine learning pipeline and the outcome classifier model used is also added. Finally, the classification results for 8 class objects is revealed and divided into three parts corresponding to ventilation devices, drilling and bolting rig machines.

7.3.1 Preliminary results of electric devices switching test

Figures 63 - 68 refer to sequential test output for every device type. The measured signal is a sinusoidally alternating current signal having values from +/- corresponding to instantaneous use of electric power. The current consumption is calculated on the basis of the signal envelope and is always positive value.

In Fig. 63 a fragment of electric devices switching test with the work of hydraulic pump is presented. During first 15 seconds, it is registered a value below 1 A which corresponds to energy consumption from other devices (such as lighting etc.) what is out of the analysis scope. In 15 second of measurement, it is visible a start-up peak up to 56 A. The next seconds current consumption is stabilized around 5,5 - 6 A which correlates with a nominal current usage.

The next device, the 1-speed fan, is presented in Fig. 64. Similarly to a hydraulic pump, there is a visible start-up peak (140A) and a stable current consumption (15A). For Fig. 65 there are visible two peaks reffering to turning on first (10 second of measurement) and second (185 second of measurement) gear of 2-speed fan. The first speed consumes around 22A, where the second speed uses 35A, respectively. The measurement output of sequential switching with two device overlapping, namely launching 1 & 2-speed fans is presented in Fig. 66. At the beginning of the measurement, the first gear of 2-speed fan is turned on and after approximately 100 seconds of measurement, the second speed is started. The fact of occurrence of two start-up peaks is

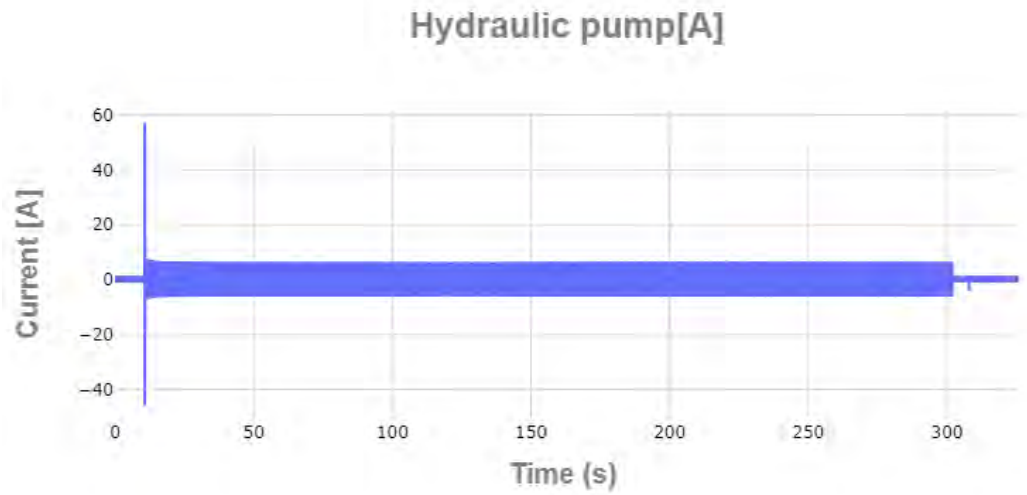

Figure 63: Switching test - hydraulic pump

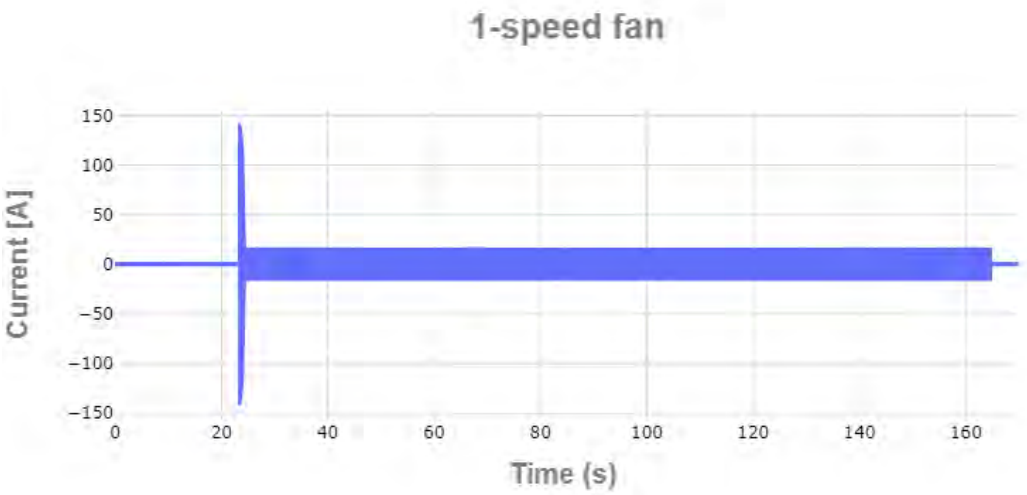

Figure 64: Switching test - 1 speed fan

characteristic and appears quite often in the recorded data. This form of getting a parametrization of such signal artifacts can be valuable from maintenance point of view, but it is not considered in this thesis. A moment after the 300th second, one can see that the 1-speed fan switching on. The second part of the diagram is the gradual switching off of the receivers, in the opposite order.

The next plots (Fig. 67,68) refer to the current consumption from the wheeled mining machines. Their current consumption is limited to drilling or bolting operations. The operations of a specific

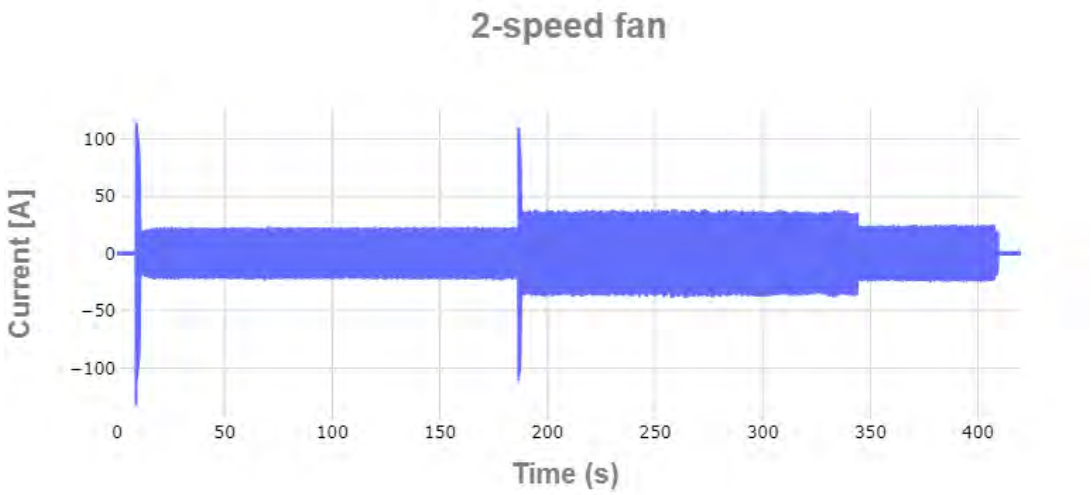

Figure 65: Switching test - 2 speed fan

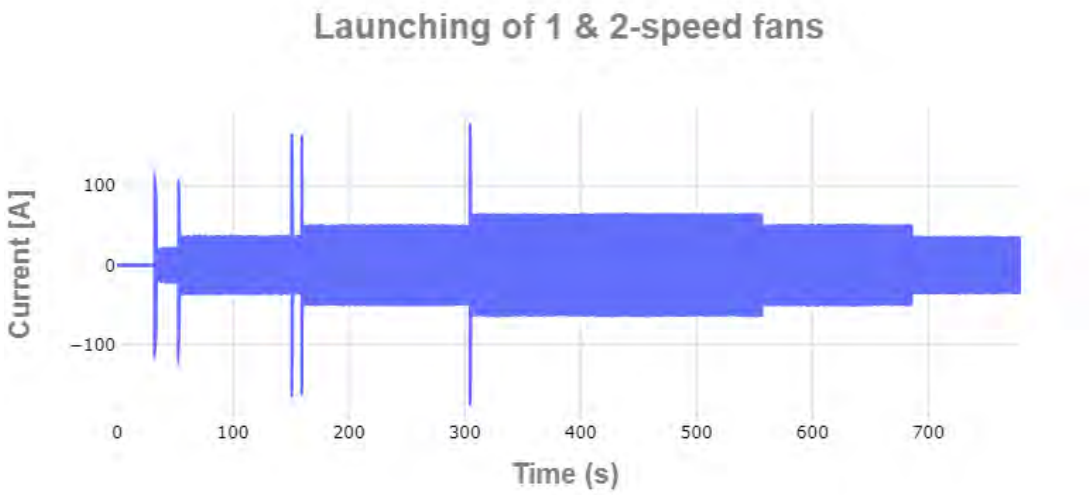

Figure 66: Switching test - 1 and 2 speed fans

machine, interpreted based on visual observation next to these machines are put with a color and text description in figures.

In summary, representation of preliminary results obtained during electric devices switching test give an insight into how specific group of devices and machines behave under standard working conditions in the mine. Based on the separated measurements for every device, the dataset can be created to gather additional information in time and frequency domain. Following that,

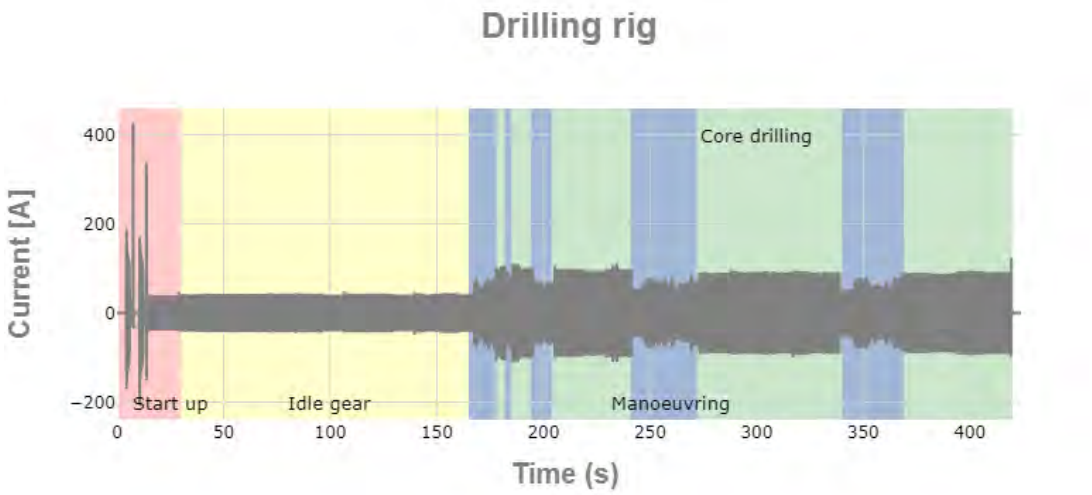

Figure 67: Switching test - drilling rig

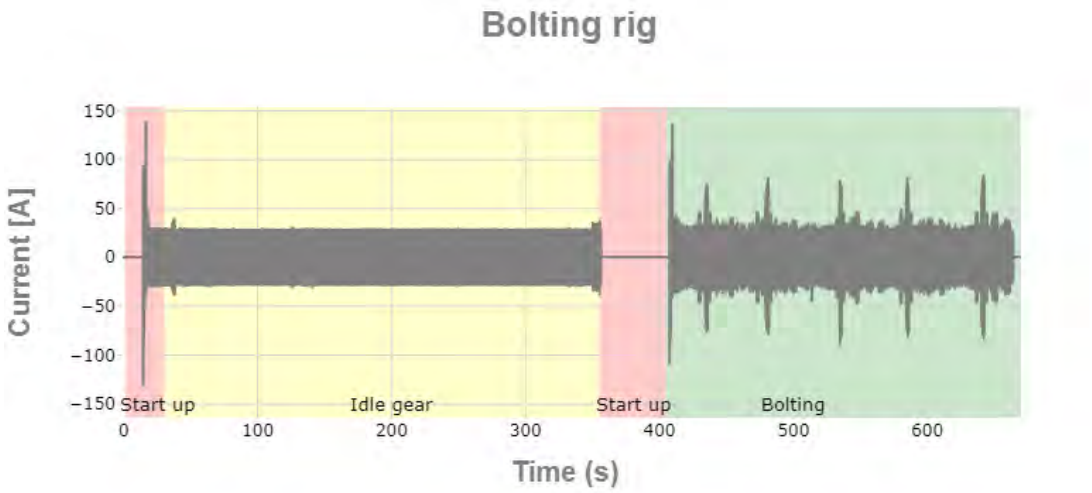

Figure 68: Switching test - bolting rig

a detailed frequency analysis and interpretation of the results is presented in next chapters. Then a classification experiment is prepared in order to assess the ability of such data source to interpret machine's work during continuous measurements.

7.3.2 Frequency domain analysis

In this section, the results of the spectrogram analysis are presented in order to use the frequency domain information to describe the operation of energomechanical devices. Following the outcomes received from Section 7.3.1, the device groups and their working regimes are revealed. In order to detect the temporal, rapid changes in signal's frequency domain, the significant emphasis is taken to choose the valid spectrogram parameters. Consequently, presented in this section (unless otherwise specified) the following were selected experimentally spectrogram parameters:

- NFFT=256
- overlap O=100
- window length n_W=128
- window type = Hamming window

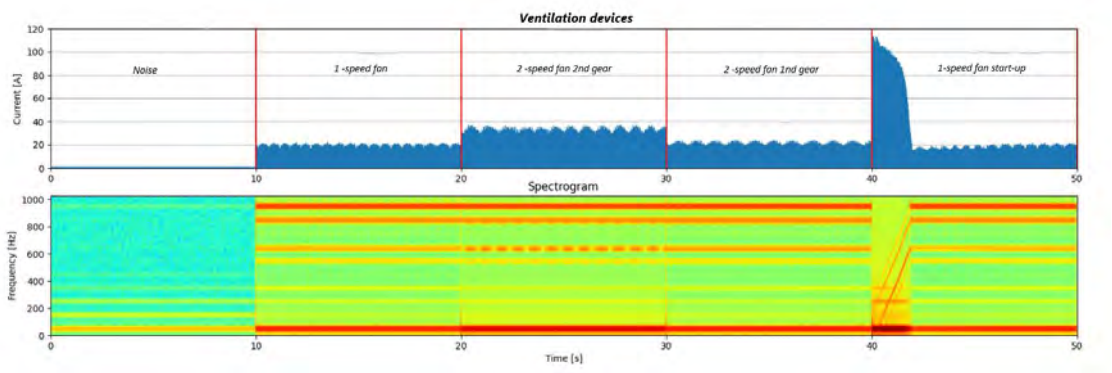

Figure 69: Ventilation devices regimes work - an instantaneous electricity consumption (top), spectrogram in the time-frequency domain (bottom)

The first group of devices being analysed in the time-frequency domain are ventilation devices. In Fig. 69 five signals that are 10-seconds long are presented as follows:

- Noise - direct current measurements with no devices turned on
- 1-speed fan - ventilation device with turned on one engine
- 2-speed fan 2nd gear - ventilation device with turned on two engines simultaneously
- 2-speed fan 1st gear - ventilation device with turned on one engine only

- 1-speed fan - ventilation device with engine start up regime

The current level consumption is visualized in top part of the figure, and the spectrogram output is given in bottom part. As it can be seen, one can observe the changes in the spectrogram values for the various bands of frequencies and their nature of change for each type of the devices.

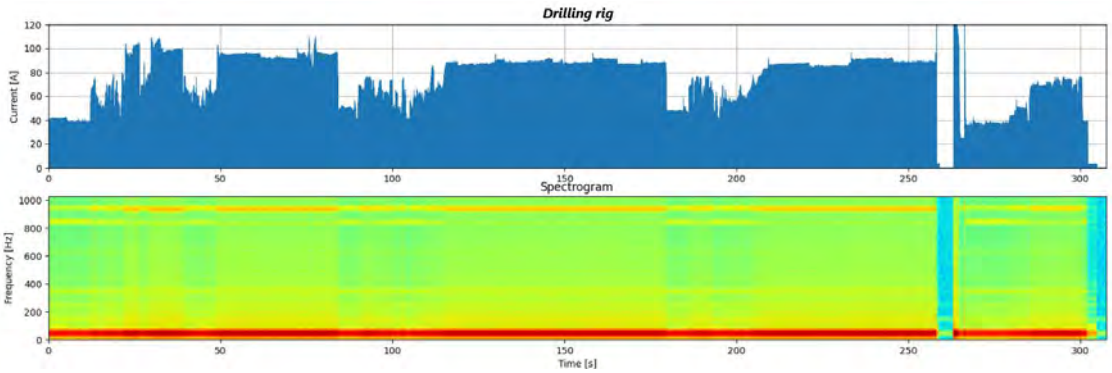

Figure 70: Drilling rig regimes work - an instantaneous electricity consumption (top), spectrogram in the time-frequency domain (bottom)

The next figure (Fig. 70) represents spectrogram results for drilling rig machine performing 3 blast holes. In this case the changes in the spectrogram energy for frequency bands above 800 Hz itensify following the changes in drilling rig work regimes. These fragments are divided into the primary drilling and the execution of e.g.: auxiliary movements of the machine.

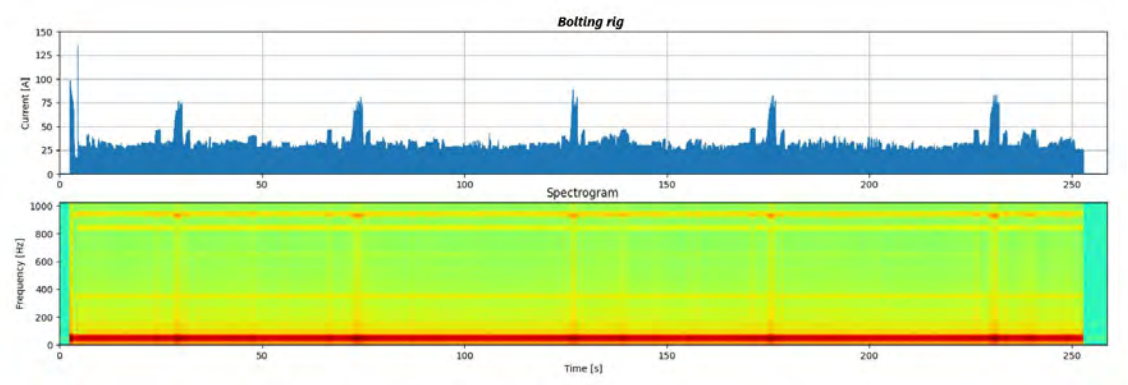

Figure 71: Bolting rig regimes work - an instantaneous electricity consumption (top), spectrogram in the time-frequency domain (bottom)

The last type of the machine being analysed is the bolting rig . The time and frequency analysis of performing the five rock bolts is presented in Fig. 71. The frequency bands with higher energy are similar to the drilling rig machine. The type of bolting rig considered here, performs the

expansion rock bolts, what can be distinguishable by the characteristic signal peaks corresponding to rock bolt tightening. This is also affected in frequency domain, what can be seen in the bottom of the figure presented above.

Due to the fact, that the carrier frequency of the signal is f_c=50 Hz, all spectrogram results presented in this section are preprocessed by the high-pass Chebyshev filter with cutoff frequency of $f_{bc} = 100$ Hz. As a digital filter, the Chebyshev type II filter is created. The chosen filter order is selected experimentally as g=11 to fulfill specific needs of optimal loss in the passband and minimum attenuation in the stopband for the given signal. All steps covering the changes of the raw signal are described in section 6.3.

The next two figures, namely Figures 72 and 73, exemplify the spectrogram results for signals from drilling rig machine performing of 3 holes. Fig. 72 shows spectrogram of the raw signal, there the highest energy (warmer colors) represent the carrier frequency of 50 Hz and other characteristic frequencies of 830 and 920 Hz. Howerer, the isolation of any characteristic frequency is difficult due to the most energetic band from signal carrier. The output from the signal filtered by high-pass filter with $f_{bc} = 100$ Hz of cutoff frequency is presented in Fig. 73. The new frequencies emerges and there are changeable due to drilling operations. Based on that, it is viable to identify the individual fragments of the drilling process based on the characteristic signal spectrum in the frequency domain. Nevertheless, this step is not a trival processing phase. As may be noticed, the frequencies below 400 Hz represent a cyclical nature of changes that is inconsistent with the changes associated with drilling sub-cycles. This part of the band can be affected by, for example, the work of hydraulic machine's subsystems and their electric engines.

Following the observation above it can be concluded that the matrix from spectrogram calculation can be reduced. The new matrix should possess the most characteristic frequency bands in order to differentiate the machine work regime types. Owing that, the dataset created for further reasoning can be limited. It is worth to mention the limitation of the method presented here. The spectrogram analysis is considerably complex, and its usage for performing the real-time analysis of the measured current signal is seriously limited. In addition to this, under conditions of the standard operation of machinery and equipment in the mining department, the subgroup of devices can work simultaneously. It affects that the frequency analysis of the signal coming from the scenario above make the frequency domain data analysis almost impossible to correctly identify and analyse the work of individual pieces of equipment. Such a case can be indicated on the basis of an analysis of the signal envelope in the time domain. These situations are represented by the sum of the work of certain sub-groups of mining equipment and machinery.

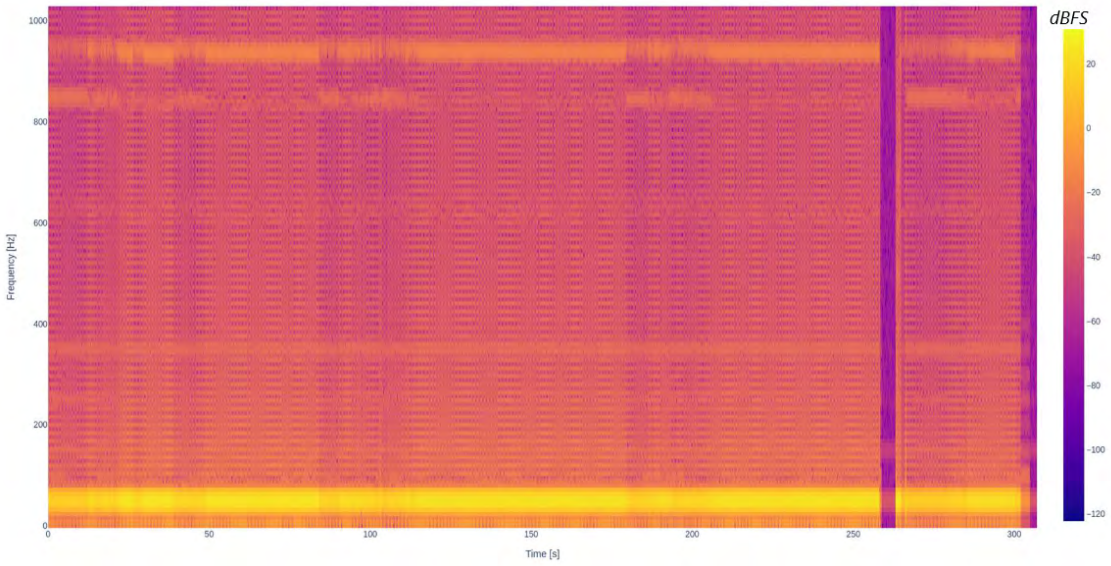

Figure 72: Spectrogram example of the nonfiltered signal of 3 drill holes obtained from drilling rig machine

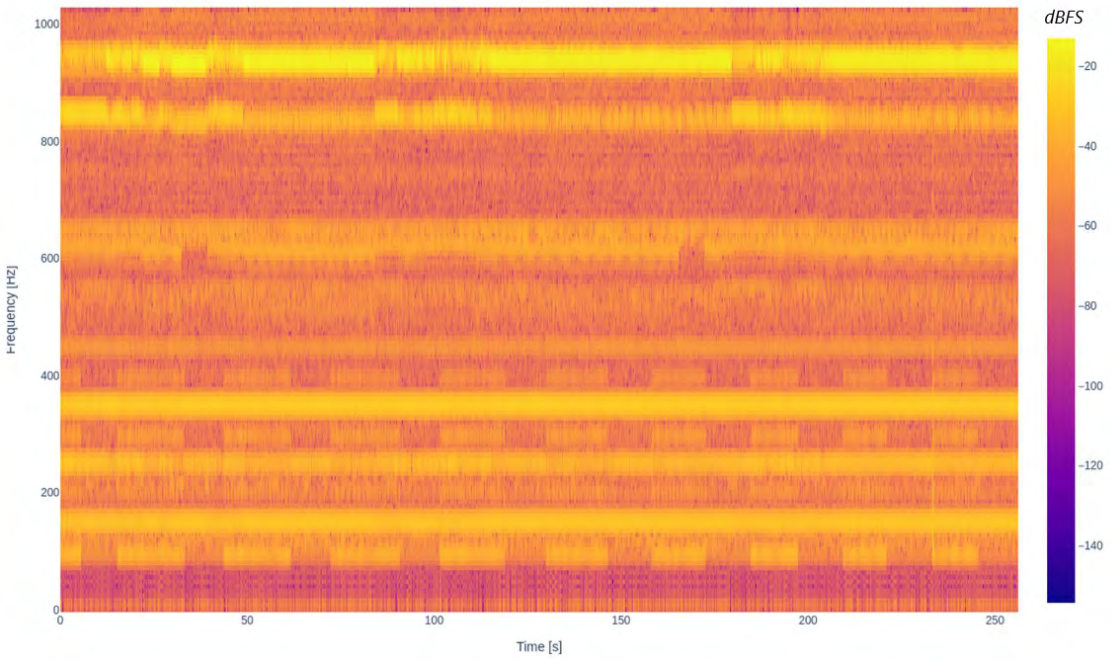

Figure 73: Spectrogram example of the filtered signal of 3 drill holes obtained from drilling rig machine (high-pass filter with 100 Hz cutoff)

7.3.3 Classification experiment results

Thanks to data revealed from electric devices switching test and initial exploratory data analysis in time and frequency domain, the next step is to use the dataset prepared to classify the types of devices and machines being turned on. To automate this step, the PyCaret, the low-code machine learning library is used [219].

class	time	current	700.78125	...	961.328125	970.3125	979.296875	988.28125
1-speed fan	2022-01-22 07:49:49.887640449	6.0	0.000179	...	0.000210	0.000241	0.000354	0.000580
bolting	2022-01-18 12:59:21.790884718	16.0	0.001328	...	0.000701	0.000854	0.001658	0.003584
bolting	2022-01-20 15:46:23.117241379	29.0	0.005943	...	0.003455	0.003404	0.003215	0.003280
two 1-speed fans with 2-speed-fan	2022-01-22 08:37:25.059829059	24.0	0.003428	...	0.002802	0.002562	0.002981	0.005163
1-speed fan with 2-speed-fan	2022-01-22 08:34:50.847457627	17.0	0.001172	...	0.001431	0.001669	0.002570	0.004011

Figure 74: Example of dataset for classification with the limited frequency of f_{lim} = 700 Hz

Parameter name	**Description**
Experiment type	classification
Target column	"class" column
Preprocess data	True, 4 steps
Features excluded	"time" column
Original dataset shape	(6218, 37)
Transformed train set shape	(4352, 36)
Transformed test set shape	(1866, 36)
Fold Generator	StratifiedKFold
Fold Number	10

Table 17: Classification experiment initial parameters

In Table 17, the set of parameters is presented in order to describe the classification experiment. Following the data processing steps from 6.3, the example of the training dataset is presented in Fig. 74. Each line contains the calculated spectrogram result for the electric current signal samples every Δt=1 second. The first column, *class* is added manually based on electric devices switching test measurements in order to describe the corresponding device or machine being turned on. The next column, *time* describes the timestamp of maximum absolute current value obtained within every Δt second. The remaining columns are added from spectrogram frequency bands from the

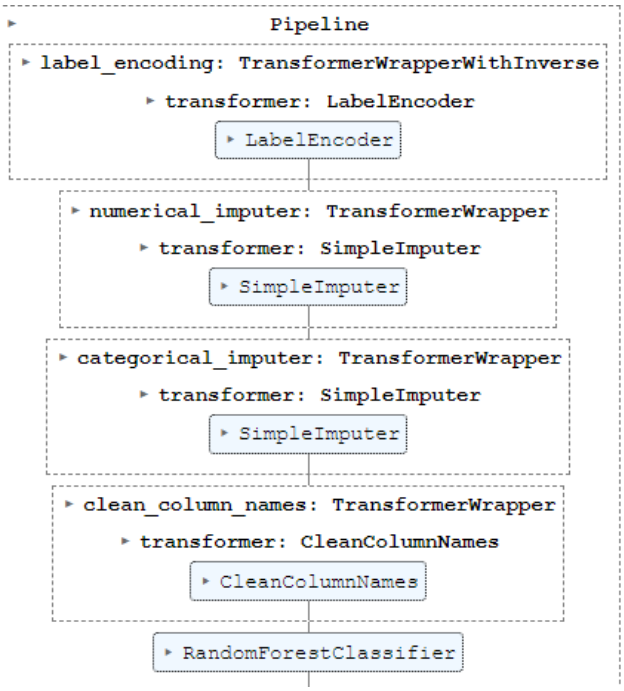

Figure 75: Transformation pipeline for classification dataset

scope of $f \in (f_{lim}, f_{max})$, where f_{lim} for the results displayed in this section is experimentally chosen f_{lim}=700 Hz.

In addition to this, several further data processing steps are considered within the machine learning experiment pipeline, namely: encoding the target column labels, usage of simple imputers for numerical and categorical columns, columns rename to escapes special characters and finally convert data back to the original representation. The pipeline steps are visualized in Fig. 75.

To start with machine learning workflow, the dataset is split into train and test subset with a ratio of 0.7. To evenly distribute every class in train and test dataset, the Stratified K-Fold cross-validator is used [220]. The next phase is to distribute the prepared data above to train the classification estimators and receive score grid with several metrics. An example of the training and cross validation step is presented in Fig. 76 with several models and metrics calculated (accuracy, Area under ROC Curve (AUC), recall, precision, F1 Score, Kappa, Mathew Correlation Coefficient (MCC), and training time (TT)), sorted by the accuracy metric [221]. With the proposed approach, the training step can be automated and run on a schedule, or based on the significant changes detection with dataset metrics (e.g. data drift detected) and the like.

For model inference and results generation, the Random Forest Classifier (RFC) is selected based on the best accuracy score. For this classifier, the Fig. 77 shows the feature importance

	Model	Accuracy	AUC	Recall	Prec.	F1	Kappa	MCC	TT (Sec)
rf	Random Forest Classifier	0.9970	0.9998	0.9970	0.9970	0.9969	0.9938	0.9938	0.1310
dt	Decision Tree Classifier	0.9947	0.9942	0.9947	0.9947	0.9947	0.9891	0.9891	0.0190
et	Extra Trees Classifier	0.9938	0.9998	0.9938	0.9939	0.9935	0.9872	0.9872	0.0660
knn	K Neighbors Classifier	0.9851	0.9942	0.9851	0.9851	0.9832	0.9688	0.9691	0.0970
qda	Quadratic Discriminant Analysis	0.9784	0.9984	0.9784	0.9799	0.9781	0.9562	0.9567	0.0080
nb	Naive Bayes	0.9667	0.9929	0.9667	0.9708	0.9678	0.9325	0.9331	0.0100
lda	Linear Discriminant Analysis	0.9582	0.9959	0.9582	0.9423	0.9480	0.9139	0.9154	0.0110
lr	Logistic Regression	0.9235	0.9637	0.9235	0.8727	0.8933	0.8264	0.8373	0.3170
ada	Ada Boost Classifier	0.8529	0.9446	0.8529	0.7828	0.8088	0.6813	0.6929	0.0980
ridge	Ridge Classifier	0.7599	0.0000	0.7599	0.6071	0.6676	0.2791	0.3823	0.0070

Figure 76: Classification estimators comparison with several metrics (sorted by accuracy)

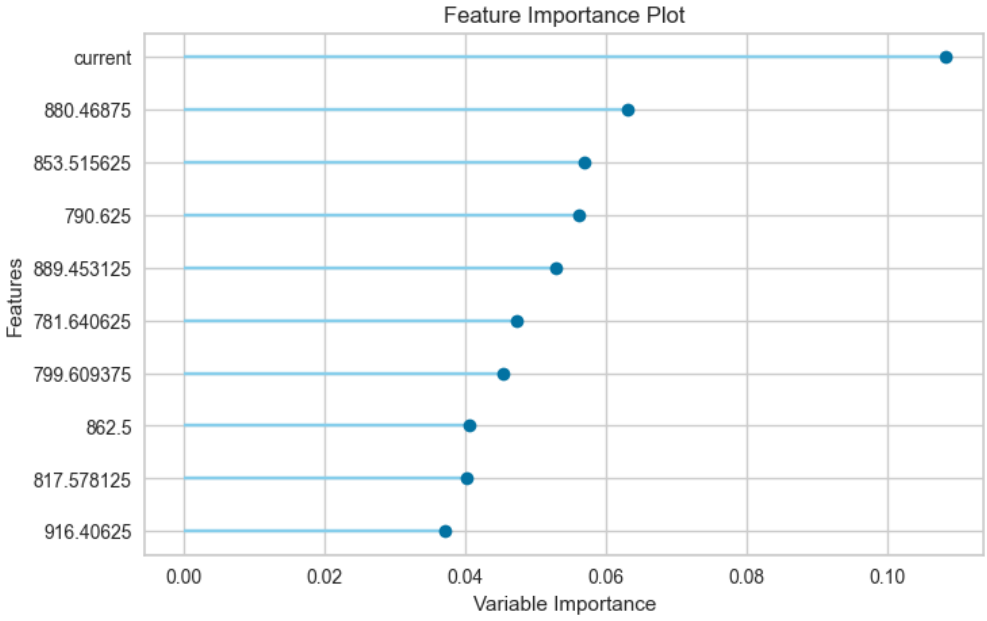

Figure 77: Feature importance plot for the selected classification model

values used for classification purposes. The created model based on the input data can classify the device or machine type work. The given classifier labels are:

- hydraulic_pump - detection of hydraulic pump work
- 1-speed fan - ventilation device with one gear single engine detected
- 2-speed fan 1st gear - ventilation device with two engines working at 1st gear detected
- 2-speed fan 2nd gear - ventilation device with two engines working at 2nd gear detected
- two 1-speed fans with 2-speed-fan - two 1-speed fan working simultaneously with 2-speed fan detected
- drilling - drilling rig machine drilling subcycle part detected
- movement - drilling rig machine manoeuvring subcycle part detected
- bolting - bolting rig machine work detected

The next figures 78, 79, 80 present the results of the classification based on current measurement data. Every figure has three subplots, where at the top of each figure it is the data representation in time domain presented. The middle subplot displays the predicted labels obtained from the classification model. The bottom subplot shows the predicted labels with rolling window applied to remove incorrect classification results, which from time to time occurs during the real data inference.

Starting from Fig. 78, a part of sequential fan activation is presented. The peaks at the top part of the plot correspond with moments when a new device is turned up. As it is presented in Section 7.3.1, values of electric current consumed by ventilation equipment are usually constant. The sum of the current taken by devices varies, and the current consumption changes from 31 A to 65 A. The classification model correctly detect the work of the 3 ventilation classes: 2-speed fan 2nd gear, 1-speed fan with 2-speed fan, and two 1-speed fans with 2-speed-fan. For some data fragments corresponding to moments of switching on a new device in the measuring area (near the peaks moments), we see different classification results. They are individual deviations and to remove them on predicted label, the rolling window calculation with $W_L = 10$ is applied.

The next part of the experiment results is the drilling rig work assessment. In Fig. 79 the selected 30 minutes scope when drilling rig worked in the mining site is presented. In the top plot part, the characteristic shape of current signal in time domain is visible. The obtained labels

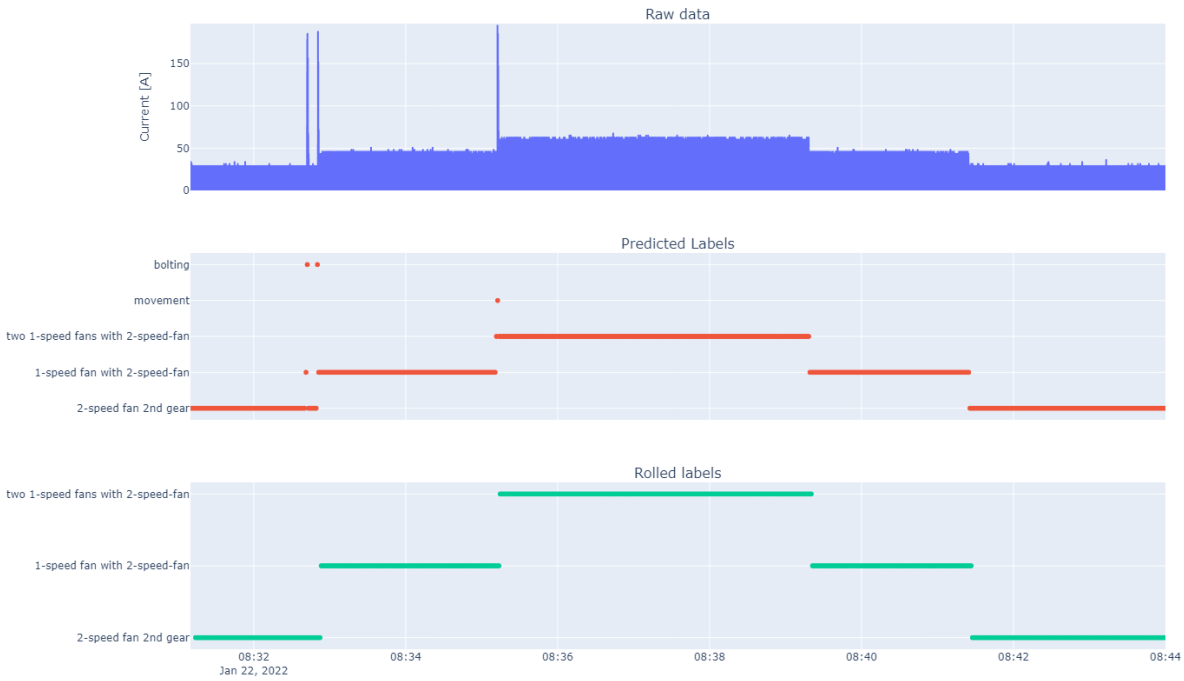

Figure 78: Predicted classess for ventilation devices detection using frequency bands higher than 700 Hz

are from the following classess: *movement*, *drilling*, and *bolting*. Whereas the first two classess are expected, the *bolting* class arises in some moments likewise. It comes from the fact, that the *movement* class, reffering to manoeuvring phase of drilling rig machine work, is significantly similar to the work of bolting rig. Hence, the certain amount of *bolting* class remains unchanged even with rolling window with $W_L = 10$ is applied in the bottom subplot. Nevertheless, the division into core drilling and manoeuvring movements coincides with the course of the current signal. Following that, the drilling rig cycles detection is possible and automated cycles count can be applied as well.

The last class being taken into consideration is the bolting rig machine work. In Fig. 80 results during the bolting rig machine work are presented. In the beginning of the chart one can see the nominal current level of 50 A, and when botling rig is turned on, the signal jumps to values around 85A. Some peaks are visible reaching values up to 115A, what is connected with the tightening the rock bolt moments. As it can be seen, the real data does not demonstrate so clearly the bolting subcycles, so machine idle gear, bolting and rock bolt tightening regime patterns are treated as one label called *bolting*. Classification model returned here two labels *bolting*, and *drilling*. At this

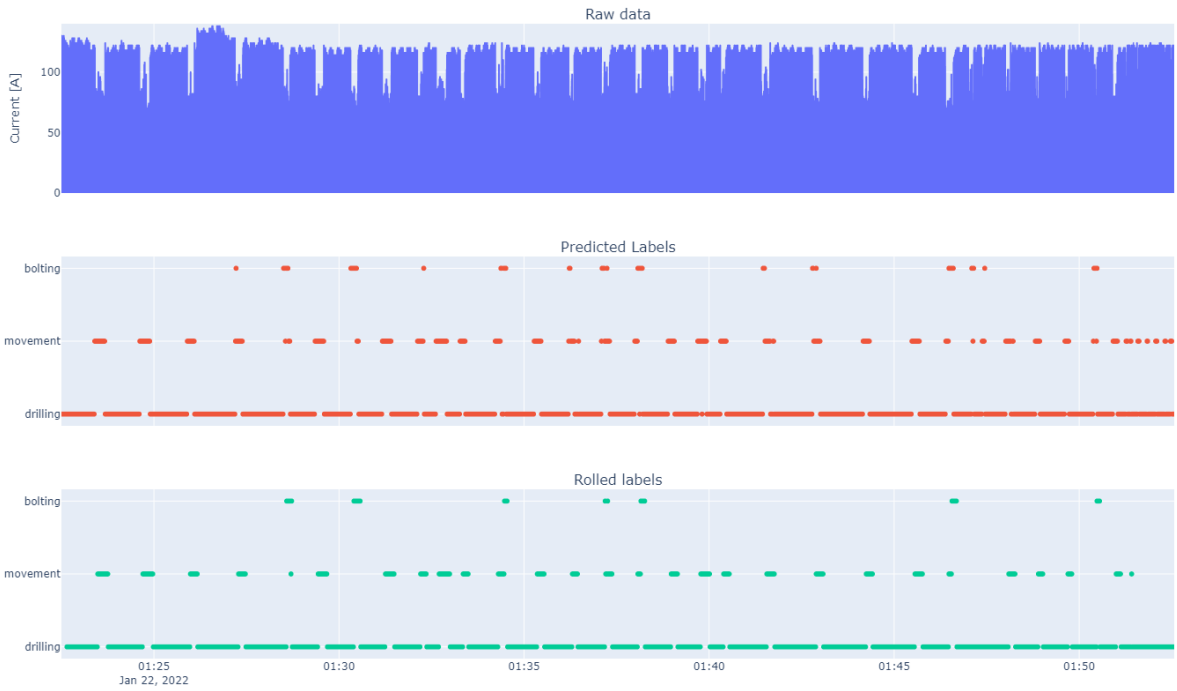

Figure 79: Predicted classess for drilling rig work phases detection using frequency bands higher than 700 Hz

point, *drilling* label is not expected here, but occur from time to time and it cannot be fully removed with rolling window applied.

The presented results mostly correctly distinguish the operation of machinery and equipment based on current measurement at a mining section. Nevertheless, it possess several limitations. While the operation of ventilation equipment is classified accurately in most cases, the operation of mining machinery causes problems. Certain parts of drilling cycles are classified as bolting and vice versa. This is a limitation due to the fact that training the machine learning model only relies on the basis of the electric devices switching test measurements. The results shown are derived from a signal which measures the sum of the electric currents consumed by all receivers at a mining section. To mitigate this, a larger sample of the training data corresponding to the variability of the operation of even the same type of device is needed. It will allow a better model to be created and will cancel out the false changes seen in drilling and bolting rig results. Moreover, it is worth to note that, the shape of the bolting signal is slightly different as compared with bolting rig work presented in Fig. 68. This may depend on the operation of another machine subtype or the work of the operator.

Figure 80: Predicted classess for bolting rig work phases detection using frequency bands higher than 700 Hz

In conclusion, the results presented in this section enable to identify the operation of the devices and machines based on current level measurement taken at a mining section electric cabinet. It is viable based on time and frequency domain analysis of the captured raw current signal, with the several data processing steps applied, and with the usage of classification model.

7.4 Results of hazardous gases data analysis

In this chapter, the results of the environmental parameters evaluation in underground mine (see Section 5.1.4) are presented. The created measurement device from Section 5.3.4 analyses CO and H_2S gas concentrations as well as temperature and humidity during the underground experiment. Device is connected to the smartphone in a constant manner to save and visualize data in real-time. In addition to this, the gas detectors from ventilation stuff (Drager PAC6500 and PAC8500), properly calibrated following the procedure (described in Section 6.4), determined a reference point for the prototype device. Together with mine ventilation crew, measurements were conducted in places where higher concentrations of gases mentioned above appeared. These types of gas accumulation can appear from a number of sources, such as the operation of the mining machinery,

local ventilation possibilities of the workings, the distance to the shaft or the time after blasting procedure.

Following the Fig. 81, several notable environmental parameter changes are expained. In this figure, CO & H_2S gas concentration measurements (in Parts Per Million (PPM) unit) are presented in first two top subplots. The third subplot represents the temperature changes (in $^{\circ}C$), and the bottom one the humidity. The overall measurement session duration was 60 minutes. During the experiment, the typical temperature (35 - 39$^{\circ}C$) and humidity (55-85$\%$) was held for an underground copper ore mine. The highest CO concentration measured do not exceed the limits for mining excavations, which is 26 ppm [191]. Point **A** in Fig. 81 represents this situation, caused by wheeled mining machines activities the in nearby excavations. The next CO rise are probably affected by these machines passing closely to the measuring route (point F). The next point of the highest hydrogen sulfide concentration is marked at point **D**, where experiment was held closely to the excavations in the given mining department where local gas emissions from the rock mass usually take place. In most other locations, the $H2S$ values were close to zero values.

Another important fragments of the measurements, reflecting the ventilation system works, are point **E** and **B**, respectively. There are places in underground net of corridors, where fresh air inlet area existed. It impacts on the decreasing of the local temperature and humidity. The slight changes in humidity are presented at **C** point, where the travel throught several air dams is observed.

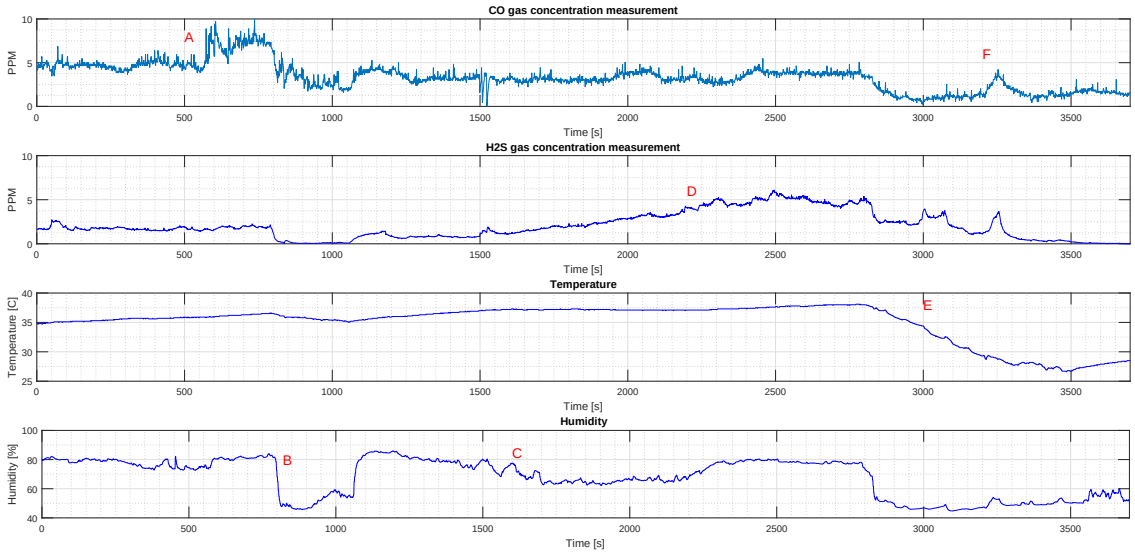

Figure 81: Measurement of the mine environmental parameters [175]

By utilizing data from the IMU sensors embedded in the mobile phone, where application for visualization purposes is run, a distance calculation was carried out with satisfactory accuracy.

Signals are recorded every 100 ms. When a rapid increase in the primary acceleration vector is detected, the smartphone application registers this as a new step. Acceleration and velocity data are collected on three axes. Consequently, when significant changes are observed, a step-by-step calculation function is activated [222]. As illustrated in Fig. 82, during the test, the distance measured is approximately 700 m. Thanks to this approach, an estimate of the total distance covered by the mine crew could be achievable after their shift.

To summarize, the presented portable measurement unit for hazardous gas detection can be used as a miner's own equipment to assess the environmental parameters. With usage of smartphone to visualize data and alert workers about the possible threats, the additional data can be gathered from smartphone sensors to estimate the value of the distance made on a duty basis.

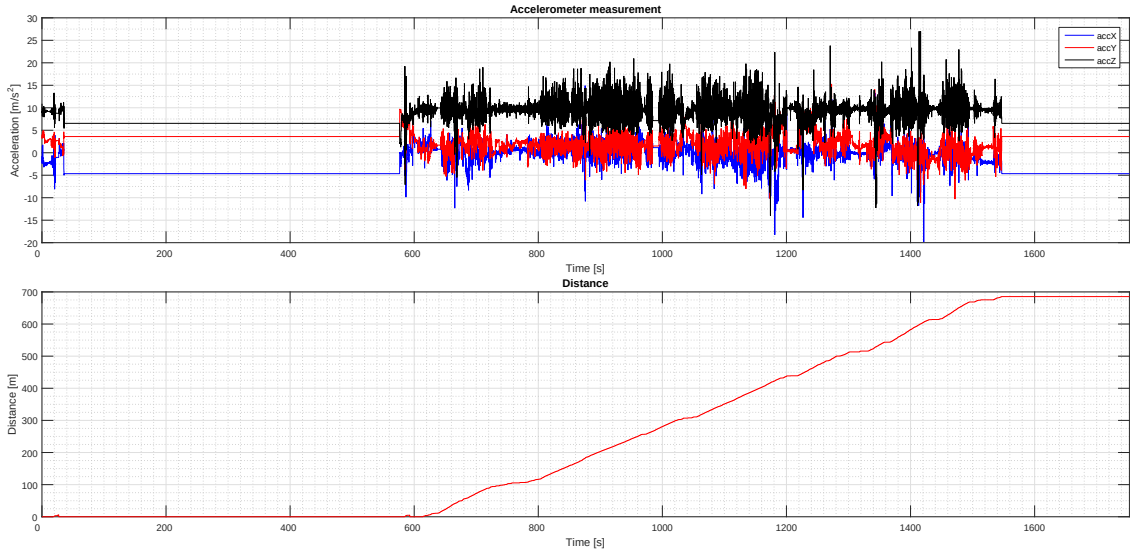

Figure 82: Calculation of distance covered based on IMU smartphone sensors [175]

The results of these analyses are described in detail in the article [175] as a part of the work supported by EIT RawMaterials GmbH under Framework Partnership Agreement No. 19018 (AMICOS. Autonomous Monitoring and Control System for Mining Plants).

7.5 Results of analysis of lidar data from inspection robot for mining transportation systems

In this section, the results of analysis of lidar data is described. A lidar sensor is mounted on the wheeled mobile robot (described in Table 4) as an example of inspection robot setup for mining transportation systems. The sensor above is directly connected to the on-board computer with ROS software. For the experiment area, the 40 m long corridor at the Wroclaw University is selected. The corridor contained several obstructions in front, above and on the sides of the robot, including recesses, doors and the wall above the lintel, creating occlusions for the lidar. Such conditions were chosen to reproduce the problems with measurement coverage of narrow linear objects. That assumption can identify the similar problems with inspection robot route assessment for mining transportation systems. Data acquisition is started during a straight path route, where the robot passes through the central part of the corridor. There are three scenarios determined for different lidar sensor configurations:

- Fixed horizontal position of the lidar sensor (horizontal lidar),
- Rotating sensor with the range of $< -45°, +45° >$ (tilting lidar),
- Rotating sensor with the full range of movement $< -90°, +90° >$ (rotating lidar).

Table 18: Density statistics for type of lidar movement [196]

Point Cloud	Mean Surface Density (MSD)	Standard deviation
Horizontal lidar	8978	5249
Tilting lidar	7581	3967
Rotating lidar	10,230	5146

In Table 18, a general statistics calculated from the whole experiment subdivided into a specific lidar movement type is presented. For each point cloud, a Mean Surface Density (MSD) and standard deviation of number of points per m^2 are calculated. The visualizations of point cloud obtained are presented in Figures 83, 84, and 85 with the same color scale. Moreover, in order to present the distribution of route coverage density for different lidar movements, a KDE is used to generate histograms presented in Fig. 86. Starting from horizonal lidar results, the distribution has three modes of 1000, 10000, and 15000 cloud points/m^2, where the mean is nearly 9000

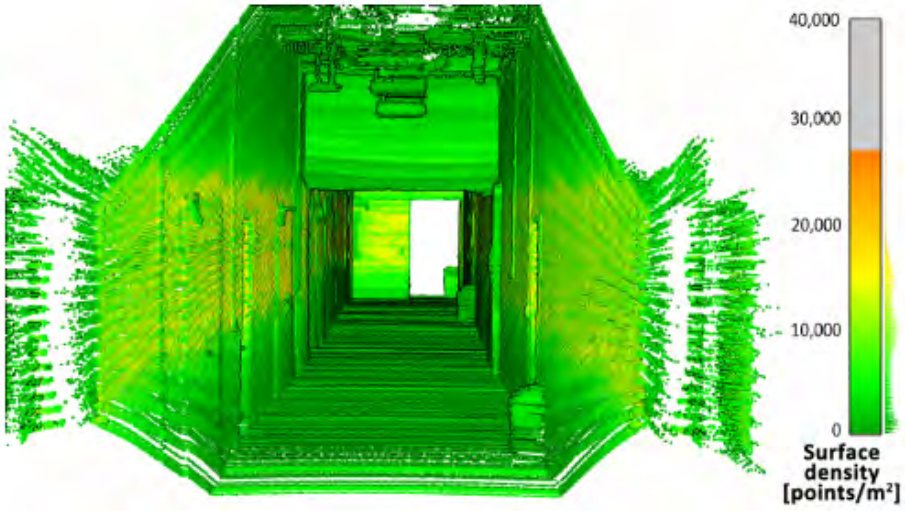

Figure 83: Point cloud density - horizontal lidar [196]

points/m^2. It affects that there are some oversampled areas (especially the corridor walls at the height of the lidar montage point on the robot mast), whereas some areas possess significantly lower data coverage (particularly visible at the beginning of the measurement). This situation is not highlighted in the movable mountage options. For tilting lidar, MSD is lower than for horizontal lidar, but the ditribution is more uniform, what corresponds to the lowest standard deviation in this experiment what is visible with the green trace in Fig. 86. Finally, the highest obtained surface density is received for rotating lidar with similar standard deviation to non-movement case.

The next phase of the experiment is to estimate the MSD for different types of objects. In Fig. 87 there are presented 6 chosen objects ((a), (b), (c), (d), (e), and (f)) existing in the corridor to examine their reconstruction quality using lidar mountage options above. First subgroup ((a), (c), (e), (f)) represents the objects with vertical surface detected, while second subgroup ((b), (d)) covers object with more complex geometry. Table 19 shows the number of cloud point obtained for every object described above. For flat object, the movable measurement types give an increase of cloud points as compared with horizontal lidar. Notably, the occlusions significantly affect measurements from the horizontal lidar for objects (a) and (f), causing some parts of these objects to be uncovered. It has also been noticed that the largest proportion increase in value is observed for objects with complex geometry, meaning that an additional axis of lidar movement has the ability to inspect objects with extensive shapes.

Enhancing the system's complexity by adding an additional actuator to rotate spinning lidar increases the data density and completeness for corridor-like scenario. Despite the fact that the

Figure 84: Point cloud density - tilting lidar [196]

Figure 85: Point cloud density - rotating lidar [196]

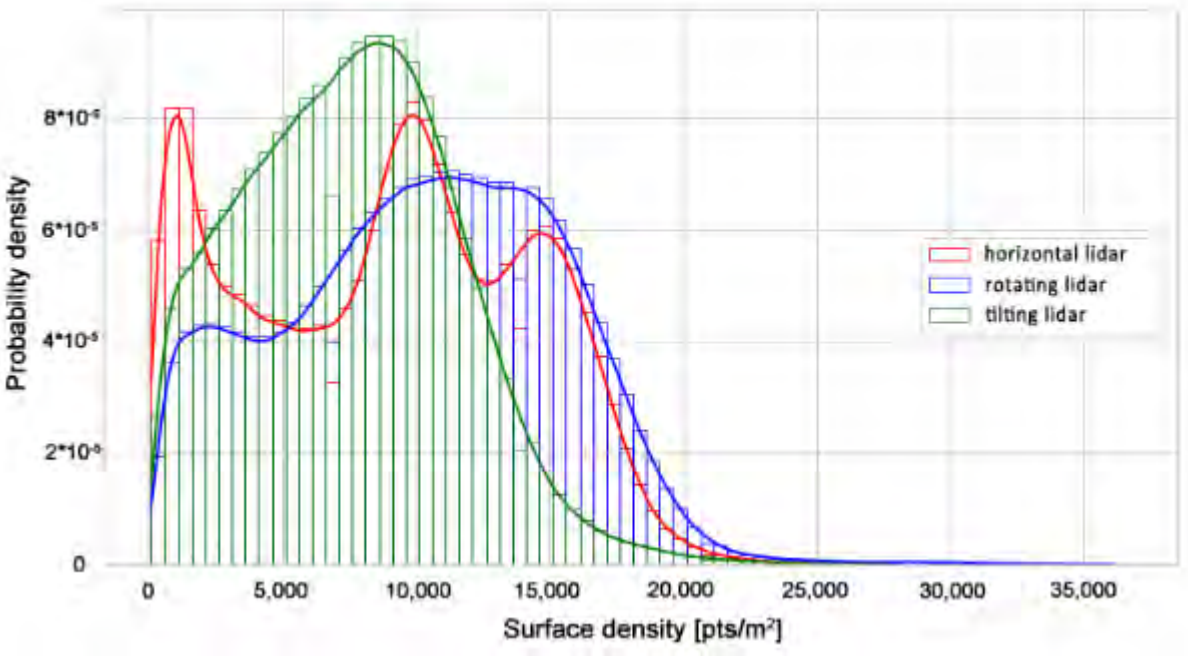

Figure 86: Surface density distributions for types of the sensor movement [196]

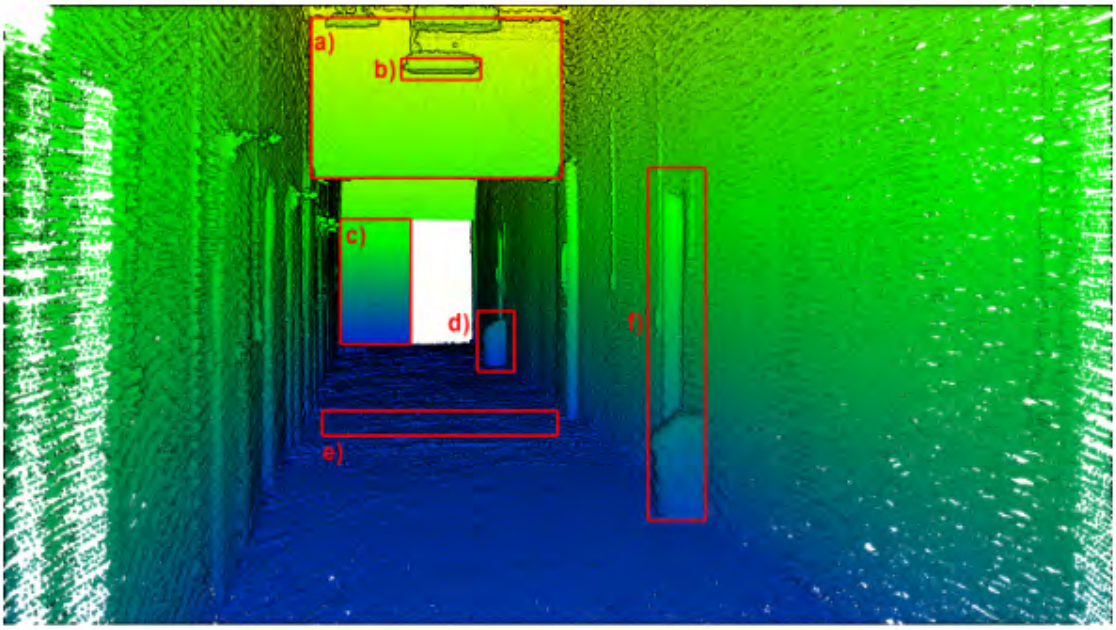

Figure 87: Objects selected for point cloud quality evaluation [196]

Table 19: Number of points for benchmark objects [196]

Measurement type	(a)	(b)	(c)	(d)	(e)	(f)
Horizontal lidar	38,113	836	64,347	1432	6013	23,576
Tilting lidar	55,151	2286	70,834	4415	25,727	20,222
Rotating lidar	86,618	5874	90,425	6289	44,671	38,065

sensor operating within its full rotational range generally has the highest MSD, a tilting sensor delivers results that are nearly as good as offered above and a considerable advancement over the static, horizontal positioning of the lidar. Especially outcomes from elements with characteristic surfaces, causing many occlusions (what is common for underground mining objects) would also support choosing one of the moving lidar mounts.

To conclude, the various elements of 3D-data quality from three typical hardware solutions employing a 3D lidar scanner for the SLAM issue are explored. A multimetric comparison is performed to examine parameters like local surface density and variation, and points per selected object. This examination allowed to gain insights into the performance of SLAM in tunnel-like scenarios, particularly regarding essential facets of inspection and mapping robotic operations in restricted, underground implementations. In underground mine inspection missions, substantial 3D data is gathered using SLAM for navigation as well as 3D analysis. Having complete representations of various objects in the point cloud is essential for machine learning algorithms to classify accurately and differentiate between objects of interest, which can then be analysed using specialized algorithms tailored to specific use cases to be applied during robotic inspection missions.

The results of these analyses are described in detail in the article [196] as a part of the work supported by EIT RawMaterials GmbH under Framework Partnership Agreement No. 19018 (AMICOS. Autonomous Monitoring and Control System for Mining Plants).

7.6 Risk analysis of cyber threats for a mining company

The proposed risk assessment method, described in Section 6.6, is used to present results obtained from the research of risk analysis of cyber threats for a mining company. Furthermore, with usage of techniques like brainstorming sessions, incident documentation, and inspection reports from mines, it is possible to assess the types of consequences and scenario frequencies that can be identified and estimated. Following the research about cybersecurity threats in industry organizations [223], SAFEME4MINE project, and a given literature ([101, 210, 224–234]), there are seven possible scenarios of cyber threats revealed. For each attack technique listed, the probability of occurrence is assessed in accordance to cybersecurity reports (Table 20). In the next Table 21, consequences of techniques compared with target of attack, and the level of mining asset automation are presented. On the basis of preparation work given above, the implementation of fuzzy rule-based risk assessment can be formulated using fuzzy logic toolbox from MATLAB software version R2020a.

Table 20: Likelihood of scenario occurrence [212]

Attack Technique	Occurrence Probability According to Cybersecurity Reports [%]
S1	72
S2	27
S3	27
S4	33
S5	9
S6	10
S7	5

Table 21: Consequences of scenario occurrence according to the targets of attack [212]

Attack Technique	Target of Attack	Consequences
I—Modern Mine		
S1 S2 S3	Databases (technical data, economic reports, personal data).	Financial loss related to data recovery (e.g., ransom), system updates (in order to reinforce uncovered weaknesses), and compensations for the employees whose data has been exposed to the attack; Loss of intellectual property, latent technology; Reputational damage.
S4 S5 S6	Mobile machinery (SCADA systems, on-board hardware related to the control of the machine); Control devices related to other machines and facilities in the mine (e.g., dewatering system, ventilation system).	Unplanned, manual inspections to be done; Increased wear and more frequent damages caused by the lack of information regarding malfunctioning; Obstructed performance analysis and optimization due to the lack of information from SCADA systems; Inability to adjust the energy supply to the actual demand; Limited access to workplaces due to ineffective water drainage; The limited ability of natural hazards' evaluation.
S7	Communication and information networks.	Unauthorized access to network devices and loss of their configuration control; Interception of the data transmitted in an internal network (even if encrypted).
II—Real-Time Mine		
S1 S2 S3	Databases (technical data, economic reports, personal data).	The same as on the previous level – a more extensive scale.
S4 S5 S6	Mobile machinery (SCADA systems, on-board hardware related to the control of the machine); Control devices related to other machines and facilities in the mine (e.g., dewatering system, ventilation system); Autonomous machines.	As on the previous level, additionally: Machinery damage resulting from the continuation of work even if exceeding the permissible working parameters; Impossibility of local autonomous work due to malfunctioning of the machine control system - decrease in productivity and/or forecasting of the mining and wear process; Reduction in the safety level resulting from the impossibility of locating workers and machines on the branches and in the mining faces; Need to switch to 'traditional' ventilation—increased costs.
S7	Communication and information networks.	The same as on the previous level—a more extensive scale.
III—Intelligent Mine		
S1 S2 S3	Databases (technical data, economic reports, personal data)	The same as on the previous level—a more extensive scale.
S4 S5 S6	Autonomous machinery; Control devices related to other machines and facilities in the mine (e.g., dewatering system, ventilation system).	As on the previous level, additionally: Damage resulting from the loss of control over the operation of machines; Damage to machines as a result of working in inappropriate environmental conditions or being in the area of natural hazards; Stopping the production of entire departments or even the entire mine as a result of failure/damage to the main part of the vertical transport infrastructure
S7	Communication and information networks.	The same as on the previous level—a more extensive scale

In the initial phase of building the suggested fuzzy model, the input parameters must undergo fuzzification. Subsequently, the linguistic scores provided by the experts are transformed into equivalent fuzzy set numbers. In the Mamdani fuzzy model, the two input variables are probability and consequences, while the output variable is the risk level. The triangular and trapezoidal fuzzy numbers (FNs) employed in the current case study to depict the linguistic scales for both input and output parameters are illustrated in Fig. 88 (based on tables: 13, 14, 15). The final step of a fuzzy risk assessment model is the determination of IF-THEN rules . Following the results of expert insights from underground safety analysis, Table 22 presents 25 rules of risk assessment, and one additional rule when no risk is defined. For example, rules 1 and 26 are defined as follows:

Rule 1*: IF probability is P1 and consequences are C1 THEN risk level is LOW.*

Rule 26*: If probability is impossible and there are no consequences, THEN the risk level is NO RISK.*

In accordance with this, the experiment is fully covered with all possible risk assessment rules and the fuzzy inference model can be created. Using the rule base above (Fig. 89 [b]), the Mamdami algorithm is used to defuzzify the obtained set of results (Fig. 89 [a]).

Table 22: Risk decision matrix [212]

Consequences Probability	C1	C2	C3	C4	C5
P5	MEDIUM HIGH	MEDIUM HIGH	MEDIUM HIGH	HIGH	HIGH
P4	MEDIUM	MEDIUM	MEDIUM HIGH	MEDIUM HIGH	HIGH
P3	MINOR	MINOR	MEDIUM	MEDIUM HIGH	MEDIUM HIGH
P2	LOW	MINOR	MINOR	MEDIUM	MEDIUM HIGH
P1	LOW	LOW	MINOR	MEDIUM	MEDIUM

Table 23 represents the risk score received from the proposed model in case that all rules posses the same weights. It is an approach in which all risks are equally important and should be sought to be minimized within presumed constraints, e.g.: organizational, time, or budget constraints. However, the weights can be structured in different order i.e. when it is assumed that 'catastrophic' consequences are more important than 'certain' probabilities in the risk assessment process.

In conclusion, the proposed method presents an approach in which the cyber-attack risk level can be assessed for mine use case. Based on the linguistic form of the presentation of expert

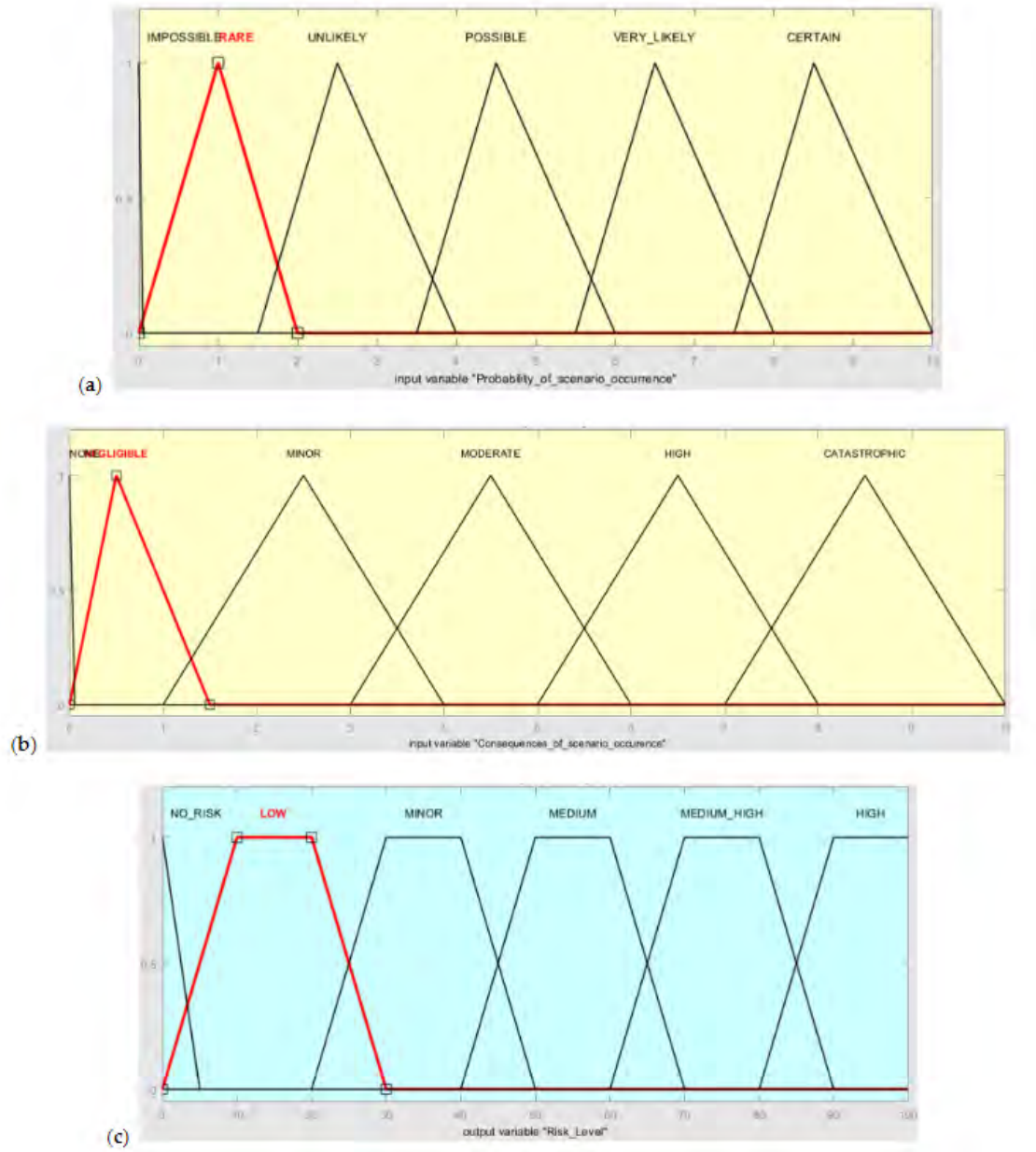

Figure 88: Membership function of (a) probability, (b) consequences, and (c) risk level [212]

knowledge of the probability of scenario occurrence and possible consequences, it is possible to evaluate the risk level with the use of fuzzy logic algorithms. The full model output is presented in Fig. 90. The surface plot symbolize the risk level based on probability of different cyber-attack scenario likehood, and consequences of a given scenario. The consequence can be interpreted as an incapability to continue operations, monetary loss, breakdown, or harm to reputation. The lowest, dark blue levels covers the situation then the final outcome of scenarios are quite likely to happen,

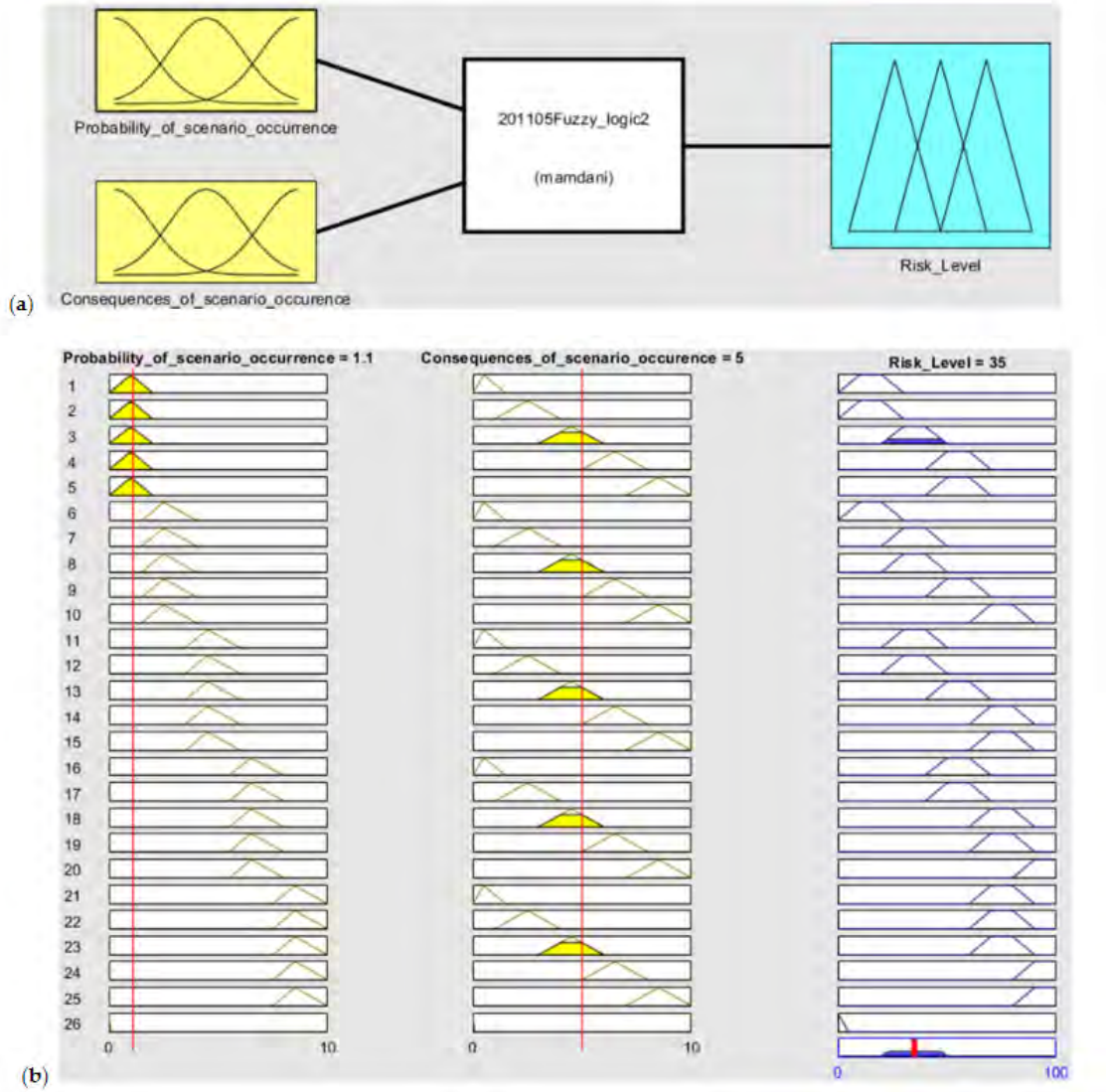

Figure 89: Mamdami model scheme (a) and rule base sample (b) [212]

but have insignificant damage potential. From a risk management perspective, confining the risk to this specific area is the most secure option. It is important to highlight that the top corner, colored yellow, theoretically signifies the most extreme and definite risk (rated 10/10 on the probability scale), which could result in catastrophic consequences for the mine. However, this represents only its highest theoretical level.

In addition to this, the quantitative estimation of the risk parameters can extend the proposed expert outcomes here with usage of real data from other risk analysis cases or other reports concerning the mensurable metrics of cyber-attack undertaken. Given that, expert opinions may

Table 23: Risk scores for scenarios vs. mine automation level (weight=1) [212]

Scenario	Risk Score (Modern Mine)	Risk Score (Real-Time Mine)	Risk Score (Intelligent Mine)
S1	55	75	75
S2	35	55	55
S3	35	55	61.7
S4	61.7	75	75
S5	55	55	55
S6	55	55	55
S7	55	55	55

be embedded in the characteristics of other mining organizations and their experiences may differ, fuzzy logic makes it possible to change the weights of risk analysis rules effortlessly.

The following cyber-attacks risk analysis method can be used to assess the cybersecurity risk, i.e. for digital transformation projects. This information can structure cybersecurity awareness and constitute the priorities for mining management and safety officers to manage project risks. Moreover, it can indicate most hazardous areas and consequently set up the risk mitigation methods. Finally, the results highlight the current state of cybersecurity in the mine and serve as a valuable reference for mine authorities in planning automation-related activities. In addition, the proposed risk assessment approach can be applied to any kind of mine, including surface and underground mining.

The results of these analyses are described in detail in the article [212] as a part of the work supported by EIT Raw Materials GmbH under the Framework Partnership Agreement no. 19036 (SAFEME4MINE. Preventive maintenance system on safety devices of mining machinery).

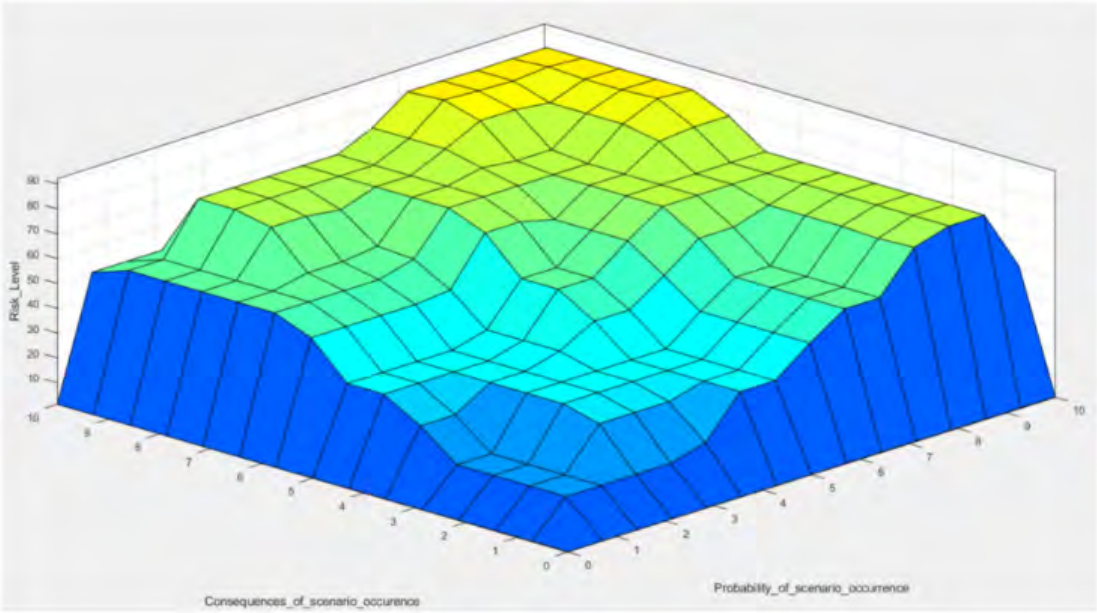

Figure 90: Surface plot of fuzzy inference system (weights = 1) [212]

8 The concept of cloud system architecture adoption for mining industry

In this section, the concept of data processing architecture for tailored mining industry needs is presented. The most emphasis is taken to present the crucial system functions and set them in the concept of usage the Cloud Resources and services. These functionalities are presented in a high-level manner. Their exact configuration and communication with other services within the system should be subjected to additional analysis.

The proposed architecture can be regarded as a preliminary list of requirements for the creation of system solutions, mainly considering code management for distributed IoT devices, machine learning experiments at the edge and management of security aspects of the delivered software. Depending on the degree of integration with Cloud Resources, some of the functionalities presented in this section are available as ready-to-use services prepared by the cloud providers. It would happen that some of them can be not accessible in terms of on-premises limitation. Following the cloud model adoption selected by the mining company, the shared responsibility model entrusts the management of different aspects by splitting the management of the physical, hardware, network, software, application and data layers between the cloud provider and the end customer.

This analysis is based on exemplary mining objects and processes, which are described in detail in the previous sections in order to prepare the information technology department for the efficient software distribution for many mining systems. However, there may also be devices measuring other technological processes in mining, the acquisition of which will require different preconditions. In this architecture concept, the greatest emphasis is taken on technological processes that are similar to the processes studied in this thesis. A number of these have been selected that differ in terms of, among other things, process variability, amount and formats of data collected. As a rule, the various measuring devices will be subject to the same principals in the context of their management, taking into account, above all, the effect of scale and the end result of data processing in order to enable organizations to make a data-driven decisions.

The high-level scheme of the concept is presented in Fig. 91. The proposed architecture consists of the two major parts called Edge Computing Resources (ECR) and (Private / Hybrid / Public) Cloud Resources (CR). The ECR are mainly IoT devices with the common ability to measure physical quantities or monitoring of mining processes as well as the capacity for data preparation and transmission to Data Artifacts Repository (DAR).

For the architecture simplicity, the functionality of taking the measurements from mining technological processes and initial data preparation are treated as the one physical device from the maintenance point of view. As intended, such a resource may be physically separated devices with a fragmented functionalities corresponding to data acquisition and edge preprocessing having the ability to communicate with each other. Still, such a unit corresponds to the use for one piece of equipment, device, machinery, mining process and so on.

The second part of the architecture contains several units corresponding to storage, analytics and aggregated data sharing resources (for visualization and reporting purposes) placed within the scope of the selected Cloud Resources area. The selected components may vary, depending on the cloud service delivery model chosen (private/hybrid/public). Nevertheless, taking into account the assumed data flow from mining devices (comma separated data from environmental measurement devices, BLOB files containing highly compressed data from measurements of highly variable processes, and .rosbag formats from inspection robot missions) the DAR should follow with a data lake concept [235, 236]. It would serve as an output data repository for IoT devices as well as an initial storage point for any analytical module usage. This storage place would stand for the raw data repository and claim as a single source of truth for any further analysis [237]. The next group of the Cloud Resources is the analytical module. Considering the need for efficient big data processing capabilities, the analytical module should consist of the distributed data processing engine to be able to transform and manage significant size of the data at once. At this step, the valid limitation should be raised that it is needed to couple the storage service location with computation power needed for data processing due to the physical limitations of big data transfer efficiency [238]. This means that the choice of the physical storage location of the cloud provider services should be the same as where the data centre operates.

Finally, the agregated data can be utilized to serve as an input for visualizations and reports for stakeholders in order to make a data-driven decisions. The level of data aggregation should follow with the business needs. At this stage it is worth to mention about the need for data management system integration that allows granular data access for different groups of employees.

In the Figure 91, some of the automated workflows (marked in circles from 1 to 7) should be applied to enable the effortless work and proper IoT devices operations at scale. There are the workflows dedicated to:

1. Software distribution for IoT devices
2. Software distribution for Edge Computing Resources

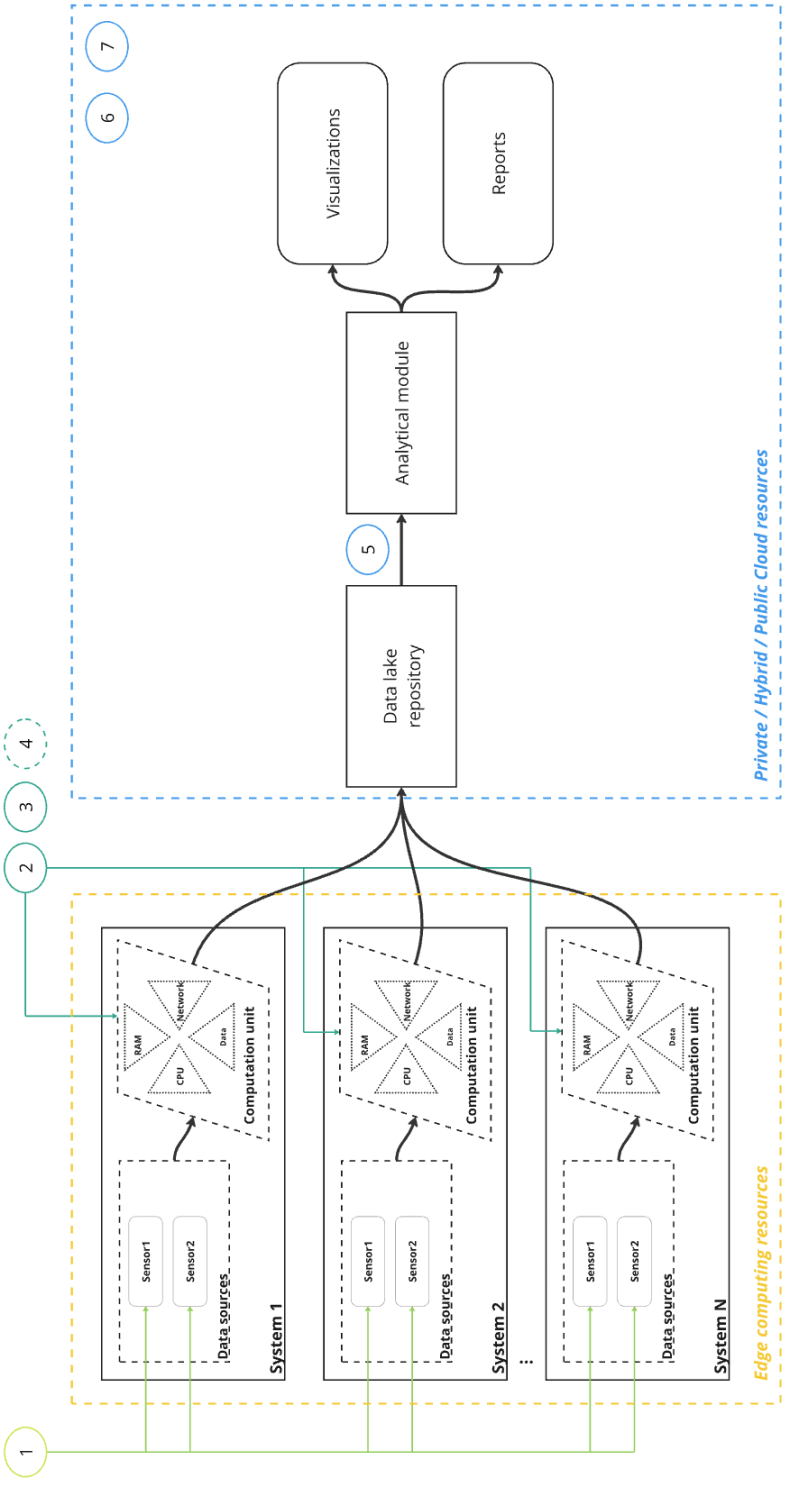

Figure 91: General scheme of edge processing with selected Cloud Resources

3. Edge machine learning workflow
4. Data transmission (streamed or in batch)
5. Scalable data processing
6. Infrastructure management (on-premises and Cloud Resources)
7. Cybersecurity analysis

The next part of this chapter refers to the detailed description of these workflows needed to be fulfilled in terms of the IoT management for mining industry needs. It is worth to mention that the mining area is extensive and that, especially for an underground mine, there are significant technological constraints due to environmental conditions (restrictions on large-scale transmission of data via wireless and wired protocols). Nevertheless, in the high-level architecture presented here, it is assumed that there are no technical limitations for this reason. In order to face the real project condition it is worth to study the well established cloud adoption pathways [239] to address the risks and reshape the business requirements.

Software distribution for IoT devices workflow

The above-mentioned workflows 1 and 2 refer to the software distribution for Edge Computing Resources. The first workflow focuses on the software distribution for IoT devices spread across mining facilities. A range of possibilities that the measuring equipment can be used are presented in Section 4. In high-profile description of the measurement devices, some of the separated modules can be distinguished. The IoT module functional scheme is presented in Fig. 92. Each IoT module matches for an entity which is coupled with the part of the mining system being the subject of measurement. It can be separated into two parts: IoT module and edge processing module. The first module refers to the software written in order to fulfill all functional requirements from the measurement and usability point of view. It covers the sensor interfaces responsible for taking measurements. In most cases it can be handled as a microcomputer / controller with ability to handle GPIO signals from sensors and save / transmit data as well as inform the users about the state with visual / sound interface.

The second module is edge processing module. The main aim is to preprocess the raw data and form them to be prepared for further transmission aiming the Data Artifacts Repository (DAR). Following the examples of devices presented in this thesis, one example of use would be the

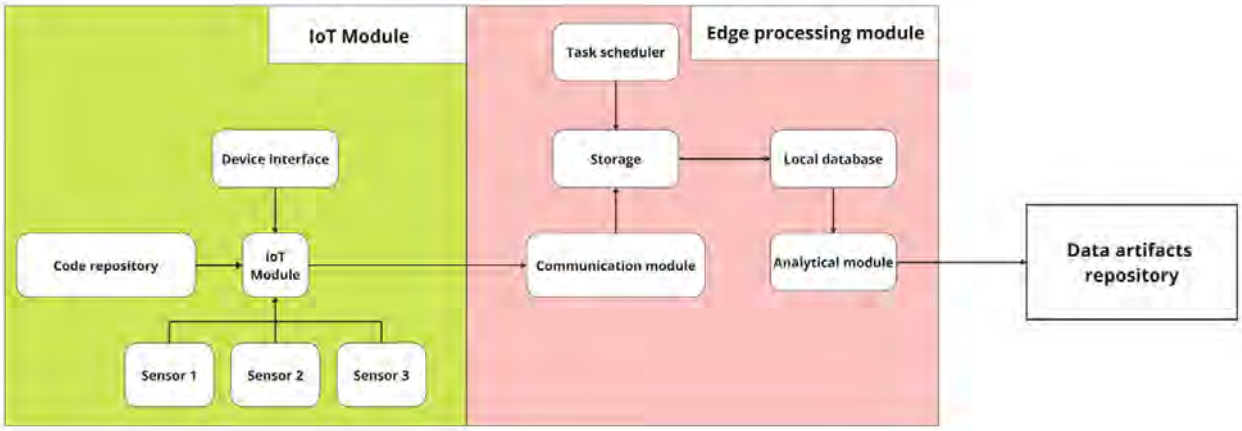

Figure 92: IoT module functional scheme

high-frequency aggregation of current signal to the binary format. This kind of edge processing can be fulfilled by the seperated device communicating with IoT module with efficient hardware components to process the data. It can be handled in a scheduled manner (covered by task scheduler) and process the incomming data in batch or in real time. The transformed data can be saved using the local database entity and be further used by the embbeded analytical module within the edge processing module and serve as part of any machine learning experiment tasks. As an example of such an inference using machine learning at the edge can aim to mining machine cycle classification. Finally, the data collected and conclusions reached can be sent to the central artifact repository (DAR).

As a baseline for source code distribution, a Source Version Control (SVC) tool can be used. With usage of set of tags for versioning the changes in hardware sensor and logger configuration, they can be properly distrubuted across the whole IoT devices landscape. Such a solution may be a facilitation in the context of a future extension of the measurement techniques implemented in the devices, where based on the tags the specific part of the software would be properly addressed to appropriate device groups.

The basic functional workflow for code management is presented in Fig. 93. Let assume a new feature request has arisen to add a new sensor to the measuring device. In step 1 prior to code merging to the main code repository a newly added code is checked via the unit-tests. After a code review completion, the updated code is deployed to the development environment (2). At this stage, a software-based digital-twin of IoT device is spinning up in order to check the integration tests with existing code. After that, the next step is an artifact generation step (3), where all code

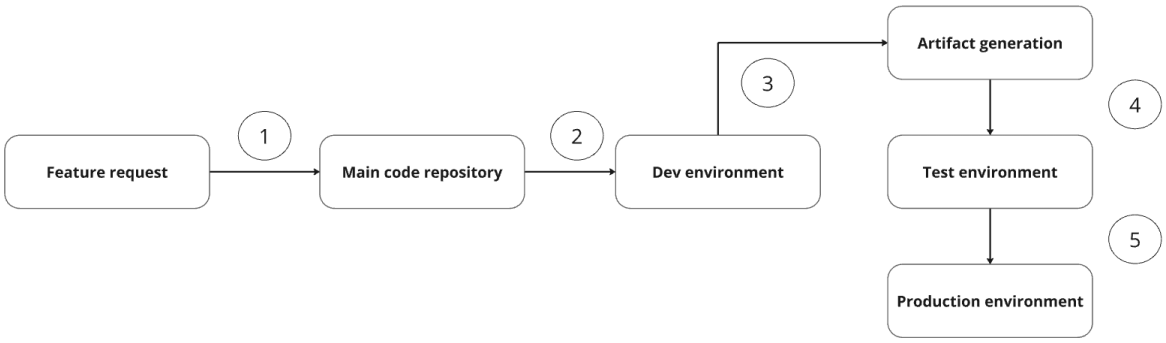

Figure 93: Software code management scheme

artifact and configuration files for embbeded devices are created. These set of the files are loaded into a physical device in order to perform the compability tests with hardware (4). If all succeeded, the final package is prepared and ready to distribute it across the devices working in production conditions (5).

Software distribution for Edge Computing Resources workflow

This workflow follows the same steps as the workflow above. In this case, the focus is not directly on the artifacts associated with the result files necessary to program the hardware and run routines responsible for conducting data acquisition. Thus, it is assumed that each of the Edge Computing Resources (ECR) has enough resources to not only manage the data acquisition from the sensors connected to the system under study, but also to preprocess the data and send it on to the central DAR.

This is based on the management of the code above, but also has to take into account the preprocessing of the data and the sending of aggregated parts of it. For this reason, the control of the software by means of tests will not check the correctness of the interaction with the sensors, but should check the correctness of the calculations and data processing performed. For such a goal, it makes sense to use containerization in testing and in the final production version to create lightweight applications running on ECR.

In this way, the edge processing modules can be decoupled from the host operating system layer and communicate with each other as separate applications. This approach allows the software developed in this way to be easily transferred between hosts both physically mounted as part of a mining systems, but also deployed on Cloud Resources. An example of such system would be

the use of containers within data acquisition for an inspection robot platform where individual containers would be responsible for independent components within the ROS operating system. Another benefit is that it makes it easier to deploy smartphone applications using containers and enable the test coverage of software development for data visualisation applications stored on smartphones. This approach also makes it significantly easier to manage different versions of smartphone operating systems and can be fully automated thanks to implementation within the workflow.

Edge machine learning workflow

In this workflow, some of the data processing methods utilize the machine learning algorithms. In the proposed architecture, they are used both within edge processing and also possible in the analytics module within Cloud Resources. It is responsible for converting some scope of data that may generate outcomes, reasoning what is further used to address the business needs. Nevertheless, many factors and biases can affect this process, in order to cover some of them it is needed to create a general workflow to facilitate it in one common way. The basic example of the proposed machine learning operation scheme is presented in Fig. 94. The first step of this workflow is a dataset preparation to shape the data with all needed features being under the review to receive the known outcomes. This step should be prepared based on in-depth exploratory data analysis for each use case. The next phase is the machine learning model(s) training with usage of the prepared dataset. At stage 2, many statistical metrics would describe the overall effectiveness of machine learning models. This step should handle a different set of metrics for different machine learning experiments (regression problems, classification, clustering etc.). If the results obtained are not satisfactory, the training step is reapeated until the all thresholds will be met (2'). The next step is the model encoding (3). It covers the works of serializing the generated machine learning models and pack them correctly. In existing data science landscape many platform generates the different types of the final model files. In order to make model interoperable, it is needed to set up the one common model file type used and covert into it. Following the proposed model preparation in above manner, the next phase is to register the model (4). It means that the model will be stored in a central model repository with additional metadata layer describing the model. Directly from that place the chosen model can be deployed to inference at the edge or Cloud Resources (5). The additional step will cover the model monitoring and its changes affecting the overall effectiveness (6). At this stage, the dataset drift (adding or removing the feature in the dataset, changes in values

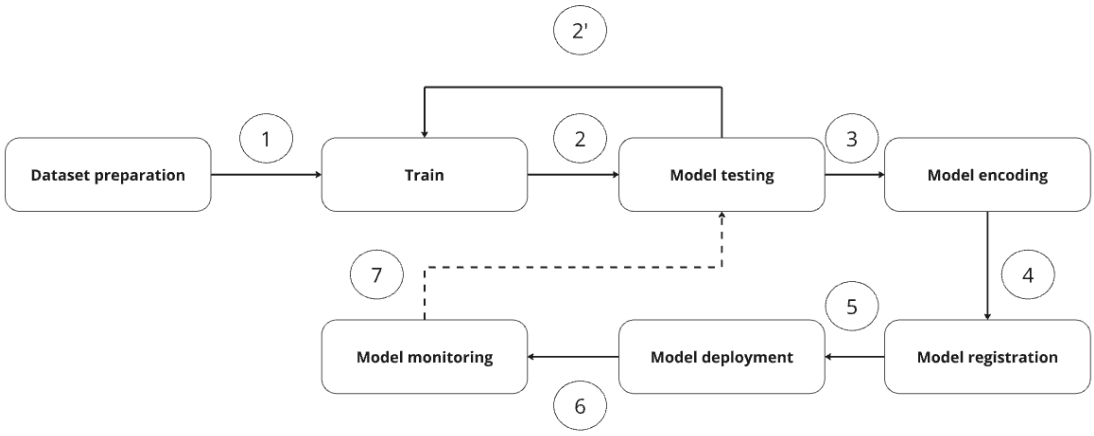

Figure 94: Machine learning operations scheme

distribution) would disturb the model. Hence, the system should come back to the training loop to update the stale model and perform the workflow again (7).

Data transmission workflow

In order to enable the data transfer of different sizes and formats to the DAR, the different ways of communication will be used. Due to the conditions of the mining company, other communication protocols will be selected taking into account the necessary spatial coverage. All communication protocols for Personal Area Network (PAN), LAN and WAN, in both wired and wireless form, can be used at different locations in the mining area backbone network. The workflow for data transmission should take into account the specific network's bandwidth limitations and to facilitate the need for frequency of information on new business events on the basis of acquired data. In order to do that, data can be transmitted from some ECR in a streaming manner, and some in batch triggered by a specific schedule or in ad-hoc manner. In addition to this, the workflow applied should also consider other aspects of data policies such as data retention, consistency, records lifecycle management during data transmission outside the mining area. At this stage, several mechanisms to ensure the system continuity should be used too. It would cover the aspects of possible infrastructure problems in the event of a network failure. Moreover, data transmission workflow can be enhanced by services improving the cybersecurity posture of the organization. To protect the internal institution network against an unauthorized access of data and services, some solutions such as Intrusion Detection System (IDS) and Intrusion Prevention System (IPS) can be taken into account [240].

Scalable data processing workflow

Working with big analytical data requires more computation resources than can be covered by a single machine. For that reason the set of virtual machines, or containers (based on level of the final service virtualization used) can be bonded together to evenly distribute the smaller parts of the data and sync the processed outputs. There are many possible options for scalable processing architecture known in the industry to store the data, such as Data Warehouse (for structured data), and Data Lake (for unstructured data and mixed data workloads) [241]. Considering the form of the data obtained from data sources described in Section 4 for the mining industry, the Data Lake concept can be a first choice for building the analytics engine.

Another major design question is to determine the data-processing workload type. For the above demand it can be distinguishable between two forms of data processing: lambda and medallion architecture. The lambda architecture joins methods of processing data in stream and batch manner. With usage of MapReduce pardigm [242], some precomputed views are calculated on batch layer over the whole dataset being processed, and some views are calculated in an incremental manner over the small data partition on the speed layer [243]. The usage of this data processing architecture within the mining area can be exemplified by the sound measurement taken by inspection robot platform. Sound data can be streamed directly in order to detect the sounds related to failures e.g.: drives in real-time and in meanwhile used for long-term deterioration detection.

The second example is the medallion architecture. The data workflow is divided into 3 layers : bronze, silver, and gold. The bronze layer refers to the raw data obtainted directly from the source. Performing data processing in that manner can be covered by Extract, Transform, Load (ETL) / Extract, Load, Transform (ELT) pipelines, which data are loaded from bronze to silver layer with all needed data transformation steps. The final stage, the gold table, contains the highest aggregated data in a form to be served directly for any visualization and reporting solutions. In this settings, the Data Lake repository can exemplify the bronze layer, where the transformed data go to silver tables, and with the additional aggregation steps, are populated to gold tables. As an example of mining data processing, the current consumption calculation of the drilling rig machine fleet can be managed in this way. In the bronze-layer table, the raw data corresponding to high-frequency sinus-shape signals can be stored. In next steps, the cumulative electricity consumption data every second will be recorded on silver tables. Finally, the aggregation of total drilling cycles performed can be saved on gold tables. Benefits coming from using the Cloud Resources for data processing focus mainly on the modular approach of such solution. It helps to accelerate the successful increasing computing capacity on demand that create an effect of scale.

Cloud Resources infrastructure management workflow

Cloud Resources management is essential to keep track of the quality of service parameters required by business needs. For the private Cloud Resources, the organization should manage all level of the hardware and software including the physical server instances, network layers and finally the application, its configuration, information and data layer. In this workflow, the emphasis is taken on the resources management hosted by cloud services providers. Following the level of the cloud model adoption by the mining organization, the different levels of the hardware virtualization parameters should be handled. From the IaaS perspective, the physical hardware management is taken by cloud provider, but the customer still keeps track of hardware-level resource such as processor type, RAM memory, storage size or network bandwidth. From PaaS perspective, the specific service-level agreement describing the hosted platform should be noted. Finally, for SaaS resources, instead of virtualization or platform-oriented parameters determination, the software parameters related to availability, reliability and redundancy of operation are described.

In most cases, Cloud Resources can be appriovisioned using the visual approach (click-and-run) using the webpage portals as well as usage of deployment scripts utilizing the custom binaries provided by Cloud Resources providers. From the management point of view, the code-centric approach, similar to IoT devices and ECR software distribution workflow is suggested. This Infrastructure as Code (IaC) approach is a more mature way of the cloud infrastructure management. It gives a consistent way of deploying resources, which can be easily reproduced to provision and deprovision set of resources at ease, giving the transparency of changes direcly from the SVC backbone. There are many open-sourced libraries fulfilling that expectations. In principle, they stand for as a wrapper of properly prepared API calls based on the valid description of the given resource parameters expressed in code form.

Cybersecurity analysis workflow

Cybersecurity analysis is an important element of information system architectures. In particular, the integration with Cloud Resources from public providers and the existence of multiple points of contact with the organization's internal network and its integration with Cloud Resources require constant monitoring and a proactive response in the event of threats. Today, cybersecurity analysis should be implemented not as an ad-hoc approach. The given architecture should be secured by design at the time of its creation. In next words, some of the deployment examples are presented. Starting from the software distribution workflow. As a part of cyber resilency, some automated

scans performing the static code analysis to monitor the existence of the known vulnerabilities and exposures can be performed. The other part of code scanning process can also cover any ambiguities, poor quality or prone-to-error implementations. Another workflow can additionally cover the implementation of secrets scanning [244]. For the balance, automatically informing the system administrators of software updates can help to mitigate risk coming from unpatched software. Switching from the code base, the container image scanning is feasible in order to use the only properly patched ones.

Cloud Resources configuration management using the Infrastructure as Code approach can check the correctness of network isolation, where i.e. the access to virtual networks, where cloud services are placed, is trully limited. It can be handled via a set of good practices in resource parameterization to identify any misconfigurations. Area under the cyber risk investigation should not be limited to the specific Cloud Resources configuration only, but these resources themselves. It is needed to check the effectiveness of any flaws which can exist within the Cloud Resources, which may also contain errors in design [111]. Another major factor, which can affect on the overall cyber resilience posture is the protection of system users and limiting their permissions. Usage of Role-Based Access Control (RBAC) mechanism for specific priviliges for custom group of users and implement it within IaC approach is highly relevant. Based on that, the system permissions should be limited to the minimum and be extended only on call. Including additional factors during users authentication is broadly used to get an access to the critical services [245].

8.1 Towards cloud adoption for mining industry

Adoption of Cloud Computing technologies can become an enormous contribution to the development of digital transformation of mining industries. In this work, the greatest impact rely on deployment of IoT devices with sensors to measure the state of the mining infrastructure as well as mining processes. Determination of key mining processes to adopt the Cloud Resources would allow for real-time monitoring of machinery, equipment, and environmental conditions. In Section 4 some of objects and processes are exemplified, which can be a good starting point of Cloud Resources adoption for distributed IoT devices. Nevertheless, any activities in this field should be preceded by an in-depth analysis, first of all, of the organization's requirements and its internal procedures related to ICT systems. Description of data policies for every use case and determination of its retention, consistency, and lifecycle is undoubtedly necessary. In addition to this, the law analysis should be also covered. As an significant development is taking place

in those fields today, more rapidly changing rules need to be taken into account. Starting with Cloud Computing Cybersecurity Standards update [246], it contains a list of many technical and management safeguards. Although this is a provision that allows government entities to use cloud solutions, the list above can be adapted for other organizations. Moreover, the european law is also developing in the field of the use of artificial intelligence. Following the latest Artificial Intelligence Act [247], it presents some use cases regarding prohibited practices.

Another important pillar towards Cloud Computing adoption is the choice of cloud implementation models. The key part of the decision to make is the cost analysis. Depending on public vs. hybrid vs. private vs. multicloud models, there will be different cost proportions related to CAPEX (capital expenditures) and OPEX (operational expenditures). These costs should primarily come from the specific cloud adoption strategy for a given part of organization digital assets. Many global cloud providers serve an advanced cost calculators to estimate the general costs for specific system requirements. For example, increasing the computation power capabilities in private or hybrid model would impact on the higher CAPEX type of costs. In contrary to that, selecting the adoption of public cloud model would divide most of the costs into OPEX costs.

In summary, the description of this high-level architecture is created as a set of good practices that, according to the author, should guide the development of an IT solution that allows the integration of IoT devices working in a mining environment with Cloud Resources. As with any implementation, it should be preceded by a risk analysis, e.g.: based on the steps outlined in Section 6.6. Like any technology, cloud services also carry certain risks. In order to minimise their negative impact on an organization's operations, these must be taken into account when architecting a solution to make it resilient to the most likely threats. In addition to this, stakeholders should take into account during the project planning phase the possible outage of cloud deployed resources. The proper implementation of cloud service redundancy options can ensure acceptable business continuity with acceptable expenses.

Finally, the use of Cloud Resources in the digitisation of mining is undoubtedly a key step in the development of a digital organization. Underground mining is one of the many industries that digital transformation is waiting for and will certainly not bypass. Details are case-specific, but the general trend has already been established, considering the most important aspects to maximize the benefits of using the cloud technologies.

9 Conclusions and future work

The research conducted by the author is focused on the application of data acquisition and analysis methods from the IoT devices applied to several technological processes from copper ore extraction. The data used in this thesis are obtained mostly from proprietary measuring devices developed for selected mining processes. For every case, the detailed technical description of the designed measurement units, as well as data processing methods, are revealed. Developed algorithms for data processing covers all steps from raw data wrangling to outcomes expression about the phenomea being under investigation. In addition to this, a description of the underground experiments and the results obtained using the proposed data processing methods are also presented. Finally, the concept of cloud system architecture adoption for mining industry is proposed as a set of requirements and best practices in order to implement a similar measuring systems at scale in the mine.

The research results obtained confirm the possibility of using the IoT-based measurement systems to assess mining processes. The dedicated measurement solutions for chosen mining processes enable getting insights into operation of e.g. the mining machines works to optimize their work. In addition to this, some examples presented in this work, can support the improvement of miners' work safety.

Going into detail, a special step is to perform experiments, prepare dedicated measurement systems and analyse process data for several technological processes and routine procedures carried out in the underground mine. For every case, the extensive description of data processing and interpretation of results obtained is presented. As an outcome, altogether with considering the fact of underground mine size, mining technologies used and variety of mining processes, there is presented the scale-effective approach for analytical procedures using Cloud Computing. Finally, the concept of cloud architecture for mining industry is revealed. Following the rule of scalling out the similar processes as presented in this thesis, several common workflows for enabling the scalable software delivery and cloud adoption for specific services needed is specified. It would help to establish reliable data workflows and efficient utilization of aggregated big data scopes in mining organization journey of digital transformation.

In details, the following achievements of this work are:

- Development of the measurement device and data processing algorithms to determine the **drilling phase corresponding to drilling rig machine work**. Instead of usage the pressure data, a non-invasive method of measuring instantaneous electric current using current clamps

is presented. The analysis of changes in the operating regime can be performed on the basis of a variable describing the machine's electrical current consumption. Comparing this with the method currently in use, which is based on the analysis of pressure variations in the hydraulic subsystems of a drilling rig, makes the novel method easier to interpret, and the methods proposed determines it well in regards to the actual variability of the process.

- The use of laser rangefinder data makes it possible to **analyse the bolting process**. By means of indirect measurement of the distance to the ceiling (indirect method for measuring the depth of a ceiling hole being drilled), it is possible to **identify bolting cycles**. With usage of non-supervised machine learning algorithms, it can be possible to automatically distinguish the bolting subcycles with usage of the rock bolts. On this basis, automated detection of the performed bolting cycles is feasible.

- Thanks to the current measurements at a mining section, **the detection of working machines and devices** based on analysis in time and frequency domains is achievable. Using the dataset from the electric devices switching test, a learning dataset for the classification algorithm is prepared and the operating moments of individual machines and equipment are successfully extracted with usage of Random Forest Classifier (RFC).

- **Integration of gas sensor with smartphone application** helps underground mining workers to assess the environmental conditions in real time. With usage of software calibration of low-price gas sensors, they can stand for a good approximation of temporary changes in the environment and warn the users about the possible gas hazards.

- The implementation of a **rotating lidar mechanism** with the operating system of the inspection robot increases the density of imaging received and the quality of the spatial imaging obtained. Owing to that, it is possible to generate a detailed mining excavation map to inspect its state and infrastructure (conveyors, conveyor belts, corridor shape, etc.).

- **A cyber risk analysis** dedicated to the mining industry is carried out, taking into account the level of integration with digital systems. A risk analysis method is proposed using indicators derived from expert knowledge and fuzzy logic. It allows the systematization of possible cyber threats within the development of a digital mine.

- Gathering all the requirements as well as constraints for the development of the IoT technology and the implementation of such systems for the mining industry, it is proposed

a concept of **cloud system architecture adoption for mining industry**. It covers several common workflows following the needs from the types of the designed devices presented in this thesis. Due to local infrastructure limitations, it is possible to implement a common framework to deploy a system where data coming from the presented IoT devices can be centrally managed.

Future work should be mainly focused on technology readiness level increase. Most of presented approaches worked at a proof of concept level. Adding new functionalities, implementation of an automated workflows and data flow management will be the main core of future activities. This thesis opens up new possibilities in the area of the study of technological processes of mining machinery and equipment and their adoption with Cloud Resources such as:

- development of new data processing methods for assessment of the abnormal behaviour of the machine operator or drilling equipment,
- optimisation of measurement data acquisition methods using laser sensors accompanying bolting processes to identify bolting cycles,
- extension the application functionality for environmental measurement kit and automation of software calibration for sensors,
- development of autonomous missions related to robotic inspection of mining equipment,
- systematisation of the software management process for large-scale deployment of IoT solutions in mines,
- increasing cyber risk research in the context of Cloud Resources adaptation and business continuity of a digitised mining company.

In the author's opinion, in regards to the current trend of industry digitalization it is viable to set up the one common architecture covering the specific needs from mining industry. As many different processes in the multi-faceted technological operations and miscellaneous types of data being aggregated are in place, thus the modular approach for maintaining the digital assets is essential. Covering the forthcoming digitisation needs of mining, it requires the use of Cloud Resources to be appropriately positioned in the IT systems architecture landscape. This will help to perform the tasks of processing large datasets and unify the management aspects of infrastructure and data processing workflows. By utilizing cloud services in different models, the end customer

- the mine - can shift the focus from managing the entire solution - to just their individual aspects from infrastructure, to platform, to data. This will enable a focus on the business objective and create new opportunities that were not possible with on-premises solutions.

List of Figures

List of Tables

List of abbreviations

BLE Bluetooth Low Energy 18

BMS Basic Monitoring System 24, 27

CC Cloud Computing v, vii, 1, 6, 8, 11, 18, 19, 147–149

CICD Continuous Integration and Continuous Deployment 20, 40

CISA Cybersecurity and Infrastructure Security Agency 37

CMS Condition Monitoring System 18

CR Cloud Resources 11, 19, 22, 86, 137–140, 142, 143, 145–148, 151, 156

DAR Data Artifacts Repository 137, 138, 140–142, 144

DCS Distributed Control System 16

DMS Drilling Monitoring System 24

DPF Diesel particulate filter 31

ECR Edge Computing Resources 137, 138, 140, 142, 144, 146

ELT Extract, Load, Transform 145

ETL Extract, Transform, Load 145

GPIO General Purpose Input/Output 60, 64, 140

HMI Human Machine Interface 27

IaaS Infrastructure as a Service 19, 146

IaC Infrastructure as Code 20, 146, 147

ICT Information and Communications Technology 38, 147

IDS Intrusion Detection System 21, 144

IMU Inertial Measurement Unit 58, 59, 63, 64, 69, 71, 85, 86, 123, 124, 156

IoT Internet of Things vii, 6, 7, 9, 11, 13, 15–18, 20–23, 36, 57, 61, 85, 137, 138, 140, 141, 146–151

IPS Intrusion Prevention System 144

KDE Kernel Density Estimator 75, 98–100, 125, 155

LAN Local Area Network 36, 93, 144

LHD Load Haul Dump Machines 14, 26

LiDAR Light Detection and Ranging 7, 36, 87, 88

MLOps Machine Learning Operations 20, 21

MSD Mean Surface Density 125, 126, 129

MWD Measurement While Drilling 13

NFFT Number of discrete Fourier transform points 112

PaaS Infrastructure as a Service 19, 146

PAN Personal Area Network 144

PCA Principal Component Analysis 83, 104

PPM Parts Per Million 31, 32, 69, 123

RBAC Role-Based Access Control 147

RFC Random Forest Classifier 117, 150

RMS Root Mean Square 97

ROS Robot Operating System 14, 36, 52, 58, 59, 73, 87, 88, 125, 143, 154

SaaS Infrastructure as a Service 19, 146

SCADA Supervisory Control and Data Acquisition 16, 37, 131, 153

SFRA Sweep Frequency Analysis Response 15

SLAM Simultaneous localization and mapping 35, 129

STFT Short-Time Fourier transform 84

SVC Source Version Control 141, 146

UAV Unmanned Aerial Vehicle 34

UGV Unmanned Ground Vehicles 34

WAN Wide Area Network 36, 144

List of mathematical symbols

Symbol	Description
$\mathbf{A}$	Current signal amplitude
ω	Angular frequency
$\mathbf{f_c}$	Signal frequency
$\mathbf{t}$	Time
$\mathbf{m(t)}$	Modulating signal
$\mathbf{x(t)}$	Amplitude-modulated signal of current
$\mathbf{X}$	Discrete signal of $\mathbf{x(t)}$
$\mathbf{Env(X)}$	Upper signal envelope of $\mathbf{X}$
$\hat{\mathbf{f}}(\mathbf{x})$	Empirical density function of $\mathbf{x(t)}$
$\mathbf{K}(\cdot)$	Kernel smoothing function
$\mathbf{n}$	Vector length (number of samples)
$\hat{\sigma}$	Standard deviation of $\mathbf{n}$ samples
$\mathbf{p}$	Length of pressure signal $\mathbf{P}$
$\mathbf{L(t)}$	Laser signal
$\mathbf{l}$	Length of laser signal $\mathbf{L}$
$\mathbf{y_{max}}$	Maximal corridor's height
$\mathbf{SMA}$	Moving average of laser signal
$\mathbf{W_1}$	Length of moving average window
$\mathbf{T_R}$	Range of interest (bolting process parametrization)
$\mathbf{D}$	Minimum penetration of the bolt drill bit
$\mathbf{E}$	Maximum penetration of the bolt drill bit
$\mathbf{r}$	Bolting rod length
$\mathbf{L_2(t)}$	Laser signal with thresholding applied
$\varnothing$	Empty set
$\mathbf{N}$	Number of signal points

List of mathematical symbols (contin.)

Symbol	Description
$\mathbf{PL}$	Starting (lower) point of the drill segment
$\mathbf{PU}$	Peak (upper) point of the drill segment
$\mathbf{C_B}$	Timestamp with cycle beginning point
$\mathbf{C_E}$	Timestamp with cycle ending point
$\mathbf{W_2}$	Length of moving average window for $\mathbf{PU}$ detection
$\mathbf{W_3}$	Length of moving average window for $\mathbf{PL}$ detection
$\mathbf{C}$	Drilling cycle
$\mathbf{c}$	Index of drilling cycles identified
$\mathbf{f_L}$	Frequency of laser signal
$\mathbf{n_L(c)}$	Vector length of the c^{th} cycle identified (number of samples)
α	Drilling progress slope (from linear interpolation of $\mathbf{C}$)
β	Intercept point of drilling progress slope (from linear interpolation of $\mathbf{C}$)
$\mathbf{PCC}$	Pearson correlation coefficient
$\mathbf{k}$	Number of clusters for clustering experiment
$\mathbf{H(z)}$	Transfer function of Chebyshev Type 2 filter
$\mathbf{z}$	Complex number
$\mathbf{a}$	Row vector of denominator coefficients
$\mathbf{b}$	Row vector of numerator coefficients
$\mathbf{d}$	Number of samples for digital filter
$\mathbf{g}$	Filter order
$\mathbf{w}$	Hamming window
$\mathbf{n_w}$	Hamming window length
$\mathbf{j}$	Imaginary unit
$\mathbf{t_P}$	Vector of time points

List of mathematical symbols (contin.)

Symbol	Description
$\mathbf{f_{lim}}$	Limited frequency bins by filter application
$\mathbf{f_{bc}}$	Band cutoff frequency
$\mathbf{f_{max}}$	Maximum frequency from Nyquist criterion
$\mathbf{GC}$	Estimation of gas concentration
$\mathbf{O}$	Raw digital output of gas sensor signal
$\mathbf{O_{min}}$	Minimum value of O
$\mathbf{O_{max}}$	Maximum value of O
$\mathbf{V}$	Reference from calibrated sensor
$\mathbf{V_{min}}$	Minimum value of V
$\mathbf{V_{max}}$	Maximum value of V
$\mathbf{s}$	Estimated step length
$\mathbf{U}$	Calibration constant of the given user
$\mathbf{a}_{\max_{\mathbf{v_i}}}$	Maximum of vertical acceleration value during i-th step
$\mathbf{a}_{\min_{\mathbf{v_i}}}$	Minimum of vertical acceleration value during i-th step
$\mathbf{R}$	Risk
$\mathbf{S}$	Scenario (undesirable event) description
$\mathbf{P_S}$	Probability of a scenario
$\mathbf{M_C}$	Measure of consequences caused by a scenario
$\mathbf{\Omega}$	Number of possible scenarios
$\mathbf{A_Z}$	Fuzzy number
$\mu_{\mathbf{1}}(\phi)$	Triangular fuzzy numbers membership function
$\mu_{\mathbf{2}}(\phi)$	Trapezoidal fuzzy numbers membership function
$\mathbf{W_L}$	Width of rolling window on predicted labels

Bibliography

[1] KGHM Polska Miedź S.A. Ore mining. https://kghm.com/en/our-business/processes/ore-mining, 2024. [Accessed 25-08-2024].

[2] Seyed Hadi Hoseinie, Hussan Al-Chalabi, and Behzad Ghodrati. Comparison between simulation and analytical methods in reliability data analysis: A case study on face drilling rigs. *Data*, 3(2):12, 2018.

[3] Paweł Śliwiński. A method of comprehensive assessment of the operational efficiency of machines and predictive maintenance based on data from the monitoring system. *Diss. PhD Thesis (in Polish),*, 2023. URL https://bip.pwr.edu.pl/strona-glowna/postepowania-o-nadanie-stopnia-doktora---publikowane-od-2023-r/pawel-sliwinski.

[4] Radosław Waloski, Waldemar Korzeniowski, Łukasz Bołoz, and Waldemar Rączka. Identification of rock mass critical discontinuities while borehole drilling. *Energies*, 14(10): 2748, 2021.

[5] Robert Zlot and Michael Bosse. Efficient large-scale three-dimensional mobile mapping for underground mines. *Journal of Field Robotics*, 31(5):758–779, 2014.

[6] M McNinch, D Parks, R Jacksha, and A Miller. Leveraging IIoT to improve machine safety in the mining industry. *Mining, metallurgy & exploration*, 36(4):675–681, 2019.

[7] Valentin Isheyskiy and José A Sanchidrián. Prospects of applying mwd technology for quality management of drilling and blasting operations at mining enterprises. *Minerals*, 10 (10):925, 2020.

[8] Manoj Khanal, Johnny Qin, Baotang Shen, and Bongani Dlamini. Preliminary investigation into Measurement While Drilling as a means to characterize the coalmine roof. *Resources*, 9(2):10, 2020.

[9] Wenpeng Liu, Jamal Rostami, and Eric Keller. Application of new void detection algorithm for analysis of feed pressure and rotation pressure of roof bolters. *International Journal of Mining Science and Technology*, 27(1):77–81, 2017.

[10] Wenpeng Liu, Jamal Rostami, Asok Ray, and Derek Elsworth. Statistical analysis of the capabilities of various pattern recognition algorithms for fracture detection based on monitoring drilling parameters. *Rock Mechanics and Rock Engineering*, 53(5):2265–2278, 2020.

[11] Sohail Manzoor, Samaneh Liaghat, Anna Gustafson, Daniel Johansson, and Håkan Schunnesson. Rock mass characterization using MWD data and photogrammetry. In *Mining Goes Digital*, pages 217–225. CRC Press, 2019.

[12] Jordan McBain and Markus Timusk. Software architecture for condition monitoring of mobile underground mining machinery: A framework extensible to intelligent signal processing and analysis. In *2012 IEEE Conference on Prognostics and Health Management*, pages 1–12, 2012.

[13] Paweł Stefaniak, Jacek Wodecki, Radosław Zimroz, Paweł Śliwiński, and Marek Andrzejewski. The multivariate analysis of monitoring system data from mining drilling machine. *International Multidisciplinary Scientific GeoConference: SGEM*, 2:913–920, 2016.

[14] Maria Stachowiak, Wioletta Koperska, Artur Skoczylas, Sergii Anufriiev, Paweł Stefaniak, and Anders Fhager. Multidimensional data analysis for drilling process in underground mines. In *APCOM 2023 Proceedings: Intelligent Mining: Innovation, Vision, and Value*, 2023.

[15] Jacek Wodecki, Anna Michalak, and Paweł Stefaniak. Review of smoothing methods for enhancement of noisy data from heavy-duty LHD mining machines. In *E3S Web of Conferences*, volume 29, page 00011. EDP Sciences, 2018.

[16] Mateusz Góralczyk, Anna Michalak, and Paweł Śliwiński. Drill bit deterioration estimation with the Random Forest Regressor. In *IOP Conference Series: Earth and Environmental Science*, volume 942, page 012013. IOP Publishing, 2021.

[17] Bartłomiej Ziętek, Jacek Wodecki, Anna Michalak, and Pawel Śliwiński. Drill bit state-oriented drilling process classification with time-series data for wheeled drilling rigs. In *IOP Conference Series: Earth and Environmental Science*, volume 942, page 012010. IOP Publishing, 2021.

[18] Ali Siamaki. Advanced analytics for drilling and blasting. In *Advanced Analytics in Mining Engineering: Leverage Advanced Analytics in Mining Industry to Make Better Business Decisions*, pages 323–343. Springer, 2022.

[19] Sebastian Arenas Bermúdez, Cristian Gerardo Zapata Otalora, and Jorge Martin Molina Escobar. Impacts of downtimes mitigation related to face drilling rigs in mining development cycles. *Archives of Mining Sciences*, pages 125–132, 2021.

[20] Juan C Gutiérrez-Diez, Ana M Castañón, and Marc Bascompta. New method to study the effectiveness of mining equipment: A case study of surface drilling rigs. *Applied Sciences*, 14(5):2185, 2024.

[21] M Erkayaoglu. Use of geospatial queries for optimum drilling and blasting practices in surface mining. In *Proceedings of the 27th International Symposium on Mine Planning and Equipment Selection-MPES 2018*, pages 57–67. Springer, 2019.

[22] Carlos Tampier, Mauricio Mascaro, and Javier Ruiz-del Solar. Autonomous loading system for load-haul-dump (LHD) machines used in underground mining. *Applied Sciences*, 11 (18):8718, 2021.

[23] Jarosław Szrek, Paweł Trybała, Mateusz Góralczyk, Anna Michalak, Bartłomiej Ziętek, and Radosław Zimroz. Accuracy evaluation of selected mobile inspection robot localization techniques in a GNSS-denied environment. *Sensors*, 21(1):141, 2020.

[24] Paweł Stefaniak, Bartosz Jachnik, Wioletta Koperska, and Artur Skoczylas. Localization of LHD machines in underground conditions using IMU sensors and DTW algorithm. *Applied Sciences*, 11(15):6751, 2021.

[25] Ian D. Miller, Fernando Cladera, Anthony Cowley, Shreyas S. Shivakumar, Elijah S. Lee, Laura Jarin-Lipschitz, Akhilesh Bhat, Neil Rodrigues, Alex Zhou, Avraham Cohen, Adarsh Kulkarni, James Laney, Camillo Jose Taylor, and Vijay Kumar. Mine tunnel exploration using multiple quadrupedal robots. *IEEE Robotics and Automation Letters*, 5(2):2840–2847, 2020.

[26] Mauricio Mascaró, Isao Parra-Tsunekawa, Carlos Tampier, and Javier Ruiz-del Solar. Topological navigation and localization in tunnels—application to autonomous load-haul-dump vehicles operating in underground mines. *Applied Sciences*, 11(14):6547, 2021.

[27] Jacek Paraszczak, Anna Gustafson, and Håkan Schunnesson. Technical and operational aspects of autonomous LHD application in metal mines. *International Journal of Mining, Reclamation and Environment*, 29(5):391–403, 2015.

[28] Amin Moniri-Morad, Masoud S Shishvan, Mario Aguilar, Malihe Goli, and Javad Sattarvand. Powered haulage safety, challenges, analysis, and solutions in the mining industry; a comprehensive review. *Results in Engineering*, page 101684, 2023.

[29] Andrea Fioravanti, Alberto Prudenzi, Giovanni Bucci, Edoardo Fiorucci, Fabrizio Ciancetta, and Simone Mari. Non intrusive electrical load identification through an online SFRA based approach. In *2020 International Symposium on Power Electronics, Electrical Drives, Automation and Motion (SPEEDAM)*, pages 694–698. IEEE, 2020.

[30] Michael Zeifman, Craig Akers, and Kurt Roth. Nonintrusive monitoring of miscellaneous and electronic loads. In *2015 IEEE International Conference on Consumer Electronics (ICCE)*, pages 305–308, 2015.

[31] Dominik Łuczak, Stefan Brock, and Krzysztof Siembab. Fault detection and localisation of a three-phase inverter with permanent magnet synchronous motor load using a convolutional neural network. *Actuators*, 12(3):125, 2023.

[32] Radu-Casian Mihailescu, David Hurtig, and Charlie Olsson. End-to-end anytime solution for appliance recognition based on high-resolution current sensing with few-shot learning. *Internet of Things*, 11:100263, 2020.

[33] Yung-Yao Chen and Yu-Hsiu Lin. A smart autonomous time-and frequency-domain analysis current sensor-based power meter prototype developed over fog-cloud analytics for demand-side management. *Sensors*, 19(20):4443, 2019.

[34] Jundika C Kurnia, Agus P Sasmito, Wai Yap Wong, and Arun S Mujumdar. Prediction and innovative control strategies for oxygen and hazardous gases from diesel emission in underground mines. *Science of the Total Environment*, 481:317–334, 2014.

[35] Mateusz Kudasik and Norbert Skoczylas. Analyzer for measuring gas contained in the pore space of rocks. *Measurement Science and Technology*, 28(10):105901, 2017.

[36] Anna Pajdak, Katarzyna Godyń, Mateusz Kudasik, and Tomasz Murzyn. The use of selected research methods to describe the pore space of dolomite from copper ore mine, Poland. *Environmental Earth Sciences*, 76:1–16, 2017.

[37] Justyna Hebda-Sobkowicz, Sebastian Gola, Radosław Zimroz, and Agnieszka Wyłomańska. Identification and statistical analysis of impulse-like patterns of carbon monoxide variation in deep underground mines associated with the blasting procedure. *Sensors*, 19(12):2757, 2019.

[38] Justyna Hebda-Sobkowicz, Sebastian Gola, Radosław Zimroz, and Agnieszka Wyłomańska. Pattern of H2S concentration in a deep copper mine and its correlation with ventilation schedule. *Measurement*, 140:373–381, 2019.

[39] Akhand Rai and Sanjay H Upadhyay. A review on signal processing techniques utilized in the fault diagnosis of rolling element bearings. *Tribology International*, 96:289–306, 2016.

[40] Robert B Randall and Jerome Antoni. Rolling element bearing diagnostics—a tutorial. *Mechanical Systems and Signal Processing*, 25(2):485–520, 2011.

[41] Jérôme Antoni and Robert Bond Randall. The spectral kurtosis: application to the vibratory surveillance and diagnostics of rotating machines. *Mechanical Systems and Signal Processing*, 20(2):308–331, 2006.

[42] Willem Abraham Roos and Philippus Stephan Heyns. In-belt vibration monitoring of conveyor belt idler bearings by using wavelet package decomposition and artificial intelligence. *International Journal of Mining and Mineral Engineering*, 12(1):48–66, 2021.

[43] A Jablonski and T Barszcz. Validation of vibration measurements for heavy duty machinery diagnostics. *Mechanical Systems and Signal Processing*, 38(1):248–263, 2013.

[44] Pawel Rzeszucinski, Maciej Orman, Cajetan T Pinto, Agnieszka Tkaczyk, and Maciej Sulowicz. Bearing health diagnosed with a mobile phone: Acoustic signal measurements can be used to test for structural faults in motors. *IEEE Industry Applications Magazine*, 24 (4):17–23, 2018.

[45] Xiangwei Liu, Deli Pei, Gabriel Lodewijks, Zhangyan Zhao, and Jie Mei. Acoustic signal based fault detection on belt conveyor idlers using machine learning. *Advanced Powder Technology*, 31(7):2689–2698, 2020.

[46] Xiong Zhang, Shuting Wan, Yuling He, Xiaolong Wang, and Longjiang Dou. Teager energy spectral kurtosis of wavelet packet transform and its application in locating the sound source of fault bearing of belt conveyor. *Measurement*, 173:108367, 2021.

[47] Ryszard Błażej, Leszek Jurdziak, Tomasz Kozłowski, and Agata Kirjanów. The use of magnetic sensors in monitoring the condition of the core in steel cord conveyor belts–tests of the measuring probe and the design of the DiagBelt system. *Measurement*, 123:48–53, 2018.

[48] Leszek Jurdziak, Ryszard Błażej, Agata Kirjanów-Błażej, Aleksandra Rzeszowska, and Paweł Kostrzewa. Improving the effectiveness of the DiagBelt+ diagnostic system - analysis of the impact of measurement parameters on the quality of signals. *Eksploatacja i Niezawodność – Maintenance and Reliability*, 26(3), 2024. ISSN 1507-2711.

[49] Anurag Choudhary, Tauheed Mian, and Shahab Fatima. Convolutional neural network based bearing fault diagnosis of rotating machine using thermal images. *Measurement*, 176: 109196, 2021.

[50] R Zimroz, M Hutter, M Mistry, P Stefaniak, K Walas, and J Wodecki. Why should inspection robots be used in deep underground mines? In *Proceedings of the 27th International Symposium on Mine Planning and Equipment Selection-MPES 2018*, pages 497–507. Springer, 2019.

[51] Mohammad Siami, Tomasz Barszcz, Jacek Wodecki, and Radoslaw Zimroz. Semantic segmentation of thermal defects in belt conveyor idlers using thermal image augmentation and U-Net-based convolutional neural networks. *Scientific Reports*, 14(1):5748, 2024.

[52] Mohammad Siami, Tomasz Barszcz, Jacek Wodecki, and Radoslaw Zimroz. Design of an infrared image processing pipeline for robotic inspection of conveyor systems in opencast mining sites. *Energies*, 15(18):6771, 2022.

[53] Parthkumar Parmar, Leszek Jurdziak, Aleksandra Rzeszowska, and Anna Burduk. Predictive modeling of conveyor belt deterioration in coal mines using AI techniques. *Energies*, 17(14): 3497, 2024.

[54] João Reis, Marlene Amorim, Nuno Melão, and Patrícia Matos. Digital transformation: a literature review and guidelines for future research. *Trends and Advances in Information Systems and Technologies: Volume 1 6*, pages 411–421, 2018.

[55] Lars Barnewold and Bernd G Lottermoser. Identification of digital technologies and digitalisation trends in the mining industry. *International Journal of Mining Science and Technology*, 30(6):747–757, 2020.

[56] Jablonski Adam and Tomasz Barszcz. Vulnerabilities and fruits of smart monitoring. *Smart Monitoring of Rotating Machinery for Industry 4.0*, pages 1–9, 2022.

[57] Erik Lund, Annika Pekkari, Jan Johansson, and Joel Lööw. Mining 4.0 and its effects on work environment, competence, organisation and society–a scoping review. *Mineral Economics*, pages 1–14, 2024.

[58] Lin Bi, Zhuo Wang, Zhaohao Wu, and Yuhao Zhang. A new reform of mining production and management modes under industry 4.0: Cloud mining mode. *Applied Sciences*, 12(6): 2781, 2022.

[59] Qinglin Qi and Fei Tao. Digital twin and big data towards smart manufacturing and industry 4.0: 360 degree comparison. *IEEE Access*, 6:3585–3593, 2018.

[60] Emmanuel Raj, David Buffoni, Magnus Westerlund, and Kimmo Ahola. Edge MLOps: An automation framework for AIoT applications. In *2021 IEEE International Conference on Cloud Engineering (IC2E)*, pages 191–200. IEEE, 2021.

[61] Dominique Dom Guinard and Vlad M Trifa. *Building the web of things: with examples in node.js and raspberry pi*. Simon and Schuster, 2016.

[62] Luigi Atzori, Antonio Iera, and Giacomo Morabito. The internet of things: A survey. *Computer networks*, 54(15):2787–2805, 2010.

[63] Fatemeh Molaei, Elham Rahimi, Hossein Siavoshi, Setareh Ghaychi Afrouz, and Victor Tenorio. A comprehensive review on Internet of Things (IoT) and its implications in the mining industry. *American Journal of Engineering and Applied Sciences*, 13(3):499–515, 2020.

[64] Paweł Stefaniak, Wioletta Koperska, Artur Skoczylas, Justyna Witulska, and Paweł Śliwiński. Methods of optimization of mining operations in a deep mine-tracking the dynamic overloads using IoT sensor. *IEEE Access*, 2023.

[65] Dominik Łuczak, Stefan Brock, and Krzysztof Siembab. Cloud based fault diagnosis by convolutional neural network as time–frequency RGB image recognition of industrial machine vibration with internet of things connectivity. *Sensors*, 23(7):3755, 2023.

[66] Byung Wan Jo, Rana Muhammad Asad Khan, Yun Sung Lee, Jun Ho Jo, and Nadia Saleem. A Fiber Bragg Grating-Based Condition Monitoring and Early Damage Detection System for the Structural Safety of Underground Coal Mines Using the Internet of Things. *Journal of Sensors*, 2018(1):9301873, 2018.

[67] N Surendranath Reddy, M Srinivasa Saketh, and Sourav Dhar. Review of sensor technology for mine safety monitoring systems: A holistic approach. In *2016 IEEE First International Conference on Control, Measurement and Instrumentation (CMI)*, pages 429–434. IEEE, 2016.

[68] Sushant Kumar Pattnaik, Soumya Ranjan Samal, Shuvabrata Bandopadhaya, Kaliprasanna Swain, Subhashree Choudhury, Jitendra Kumar Das, Albena Mihovska, and Vladimir Poulkov. Future wireless communication technology towards 6G IoT: An application-based analysis of IoT in real-time location monitoring of employees inside underground mines by using BLE. *Sensors*, 22(9):3438, 2022.

[69] Byung Wan Jo and Rana Muhammad Asad Khan. An event reporting and early-warning safety system based on the internet of things for underground coal mines: A case study. *Applied Sciences*, 7(9):925, 2017.

[70] ByungWan Jo and Rana Muhammad Asad Khan. An internet of things system for underground mine air quality pollutant prediction based on azure machine learning. *Sensors*, 18(4):930, 2018.

[71] Yufeng Jiang, Wei Chen, Xue Zhang, Xuejun Zhang, and Guowei Yang. Real-time monitoring of underground miners' status based on mine IoT system. *Sensors*, 24(3):739, 2024.

[72] Wojciech Staszewski, Adam Jablonski, and Tomasz Barszcz. New possibilities of redundant data transmission for intelligent sensor networks. In *Proc. MFPT-Intell. Technol. Equip. Hum. Perform. Monit.*, pages 180–189, 2018.

[73] Adam Jabłoński, Tomasz Barszcz, and Marzena Bielecka. Automatic validation of vibration signals in wind farm distributed monitoring systems. *Measurement*, 44(10):1954–1967, 2011.

[74] Adam Jablonski and Tomasz Barszcz. Overview of practical aspects of evaluation of spectral scalar indicators for trend analysis in condition monitoring. In *Workshop on Nonstationary Systems and Their Applications*, pages 207–216. Springer, 2021.

[75] Reihaneh H Hariri, Erik M Fredericks, and Kate M Bowers. Uncertainty in big data analytics: survey, opportunities, and challenges. *Journal of Big data*, 6(1):1–16, 2019.

[76] Qi Zhang, Lu Cheng, and Raouf Boutaba. Cloud computing: state-of-the-art and research challenges. *Journal of internet services and applications*, 1:7–18, 2010.

[77] D Parkhill. The challenge of the computer utility. AddisonWesley. *Reading*, 1966.

[78] Hui Zhang, Guofei Jiang, Kenji Yoshihira, Haifeng Chen, and Akhilesh Saxena. Intelligent workload factoring for a hybrid cloud computing model. In *2009 Congress on Services-I*, pages 701–708. IEEE, 2009.

[79] Armando Fox, Rean Griffith, Anthony Joseph, Randy Katz, Andrew Konwinski, Gunho Lee, David Patterson, Ariel Rabkin, Ion Stoica, et al. Above the clouds: A berkeley view of cloud computing. *Dept. Electrical Eng. and Comput. Sciences, University of California, Berkeley, Rep. UCB/EECS*, 28(13):2009, 2009.

[80] Surajit Chaudhuri and Umeshwar Dayal. An overview of data warehousing and OLAP technology. *ACM Sigmod record*, 26(1):65–74, 1997.

[81] Huang Fang. Managing data lakes in big data era: What's a data lake and why has it became popular in data management ecosystem. In *2015 IEEE International Conference on Cyber Technology in Automation, Control, and Intelligent Systems (CYBER)*, pages 820–824, 2015.

[82] Enji Sun, Xingkai Zhang, and Zhongxue Li. The internet of things (IoT) and cloud computing (CC) based tailings dam monitoring and pre-alarm system in mines. *Safety science*, 50(4):811–815, 2012.

[83] Jiacheng Xie, Shuguang Liu, and Xuewen Wang. Framework for a closed-loop cooperative human Cyber-Physical System for the mining industry driven by VR and AR: MHCPS. *Computers & Industrial Engineering*, 168:108050, 2022.

[84] Nabil El Bazi, Mustapha Mabrouki, Oussama Laayati, Nada Ouhabi, Hicham El Hadraoui, Fatima-Ezzahra Hammouch, and Ahmed Chebak. Generic multi-layered digital-twin-framework-enabled asset lifecycle management for the sustainable mining industry. *Sustainability*, 15(4):3470, 2023.

[85] Nabil Elbazi, Mustapha Mabrouki, Ahmed Chebak, and FatimaEzzahrae Hammouch. Digital twin architecture for mining industry: case study of a stacker machine in an experimental open-pit mine. In *2022 4th Global Power, Energy and Communication Conference (GPECOM)*, pages 232–237. IEEE, 2022.

[86] Christopher Newman, Zach Agioutantis, and Nathaniel Schaefer. Development of a web-platform for mining applications. *International Journal of Mining Science and Technology*, 28(1):95–99, 2018.

[87] Liangcai Fang, Chungui Ge, Guolin Zu, Xinkun Wang, Weiguo Ding, Changliang Xiao, and Liang Zhao. A mobile edge computing architecture for safety in mining industry. In *2019 IEEE SmartWorld, Ubiquitous Intelligence & Computing, Advanced & Trusted Computing, Scalable Computing & Communications, Cloud & Big Data Computing, Internet of People and Smart City Innovation (SmartWorld/SCALCOM/UIC/ATC/CBDCom/IOP/SCI)*, pages 1494–1498. IEEE, 2019.

[88] Yuchun Zhang, Liang Zhao, Kaiqi Yang, and Lexi Xu. Mobile edge computing for intelligent mining safety: a case study of ventilator. In *2020 IEEE intl conf on parallel & distributed processing with applications, big data & cloud computing, sustainable computing & communications, social computing & networking (ISPA/BDCloud/SocialCom/SustainCom)*, pages 1300–1305. IEEE, 2020.

[89] Huimin Lu, Mei Wang, and Arun Kumar Sangaiah. Human emotion recognition using an EEG cloud computing platform. *Mobile Networks and Applications*, 25:1023–1032, 2020.

[90] K Soroko, P Zgrzebski, R Stach, and S Gola. Improving underground mine climate conditions using ventilation dams to seal abandoned areas in polish copper mines. *CIM Journal*, 11(3):188–197, 2020.

[91] Piotr Bardzinski, Leszek Jurdziak, Witold Kawalec, and Robert Krol. Copper ore quality tracking in a belt conveyor system using simulation tools. *Natural Resources Research*, 29: 1031–1040, 2020.

[92] Mark Jasinski, Elżbieta Jasińska, Michal Jasiński, and Lukasz Jasiński. Computer-aided appliances to underground machines maintenance – selected issues. In *2018 10th International Conference on Electronics, Computers and Artificial Intelligence (ECAI)*, pages 1–4, 2018. doi: 10.1109/ECAI.2018.8679066.

[93] Andrej Dyck, Ralf Penners, and Horst Lichter. Towards definitions for release engineering and DevOps. In *2015 IEEE/ACM 3rd International Workshop on Release Engineering*, pages 3–3. IEEE, 2015.

[94] Esteban Elias Romero, Carlos David Camacho, Carlos Enrique Montenegro, Óscar Esneider Acosta, Rubén González Crespo, Elvis Eduardo Gaona, and Marcelo Herrera Martínez. Integration of DevOps practices on a noise monitor system with CircleCI and Terraform. *ACM Transactions on Management Information Systems (TMIS)*, 13(4):1–24, 2022.

[95] Dominik Kreuzberger, Niklas Kühl, and Sebastian Hirschl. Machine learning operations (MLOps): Overview, definition, and architecture. *IEEE access*, 11:31866–31879, 2023.

[96] Hubert Baniecki, Wojciech Kretowicz, Piotr Piątyszek, Jakub Wiśniewski, et al. Dalex: responsible machine learning with interactive explainability and fairness in python. *Journal of Machine Learning Research*, 22(214):1–7, 2021.

[97] Yan Liu, Zhijing Ling, Boyu Huo, Boqian Wang, Tianen Chen, and Esma Mouine. Building a platform for machine learning operations from open source frameworks. *IFAC-PapersOnLine*, 53(5):704–709, 2020.

[98] DR Niranjan et al. Jenkins pipelines: A novel approach to machine learning operations (MLOps). In *2022 International Conference on Edge Computing and Applications (ICECAA)*, pages 1292–1297. IEEE, 2022.

[99] Antonio M Burgueño-Romero, Antonio Benítez-Hidalgo, Cristóbal Barba-González, and José F Aldana-Montes. Towards an open-source MLOps architecture. *IEEE Software*, 2024.

[100] Philipp Ruf, Manav Madan, Christoph Reich, and Djaffar Ould-Abdeslam. Demystifying MLOps and presenting a recipe for the selection of open-source tools. *Applied Sciences*, 11 (19):8861, 2021.

[101] Terje Aven. The risk concept—historical and recent development trends. *Reliability Engineering & System Safety*, 99:33–44, 2012.

[102] Technical Committee ISO/TC 262. PN-ISO 31000:2018-08: Risk management—principles and guidelines. `https://www.iso.org/obp/ui#iso:std:iso:31000:ed-2:v1:en`, 2018. [Accessed 11-11-2024].

[103] Technical Committee ISO/TC 262. ISO 31073:2022. `https://www.iso.org/obp/ui#iso:std:iso:31073:ed-1:v1:en`, 2022. [Accessed 11-11-2024].

[104] Katja Tuma, Gül Calikli, and Riccardo Scandariato. Threat analysis of software systems: A systematic literature review. *Journal of Systems and Software*, 144:275–294, 2018.

[105] EY. Top 10 risks and opportunities for mining and metals companies in 2025. `https://www.ey.com/en_gl/insights/energy-resources/risks-opportunities`, 2024. [Accessed 11-11-2024].

[106] EY. Top 10 business risks and opportunities – 2020. `https://web.archive.org/web/20211205220704/https://www.ey.com/en_gl/mining-metals/10-business-risks-facing-mining-and-metals`, 2020. [Accessed 11-11-2024].

[107] Julian Jang-Jaccard and Surya Nepal. A survey of emerging threats in cybersecurity. *Journal of Computer and System Sciences*, 80(5):973–993, 2014.

[108] Patricia AS Ralston, James H Graham, and Jefferey L Hieb. Cyber security risk assessment for SCADA and DCS networks. *ISA transactions*, 46(4):583–594, 2007.

[109] Kamran Shaukat, Suhuai Luo, Vijay Varadharajan, Ibrahim A Hameed, and Min Xu. A survey on machine learning techniques for cyber security in the last decade. *IEEE access*, 8: 222310–222354, 2020.

[110] Ying Zhang, Peisong Li, and Xinheng Wang. Intrusion detection for IoT based on improved genetic algorithm and deep belief network. *IEEE Access*, 7:31711–31722, 2019.

[111] Biniam Fisseha Demissie and Silvio Ranise. Assessing the Effectiveness of the Shared Responsibility Model for Cloud Databases: the Case of Google's Firebase. In *2021 IEEE International Conference on Smart Data Services (SMDS)*, pages 121–131. IEEE, 2021.

[112] Viktor Engström, Pontus Johnson, Robert Lagerström, Erik Ringdahl, and Max Wällstedt. Automated security assessments of Amazon Web services environments. *ACM Transactions on Privacy and Security*, 26(2):1–31, 2023.

[113] Stanislaw Piasecki, Lachlan Urquhart, and Derek McAuley. Defence against the dark artefacts: Smart home cybercrimes and cybersecurity standards. *Computer law & Security review*, 42:105542, 2021.

[114] Pascal Oser, Rens W van der Heijden, Stefan Lüders, and Frank Kargl. Risk prediction of IoT devices based on vulnerability analysis. *ACM Transactions on Privacy and Security*, 25 (2):1–36, 2022.

[115] Olufogorehan Tunde-Onadele, Jingzhu He, Ting Dai, and Xiaohui Gu. A study on container vulnerability exploit detection. In *2019 IEEE International Conference on Cloud Engineering (IC2E)*, pages 121–127. IEEE, 2019.

[116] Mine Master. Face master 1.7 specification. `https://www.minemaster.eu/product/face-master-1-7/`, 2024. [Accessed 24-07-2024].

[117] Krzysztof Okrent. Studying the impact of the drilling process on the durability of cutting tools. *Diss. PhD Thesis (in Polish)*, 2012. URL `https://winntbg.bg.agh.edu.pl/rozprawy2/10566/full10566.pdf`.

[118] Oihane C Basurko and Zigor Uriondo. Condition-based maintenance for medium speed diesel engines used in vessels in operation. *Applied Thermal Engineering*, 80:404–412, 2015.

[119] Xiang Rao, Chenxing Sheng, Zhiwei Guo, and Chengqing Yuan. A review of online condition monitoring and maintenance strategy for cylinder liner-piston rings of diesel engines. *Mechanical Systems and Signal Processing*, 165:108385, 2022.

[120] Patrycja Janiszewska. Mine Master made self-propelled drilling and bolting rigs designed for underground mining. *Mining–Informatics, Automation and Electrical Engineering*, 58: 7–11, 2020.

[121] Artur Kozłowski and Łukasz Bołoz. Battery electric roof bolter versus diesel roof bolter—results of field trials at a polish copper mine. *Energies*, 17(12):3033, 2024.

[122] Mine Master. Roof master 1.7.0 datasheet specification. `https://www.minemaster.eu/sites/default/files/ulotka%20Roof%20Master%201.7_0.pdf`, 2020. [Accessed 2-09-2023].

[123] Jucai Chang, Kai He, Zhiqiang Yin, Wanfeng Li, Shihui Li, and Dongdong Pang. Study on the instability characteristics and bolt support in deep mining roadways based on the surrounding rock stability index: example of pansan coal mine. *Advances in Civil Engineering*, 2020(1):8855335, 2020.

[124] A. Pietrzyński, M. Zaleska-Kuczmierczyk, and J. Janowski. *Exploitation systems, mining methods and types of excavation support; Monograph of KGHM Polska Miedź S.A.* CBPM "Cuprum" Sp. z o.o. , Wroclaw on behalf of KGHM Polska Miedź SA, ISBN 83–905296–0–2 (in Polish), Lubin, 1996.

[125] Biraj Lama and Moe Momayez. Review of non-destructive methods for rock bolts condition evaluation. *Mining*, 3(1):106–120, 2023.

[126] Jung-Doung Yu, Myeong-Ho Bae, In-Mo Lee, and Jong-Sub Lee. Nongrouted ratio evaluation of rock bolts by reflection of guided ultrasonic waves. *Journal of Geotechnical and Geoenvironmental Engineering*, 139(2):298–307, 2013.

[127] DH Steve Zou, Jiulong Cheng, Renjie Yue, and Xiaoyun Sun. Grout quality and its impact on guided ultrasonic waves in grouted rock bolts. *Journal of Applied Geophysics*, 72(2): 102–106, 2010.

[128] V Madenga, DH Zou, and C Zhang. Effects of curing time and frequency on ultrasonic wave velocity in grouted rock bolts. *Journal of Applied Geophysics*, 59(1):79–87, 2006.

[129] Victor Giurgiutiu. Structural health monitoring (SHM) of aerospace composites. In *Polymer Composites in the Aerospace Industry*, pages 491–558. Elsevier, 2020.

[130] Bo Wang, Linsheng Huo, Dongdong Chen, Weijie Li, and Gangbing Song. Impedance-based pre-stress monitoring of rock bolts using a piezoceramic-based smart washer—a feasibility study. *Sensors*, 17(2):250, 2017.

[131] Jung-Doung Yu, Ki-Hong Kim, and Jong-Sub Lee. Nondestructive health monitoring of soil nails using electromagnetic waves. *Canadian Geotechnical Journal*, 55(1):79–89, 2018.

[132] Krzysztof Skrzypkowski. Case studies of rock bolt support loads and rock mass monitoring for the room and pillar method in the Legnica-Głogów copper district in Poland. *Energies*, 13(11):2998, 2020.

[133] Anna Bajus. Cost analysis by positions on the example of the KGHM Polska Miedź SA mining plants. *Zeszyty Naukowe Instytutu Gospodarki Surowcami Mineralnymi Polskiej Akademii Nauk*, 2019.

[134] KGHM Polska Miedź S.A. Plan for the renovation of power grids and facilities - 2024 (in polish). `https://kghm.com/sites/default/files/tabela_plan_remontow_osd_kghm_polska_miedz_s.a._na_rok_2024.pdf`, 2024. [Accessed 13-08-2024].

[135] KGHM Polska Miedź S.A. Plan for the renovation of power grids and facilities - 2023 (in polish). `https://kghm.com/sites/default/files/2024-01/plan_remontow_osd_kghm_polska_miedz_s.a._na_rok_2023.pdf`, 2024. [Accessed 13-08-2024].

[136] KGHM Polska Miedź S.A. Plan for the renovation of power grids and facilities - 2018 (in polish). `https://kghm.com/sites/default/files/plan-remontow-osd-kghm-na-2018-rok.pdf`, 2024. [Accessed 13-08-2024].

[137] Stefan Gierlotka. Rozwój elektryfikacji kopalń węgla kamiennego. *Hereditas Minariorum*, 3:225–236, 2016.

[138] Marco Civera and Cecilia Surace. A comparative analysis of signal decomposition techniques for structural health monitoring on an experimental benchmark. *Sensors*, 21 (5):1825, 2021.

[139] Menglong Wu, Nanyan Hu, Yicheng Ye, Qihu Wang, and Xianhua Wang. Multi-hazard risk characterization and collaborative control oriented to space in non-coal underground mines. *Scientific Reports*, 12(1):16452, 2022.

[140] Norbert Skoczylas, Katarzyna Kozieł, and Libor Sitek. The principles of evaluating the risk of rock and gas outburst in copper ore mines. *Rock Mechanics and Rock Engineering*, pages 1–18, 2024.

[141] KGHM Polska Miedź S.A. Mining assets of KGHM Polska Miedź S.A. in the Legnica-Głogów Copper District. Technical report, KGHM Polska Miedź S.A, M. Skłodowskiej-Curie 48, September 2012.

[142] Aleksandra Banasiewicz, Anna Janicka, Anna Michalak, and Radosław Włostowski. Photocatalysis as a method for reduction of ambient NOx in deep underground mines. *Measurement*, 200:111453, 2022.

[143] William Jacobs, Melinda R Hodkiewicz, and Thomas Bräunl. A cost–benefit analysis of electric loaders to reduce diesel emissions in underground hard rock mines. *IEEE Transactions on industry applications*, 51(3):2565–2573, 2014.

[144] Tee L Guidotti. Hydrogen sulfide intoxication. In *Handbook of clinical neurology*, volume 131, pages 111–133. Elsevier, 2015.

[145] Katy O Goyak and R Jeffrey Lewis. Application of adverse outcome pathway networks to integrate mechanistic data informing the choice of a point of departure for hydrogen sulfide exposure limits. *Critical Reviews in Toxicology*, 51(3):193–208, 2021.

[146] Bo Tan, Zhuangzhuang Shao, Hongyi Wei, Guangyuan Yang, Xiaoman Zhu, Bin Xu, and Feichao Zhang. Status of research on hydrogen sulphide gas in chinese mines. *Environmental Science and Pollution Research*, 27:2502–2521, 2020.

[147] Mark Goldstein. Carbon monoxide poisoning. *Journal of Emergency Nursing*, 34(6): 538–542, 2008.

[148] İpek Özmen and Emine Aksoy. Respiratory emergencies and management of mining accidents. *Turkish Thoracic Journal*, 16(Suppl 1):S18, 2015.

[149] Maria Stachowiak, Wioletta Koperska, Paweł Stefaniak, Artur Skoczylas, and Sergii Anufriiev. Procedures of detecting damage to a conveyor belt with use of an inspection legged robot for deep mine infrastructure. *Minerals*, 11(10):1040, 2021.

[150] KGHM Zanam. Belt conveyor haulage systems. `https://www.kghmzanam.com/kategoria/systemy-odstawy-tasmowej/`, 2024. [Online; accessed 16-August-2024].

[151] Jarosław Szrek, Janusz Jakubiak, and Radoslaw Zimroz. A mobile robot-based system for automatic inspection of belt conveyors in mining industry. *Energies*, 15(1):327, 2022.

[152] Radoslaw Zimroz, Monika Hardygóra, and Ryszard Blazej. Maintenance of belt conveyor systems in Poland - an overview. In *Proceedings of the 12th International Symposium Continuous Surface Mining-Aachen 2014*, pages 21–30. Springer, 2015.

[153] Leszek Jurdziak, Damian Kaszuba, Witold Kawalec, and Robert Król. Idea of identification of copper ore with the use of process analyser technology sensors. In *IOP Conference Series: Earth and Environmental Science*, volume 44, page 042037. IOP Publishing, 2016.

[154] Piotr Kruczek, Jakub Sokołowski, Jakub Obuchowski, Mateusz Sawicki, Agnieszka Wyłomańska, and Radosław Zimroz. Fault detection in belt conveyor drive unit via multiple source data. In *Cyclostationarity: Theory and Methods III: Contributions to the 9th Workshop on Cyclostationary Systems and Their Applications, Grodek, Poland, 2016*, pages 173–186. Springer, 2017.

[155] Srijeet Halder and Kereshmeh Afsari. Robots in inspection and monitoring of buildings and infrastructure: A systematic review. *Applied Sciences*, 13(4):2304, 2023.

[156] Hamid Shiri, Jacek Wodecki, Bartłomiej Ziętek, and Radosław Zimroz. Inspection robotic UGV platform and the procedure for an acoustic signal-based fault detection in belt conveyor idler. *Energies*, 14(22):7646, 2021.

[157] Artur Skoczylas, Paweł Stefaniak, Sergii Anufriiev, and Bartosz Jachnik. Belt conveyors rollers diagnostics based on acoustic signal collected using autonomous legged inspection robot. *Applied Sciences*, 11(5):2299, 2021.

[158] Tomasz Buratowski, Jerzy Garus, Mariusz Giergiel, and Andrii Kudriashov. Real-time 3D mapping in isolated industrial terrain with use of mobile robotic vehicle. *Electronics*, 11 (13):2086, 2022.

[159] Robert Lösch, Steve Grehl, Marc Donner, Claudia Buhl, and Bernhard Jung. Design of an autonomous robot for mapping, navigation, and manipulation in underground mines. In *2018 IEEE/RSJ International Conference on Intelligent Robots and Systems (IROS)*, pages 1407–1412. IEEE, 2018.

[160] Héctor Azpúrua, Adriano Rezende, Guilherme Potje, Gilmar Pereira da Cruz Júnior, Rafael Fernandes, Victor Miranda, Levi Welington de Resende Filho, Jacó Domingues, Filipe Rocha, Frederico Luiz Martins de Sousa, et al. Towards semi-autonomous robotic inspection and mapping in confined spaces with the EspeleoRobô. *Journal of Intelligent & Robotic Systems*, 101:1–27, 2021.

[161] KGHM Polska Miedź S.A. W pracy: SCADA, która proces nadzoruje (in polish). `https://kghm.com/pl/w-pracy`, 2024. [Online; accessed 22-August-2024].

[162] CISA. Guide to getting started with a cybersecurity risk assessment. Technical report, Cybersecurity & Infrastructure Security Agency, August 2024.

[163] CVE Numbering Authorities. Common Vulnerabilities and Exposures. `https://www.cve.org/About/Overview`, 2024. [Online; accessed 22-August-2024].

[164] Cybersecurity & Infrastructure Security Agency. Known exploited vulnerabilities catalog. `https://www.cisa.gov/known-exploited-vulnerabilities-catalog`, 2024. [Online; accessed 22-August-2024].

[165] The European Union Agency for Cybersecurity (ENISA). Threat landscape. `https://www.enisa.europa.eu/topics/cyber-threats/threats-and-trends`, 2024. [Online; accessed 22-August-2024].

[166] KGHM Polska Miedź S.A. W pracy: Energia na cenzurowanym (in polish). `https://kghm.com/pl/w-pracy`, 2024. [Online; accessed 22-August-2024].

[167] Maria Ilaria Lunesu, Roberto Tonelli, Lodovica Marchesi, and Michele Marchesi. Assessing the risk of software development in agile methodologies using simulation. *IEEE Access*, 9: 134240–134258, 2021.

[168] Keke Gai, Meikang Qiu, and Sam Adam Elnagdy. A novel secure big data cyber incident analytics framework for cloud-based cybersecurity insurance. In *2016 IEEE 2nd International Conference on Big Data Security on Cloud (BigDataSecurity), IEEE International Conference on High Performance and Smart Computing (HPSC), and IEEE International Conference on Intelligent Data and Security (IDS)*, pages 171–176. IEEE, 2016.

[169] Mineral and Energy Economy Research Institute of the Polish Academy of Sciences. Mineral Resources & Energy Congress (SEP) 2024. `https://szkolaeksploatacji.pl/wp-content/knowledge/flipbook/_materialy_sep_koncowe/2024/index.html`, 2024. [Accessed 04-02-2025].

[170] Artur Dyczko. Cybersecurity of IT/OT systems in key functional areas of a mining plant operating on the basis of the idea of INDUSTRY 4.0. *Mining Machines*, 42, 2024.

[171] Krzysztof Fuławka, Lech Stolecki, Marcin Szumny, Witold Pytel, Izabela Jaśkiewicz-Proć, Michel Jakić, Michael Nöger, and Philipp Hartlieb. Roof fall hazard monitoring and evaluation—state-of-the-art review. *Energies*, 15(21):8312, 2022.

[172] Piotr Mertuszka, Bartlomiej Kramarczyk, Mateusz Pytlik, Marcin Szumny, Katarzyna Jaszcz, and Tomasz Jarosz. Implementation and verification of effectiveness of bulk emulsion explosive with improved energetic parameters in an underground mine environment. *Energies*, 15(17):6424, 2022.

[173] Jacek Wodecki, Mateusz Góralczyk, Pavlo Krot, Bartłomiej Ziętek, Jaroslaw Szrek, Magdalena Worsa-Kozak, Radoslaw Zimroz, Paweł Śliwiński, and Andrzej Czajkowski. Process monitoring in heavy duty drilling rigs—data acquisition system and cycle identification algorithms. *Energies*, 13(24):6748, 2020.

[174] Bartłomiej Ziętek, Paweł Śliwiński, Jarosław Szrek, and Radosław Zimroz. Laser-based measurement system for drilling and bolting operations monitoring in deep underground copper ore mine. *Measurement*, 253:117425, 2025. ISSN 0263-2241. doi: https://doi.org/10.1016/j.measurement.2025.117425.

[175] Bartłomiej Ziętek, Aleksandra Banasiewicz, Radosław Zimroz, Jarosław Szrek, and Sebastian Gola. A portable environmental data-monitoring system for air hazard evaluation in deep underground mines. *Energies*, 13(23), 2020. ISSN 1996-1073.

[176] Paweł Trybała, Jarosław Szrek, Fabio Remondino, Paulina Kujawa, Jacek Wodecki, Jan Blachowski, and Radosław Zimroz. MIN3D Dataset: MultI-seNsor 3D Mapping with an Unmanned Ground Vehicle. *PFG–Journal of Photogrammetry, Remote Sensing and Geoinformation Science*, 91(6):425–442, 2023.

[177] P Trybała, J Szrek, F Remondino, J Wodecki, and R Zimroz. Calibration of a multi-sensor wheeled robot for the 3D mapping of underground mining tunnels. *The International Archives of the Photogrammetry, Remote Sensing and Spatial Information Sciences*, 48: 135–142, 2022.

[178] Feng Gao, Xin Li, Xin Xiong, Haichuan Lu, and Zengwu Luo. Refined design and optimization of underground medium and long hole blasting parameters—a case study of the gaofeng mine. *Mathematics*, 11(7):1612, 2023.

[179] Open Robotics. ROS: velodyne_driver. `https://wiki.ros.org/velodyne_driver?distro=melodic`, 2024. [Online; accessed 10-July-2024].

[180] Open Robotic. RViz: User Guide. `https://wiki.ros.org/rviz/UserGuide`, 2024. [Online; accessed 11-July-2024].

[181] Shailja Tripathi, Laxmi Pandit, et al. Analysis of factors influencing adoption of internet of things: a system dynamics approach. *Theoretical Economics Letters*, 9(07):2606, 2019.

[182] DFRobot. DFRobot DS3231M github.com. `https://github.com/DFRobot/DFRobot_DS3231M`, 2023. [Accessed 07-09-2023].

[183] Adafruit. Adafruit CircuitPython MPU6050. `https://github.com/adafruit/Adafruit_CircuitPython_MPU6050`, 2023. [Accessed 07-09-2023].

[184] Fluke. Fluke i400 AC Current Clamp data sheet. `https://dam-assets.fluke.com/s3fs-public/fluke-i400.pdf?pgTa0A6AEwbFAUkykZ6GCpX14A_DWwcO`, 2024. [Accessed 20-05-2024].

[185] Hanwei Eletronics CO LTD. MQ9 gas sensor. https://www.mouser.com/datasheet/2/830/SEN0134_MQ_9-2488817.pdf, 2020. [Online; accessed 25-May-2024].

[186] Ltd Zhengzhou Winsen Electronics Technology Co. MQ136 gas sensor. https://cdn.sparkfun.com/assets/d/e/3/8/6/MQ136__Ver1.4__-_Manual.pdf, 2015. [Online; accessed 25-May-2024].

[187] Wavesen. HC06 Bluetooth datasheet. https://www.olimex.com/Products/Components/RF/BLUETOOTH-SERIAL-HC-06/resources/hc06.pdf, 2020. [Online; accessed 26-May-2024].

[188] Hubert Henry Ward and Hubert Henry Ward. Using bluetooth with PIR motion sensors. *Programming Arduino Projects with the PIC Microcontroller: A Line-by-Line Code Analysis and Complete Reference Guide for Embedded Programming in C*, pages 343–387, 2022.

[189] Ben Wittbrodt and Joshua M. Pearce. The effects of PLA color on material properties of 3-D printed components. *Additive Manufacturing*, 8:110–116, 10 2015.

[190] V. Mirón, S. Ferrándiz, D. Juárez, and A. Mengual. Manufacturing and characterization of 3D printer filament using tailoring materials. *Procedia Manufacturing*, 13:888–894, 2017.

[191] Minister of Energy. Regulation of the Minister of Energy related to operations of underground mining (available in polish: Rozporzadzenie Ministra Energii z dnia 23 listopada 2016 r., w sprawie szczegółowych wymagań dotyczacych prowadzenia ruchu podziemnych zakładów górniczych (dz. u. z 2017r., poz. 1118), 2017. https://www.dziennikustaw.gov.pl/du/2017/1118/1.

[192] platformio.org. IDE for embedded development. https://platformio.org/, 2020. [Online; accessed 26-May-2024].

[193] gs.statcounter.com. Mobile OS Market share. https://gs.statcounter.com/os-market-share/mobile/worldwide/, 2024. [Online; accessed 26-May-2024].

[194] Inc. Open Source Robotics Foundation. ROS - Robot Operating System. https://ros.org/, 2024. [Online; accessed 12-June-2024].

[195] ROBOTIS. DYNAMIXEL AX-12A datasheet. https://www.robotis.us/dynamixel-ax-12a, 2024. [Online; accessed 12-June-2024].

[196] Paweł Trybała, Jarosław Szrek, Błażej Dębogórski, Bartłomiej Ziętek, Jan Blachowski, Jacek Wodecki, and Radosław Zimroz. Analysis of lidar actuator system influence on the quality of dense 3D point cloud obtained with SLAM. *Sensors*, 23(2):721, 2023.

[197] Lawrence Marple. Computing the discrete-time "analytic" signal via FFT. *IEEE Transactions on signal processing*, 47(9):2600–2603, 1999.

[198] Hill Peter D. Kernel estimation of a distribution function. *Communications in Statistics-Theory and Methods*, 14(3):605–620, 1985.

[199] Bernard W Silverman. *Density estimation for statistics and data analysis*. Routledge, 2018.

[200] Jacob Benesty, Jingdong Chen, Yiteng Huang, and Israel Cohen. Pearson correlation coefficient. *Springer Topics in Signal Processing*, 2:1 – 4, 2009.

[201] Matteo Mazziotta and Adriano Pareto. Normalization methods for spatio-temporal analysis of environmental performance: Revisiting the min–max method. *Environmetrics*, 33(5), 2022.

[202] Michael E Tipping and Christopher M Bishop. Mixtures of probabilistic principal component analyzers. *Neural computation*, 11(2):443–482, 1999.

[203] R.G. Lyons. *Understanding Digital Signal Processing*. Prentice Hall professional technical reference. Prentice Hall/PTR, 2004. ISBN 9780131089891.

[204] A.V. Oppenheim, R.W. Schafer, and J.R. Buck. *Discrete-time Signal Processing*. Prentice Hall international editions. Prentice Hall, 1999. ISBN 9780137549207.

[205] Estefania Munoz Diaz and Ana Luz Mendiguchia Gonzalez. Step detector and step length estimator for an inertial pocket navigation system. In *2014 International Conference on Indoor Positioning and Indoor Navigation (IPIN)*, pages 105–110, 2014.

[206] Yunye Jin, Hong-Song Toh, Wee-Seng Soh, and Wai-Choong Wong. A robust dead-reckoning pedestrian tracking system with low cost sensors. In *2011 IEEE International Conference on Pervasive Computing and Communications (PerCom)*, pages 222–230, 2011.

[207] Yuya Maruyama, Shinpei Kato, and Takuya Azumi. Exploring the performance of ROS2. In *Proceedings of the 13th international conference on embedded software*, pages 1–10, 2016.

[208] Paweł Trybała. 3D Surveying of Mining Environments using Simultaneous Localization and Mapping. *Diss. PhD Thesis (in Polish), available at:* `https://bip.pwr.edu.pl/strona-glowna/postepowania-o-nadanie-stopnia-doktora---publikowane-od-2023-r/pawel-trybala`, 2023.

[209] Wael R Abdellah, Jong-Gwan Kim, Mohamed MA Hassan, and Mahrous AM Ali. The key challenges towards the effective implementation of digital transformation in the mining industry. *Geosystem Engineering*, 25(1-2):44–52, 2022.

[210] Stanley Kaplan and B John Garrick. On the quantitative definition of risk. *Risk analysis*, 1 (1):11–27, 1981.

[211] Debi Prasad Tripathy and Charan Kumar Ala. Risk assessment in underground coalmines using fuzzy logic in the presence of uncertainty. *Journal of The Institution of Engineers (India): Series D*, 99:157–163, 2018.

[212] Agnieszka A Tubis, Sylwia Werbińska-Wojciechowska, Mateusz Góralczyk, Adam Wróblewski, and Bartłomiej Ziętek. Cyber-attacks risk analysis method for different levels of automation of mining processes in mines based on fuzzy theory use. *Sensors*, 20(24): 7210, 2020.

[213] J Antoniak. W kierunku kopalni przyszłości. *Surowce i Maszyny Budowlane*, 4:35–40, 2010.

[214] W Pratt Rogers, M Mustafa Kahraman, Frank A Drews, Kody Powell, Joel M Haight, Yaxue Wang, Kritika Baxla, and Mohit Sobalkar. Automation in the mining industry: Review of technology, systems, human factors, and political risk. *Mining, metallurgy & exploration*, 36:607–631, 2019.

[215] Deloitte. Intelligent Mining. Delivering Real Value. `https://www.deloitte.com/content/dam/assets-shared/legacy/docs/gx-intelligent-mining-mar-2018.pdf`, 2018. [Online; accessed 29-May-2023].

[216] Cengiz Kahraman, Ufuk Cebeci, and Ziya Ulukan. Multi-criteria supplier selection using fuzzy AHP. *Logistics information management*, 16(6):382–394, 2003.

[217] F. Pedregosa, G. Varoquaux, A. Gramfort, V. Michel, B. Thirion, O. Grisel, M. Blondel, P. Prettenhofer, R. Weiss, V. Dubourg, J. Vanderplas, A. Passos, D. Cournapeau, M. Brucher, M. Perrot, and E. Duchesnay. Scikit-learn: Machine learning in Python. *Journal of Machine Learning Research*, 12:2825–2830, 2011.

[218] Congming Shi, Bingtao Wei, Shoulin Wei, Wen Wang, Hai Liu, and Jialei Liu. A quantitative discriminant method of elbow point for the optimal number of clusters in clustering algorithm. *EURASIP Journal on Wireless Communications and Networking*, 2021 (1), February 2021. ISSN 1687-1499.

[219] Moez Ali. *PyCaret: An open source, low-code machine learning library in Python*, April 2020. URL `https://www.pycaret.org`. PyCaret version 1.0.0.

[220] TR Mahesh, Oana Geman, Martin Margala, Manisha Guduri, et al. The stratified k-folds cross-validation and class-balancing methods with high-performance ensemble classifiers for breast cancer classification. *Healthcare Analytics*, 4:100247, 2023.

[221] Ni Wayan Surya Wardhani, Masithoh Yessi Rochayani, Atiek Iriany, Agus Dwi Sulistyono, and Prayudi Lestantyo. Cross-validation metrics for evaluating classification performance on imbalanced data. In *2019 International Conference on Computer, Control, Informatics and its Applications (IC3INA)*, pages 14–18. IEEE, 2019.

[222] P. Stefaniak, J. Wodecki, A. Michalak, A. Wyłomańska, and R. Zimroz. Data acquisition system for position tracking and human-selected physiological and environmental parameters in underground mine. In *Proceedings of the 18th Symposium on Environmental Issues and Waste Management in Energy and Mineral Production*, pages 241–248. Springer International Publishing, 2018.

[223] Great Britain Government. Cyber Security Breaches Survey; main report. Technical report, Department for Culture Media and Sport, London, 2017.

[224] N Huq. Cyber Threats to the Mining Industry. A Trendlabs research paper. `https://documents.trendmicro.com/assets/wp/wp-cyber-threats-to-the-mining-industry.pdf`, 2024. [Accessed 31-08-2024].

[225] Mariusz Kostrzewski, Pavol Varjan, and Josef Gnap. Solutions dedicated to internal logistics 4.0. *Sustainable Logistics and Production in Industry 4.0: New Opportunities and Challenges*, pages 243–262, 2020.

[226] Mariusz Kostrzewski. Sensitivity analysis of selected parameters in the order picking process simulation model, with randomly generated orders. *Entropy*, 22(4):423, 2020.

[227] World Economic Forum. Global Risks Report 2017; Technical Report. https://www.weforum.org/reports/the-global-risks-report-2017, 2017. [Accessed 31-08-2024].

[228] International Organization for Standardization. PN-ISO 31000:2018-08: Risk Management—Principles and Guidelines;. https://www.iso.org/obp/ui#iso:std:iso:31000:ed-2:v1:en, 2018. [Accessed 31-08-2024].

[229] Floris Goerlandt and Jakub Montewka. Maritime transportation risk analysis: Review and analysis in light of some foundational issues. *Reliability Engineering & System Safety*, 138: 115–134, 2015.

[230] Terje Aven and Bodil S Krohn. A new perspective on how to understand, assess and manage risk and the unforeseen. *Reliability Engineering & System Safety*, 121:1–10, 2014.

[231] Terje Aven and Vidar Kristensen. Perspectives on risk: review and discussion of the basis for establishing a unified and holistic approach. *Reliability Engineering & System Safety*, 90 (1):1–14, 2005.

[232] Terje Aven. Perspectives on risk in a decision-making context–review and discussion. *Safety science*, 47(6):798–806, 2009.

[233] Terje Aven. Practical implications of the new risk perspectives. *Reliability Engineering & System Safety*, 115:136–145, 2013.

[234] EY Paul Mitchell. Does cyber risk only become a priority once you've been attacked? https://www.ey.com/en_gl/insights/energy-resources/does-cyber-risk-only-become-a-priority-once-you-ve-been-attacked, 2022. [Accessed 31-08-2024].

[235] Pegdwendé Sawadogo and Jérôme Darmont. On data lake architectures and metadata management. *Journal of Intelligent Information Systems*, 56(1):97 – 120, 2021.

[236] Huang Fang. Managing data lakes in big data era: What's a data lake and why has it became popular in data management ecosystem. In *2015 IEEE International Conference on Cyber*

Technology in Automation, Control, and Intelligent Systems (CYBER), pages 820–824. IEEE, 2015.

[237] Candy Pang and Duane Szafron. Single Source of Truth (SSOT) for Service Oriented Architecture (SOA). In Xavier Franch, Aditya K. Ghose, Grace A. Lewis, and Sami Bhiri, editors, *Service-Oriented Computing*, pages 575–589, Berlin, Heidelberg, 2014. Springer Berlin Heidelberg. ISBN 978-3-662-45391-9.

[238] Marco Stolpe. The internet of things: Opportunities and challenges for distributed data analysis. *SIGKDD Explor. Newsl.*, 18(1):15–34, August 2016. ISSN 1931-0145.

[239] CISA. Considerations for public safety cloud computing adoption. Technical report, Cybersecurity & Infrastructure Security Agency, August 2024.

[240] Keith Stouffer, Keith Stouffer, Michael Pease, CheeYee Tang, Timothy Zimmerman, Victoria Pillitteri, Suzanne Lightman, Adam Hahn, Stephanie Saravia, Aslam Sherule, et al. *Guide to operational technology (OT) security*. US Department of Commerce, National Institute of Standards and Technology, 2023.

[241] Amr A Munshi and Yasser Abdel-Rady I Mohamed. Data lake lambda architecture for smart grids big data analytics. *IEEE Access*, 6:40463–40471, 2018.

[242] Jeffrey Dean and Sanjay Ghemawat. MapReduce: simplified data processing on large clusters. *Communications of the ACM*, 51(1):107–113, 2008.

[243] Ahmed Eldawy and Mohamed F Mokbel. Spatialhadoop: A MaRreduce framework for spatial data. In *2015 IEEE 31st International Conference on Data Engineering*, pages 1352–1363. IEEE, 2015.

[244] Setu Kumar Basak, Jamison Cox, Bradley Reaves, and Laurie Williams. A comparative study of software secrets reporting by secret detection tools. In *2023 ACM/IEEE International Symposium on Empirical Software Engineering and Measurement (ESEM)*, pages 1–12. IEEE, 2023.

[245] Aleksandr Ometov, Sergey Bezzateev, Niko Mäkitalo, Sergey Andreev, Tommi Mikkonen, and Yevgeni Koucheryavy. Multi-factor authentication: A survey. *Cryptography*, 2(1):1, 2018.

[246] Ministry of Digitalisation (Ministerstwo Cyfryzacji). Update of Cloud Computing Cybersecurity Standards - public consultations (in polish), 2024. https://www.gov.pl/web/cyfryzacja/ministerstwo-cyfryzacji-zaprasza-do-konsultacji-aktualizacji-standardow-cyberbezpieczenstwa-chmur-obliczeniowych.

[247] Council of European Union. Council regulation (EU) no 2024/1689 (Artificial Intelligence Act), 2024. https://eur-lex.europa.eu/legal-content/EN/TXT/?uri=CELEX:32024R1689.